63-3-3

403053

ASD-TDR-63-223
PART I

403 053

FEASIBILITY INVESTIGATION OF CHEMICALLY SPRAYED THIN FILM PHOTOVOLTAIC CONVERTERS

TECHNICAL DOCUMENTARY REPORT NO. ASD-TDR-63-223, PART I

MARCH 1963

DIRECTORATE OF AEROMECHANICS
AERONAUTICAL SYSTEMS DIVISION
AIR FORCE SYSTEMS COMMAND
WRIGHT-PATTERSON AIR FORCE BASE, OHIO

PROJECT NO. 8173, TASK NO. 817301

(PREPARED UNDER CONTRACT NO. AF 33(657)-7919
BY THE NATIONAL CASH REGISTER COMPANY, DAYTON, OHIO;
R. R. CHAMBERLIN, J. S. SKARMAN, D. E. KOOPMAN,
AND L. E. BLAKELY, JR.)

ASD-TDR-63-223
PART I

FEASIBILITY INVESTIGATION OF CHEMICALLY SPRAYED THIN FILM PHOTOVOLTAIC CONVERTERS

TECHNICAL DOCUMENTARY REPORT NO. ASD-TDR-63-223, PART I

MARCH 1963

DIRECTORATE OF AEROMECHANICS
AERONAUTICAL SYSTEMS DIVISION
AIR FORCE SYSTEMS COMMAND
WRIGHT-PATTERSON AIR FORCE BASE, OHIO

PROJECT NO. 8173, TASK NO. 817301

(PPEPARED UNDER CONTRACT NO. AF 33(657)-7919
BY THE NATIONAL CASH REGISTER COMPANY, DAYTON, OHIO;
R. R. CHAMBERLIN, J. S. SKARMAN, D. E. KOOPMAN,
AND L. E. BLAKELY, JR.)

NOTICES

When Government drawings, specifications, or other data are used for any purpose other than in connection with a definitely related Government procurement operation, the United States Government thereby incurs no responsibility nor any obligation whatsoever; and the fact that the Government may have formulated, furnished, or in any way supplied the said drawings, specifications, or other data, is not to be regarded by implication or otherwise as in any manner licensing the holder or any other person or corporation, or conveying any rights or permission to manufacture, use, or sell any patented invention that may in any way be related thereto.

Qualified requesters may obtain copies of this report from the Armed Services Technical Information Agency (ASTIA), Arlington Hall Station, Arlington 12, Virginia.

This report has been released to the Office of Technical Services, U.S. Department of Commerce, Washington 25, D.C., for sale to the general public.

Copies of this report should not be returned to the Aeronautical Systems Division unless return is required by security considerations, contractual obligations, or notice on a specific document.

FOREWORD

This report was prepared by The National Cash Register Company as a technical summary report covering the research and development on Contract AF 33(657)-7919, Project No. 8173, Task No. 817301. The project was initiated by the Flight Accessories Laboratory of the Flight Vehicle Power Branch. The work was administrated under the direction of the Aeronautical Systems Division, Wright Patterson Air Force Base, with Mr. L. D. Massie as Project Engineer.

This contract and technical report are concerned with the work from 1 February 1962 through January 1963. The following technical personnel have contributed to the project during this period of Contract AF 33(657)-7919: R. R. Chamberlin, J. S. Skarman, F. P. Gugliotta, D. E. Koopman, F. G. Ullman, L. E. Blakely, G. L. Hartman, D. J. Huber, and R. L. Boor. Project direction has been provided by R. R. Chamberlin. D. E. Koopman directed the crystallographic studies, with F. G. Ullman and L. E. Blakely the work on anti-reflection coatings.

Acknowledgment is made to Dr. A. F. Prebus of Ohio State University who provided electronmicroscope support and to Dr. W. M. Becker of Purdue University who was consulted on problems of basic mechanisms.

ABSTRACT

This technical report presents the results of the first phase of Contract AF 33(657)-7919. The objectives of this phase were: (1) to demonstrate the feasibility of fabricating a thin film photovoltaic converter using a chemical spray process for the deposition of the active elements, and (2) to fabricate for delivery six experimental cells, four using CdS and two using CdSe as the n-type semiconducting layer.

Research with these materials has shown the feasibility of fabricating photovoltaic converters using thin films of cadmium and copper sulfide (.6 μ and .05 μ respectively) and has shown that the deposition process used is applicable to large area, multiple layer (CdS-CdSe-Cu_2S) configurations, solid solution (Cd(S, Se)-Cu_2S) cells, and continuous line production. This research has also shown that a heterogeneous junction photovoltaic converter can be formed using CdS and Cu_2S.

Six (4 CdS and 2 CdSe) cells of 16 in^2 area were fabricated for delivery. The four CdS cells had an average efficiency of .2% and the two CdSe cells had an average efficiency of less than .01%. The efficiencies of the four inch square cells do not indicate the potential of the chemical spray process since CdS cells of one square inch were made with 1.2% efficiency and CdS cells of one square centimeter were made with 3.5% efficiency. All of these cells were of the back wall (incident irradiation travels through the substrate) configuration using one eighth inch hard glass as the substrate.

TABLE OF CONTENTS

LIST OF ILLUSTRATIONS

LIST OF ILLUSTRATIONS (continued)

LIST OF ILLUSTRATIONS (continued)

LIST OF TABLES

INTRODUCTION

The objective of the applied research described in this technical report was to show the feasibility of depositing with a unique chemical spray process the semiconducting layers or films necessary to form a thin film photovoltaic structure. It was intended that thin film photovoltaic converters be made using either cadmium sulfide or cadmium selenide.

The fabrication of thin layer photovoltaic converters using cadmium sulfide is definitely not new, however, the applied research accomplished under Contract AF 33(657)-7919 has resulted in some unique cell structures and an improved method of forming a distinct heterojunction using copper sulfide and cadmium sulfide.

This work under AF 33(657)-7919 has as its final objective the fabrication of a flexible thin film photovoltaic array of at least one square foot in area with sufficient efficiency such that the watts per pound ratio is greater than that obtainable with presently available solar power sources. The first phase effort involving the demonstration of feasibility of the chemical spray process was accomplished using glass substrates and the back wall configuration. This first effort has resulted in the fabrication of 1 cm^2 cells of greater than 3.5%; the demonstration of several new thin film cells; and the demonstration of a thin film photovoltaic structure which has an improved environmental stability.

The types of structures fabricated together with some comments of their behavior is contained in Section I, with Section II covering in detail the crystallographic aspect of the films formed by the chemical spray process. Section III covers briefly the experiments involving possible improvements through the use of anti-reflection coatings with Section IV covering the various aspects of cell fabrication and their characteristics.

The appendix of this report contains the thermal and electrical characteristics of the experimental 4 inch by 4 inch cells delivered under this contract.

Manuscript released by the authors February 1963 for publication as an ASD Technical Documentary Report.

TECHNICAL DISCUSSION

I. PHOTOVOLTAIC MATERIALS

INTRODUCTION

Previous researchers in the cadmium sulfide photovoltaic converter field have fabricated cells using vacuum deposited layers ranging up to 15 mils[1-3] in thickness in the early efforts to make broad area photovoltaic converters. Recently these researchers have reduced their layer thicknesses to the 15 to 40 micron range[4,5] with some improvement in the cell's efficiencies. The improvements which have been gained appear to be due primarily to improvement in the deposition of the cadmium sulfide film and not to any significant change in the method of forming the barrier.

The research conducted during the first phase of Contract AF 33(657)-7919 has been concerned primarily with:

1. Deposition of CdS and CdSe films of less than 1 micron thickness
2. Formation of a barrier using a film of a p-type material
3. Evaluating the physical characteristics of the deposited films
4. Determining parameters that limit array size
5. Development of a model which appears suitable for a CdS photovoltaic converter

TECHNICAL DISCUSSION

1. Semiconducting Film Requirements

As this research program was to be ultimately directed toward gaining the necessary technology for the experimental production of photovoltaic converters for aerospace application, it was decided early in the first phase that a demonstration of process feasibility with films in the 1 micron thickness range would be of greatest value. The advantage of very thin films with regards to flexibility and weight is obvious with front wall cells. Although it has not been considered as a serious possibility for aerospace application, the back wall cell on a transparent substrate also would be benefited, if the first semiconducting (n-type) layer has a minimum thickness so that a maximum amount of the incident energy arrives at the barrier.

Table 1 gives the values of open circuit voltage (hereafter designated O. C. V. or V_{oc}) and short circuit current (hereafter designated

S. C. C. or I_{sc}) obtained with cells made by intentionally changing the thickness of the n-type film. Other factors, such as the deposition parameters of the n-type film, the deposition parameters of the p-type film, the thickness of the p-type film and all heat treatments, were the same for all cells, within experimental error.

TABLE 1

Thickness	V_{oc}	I_{sc}
4000 A°	.30 V	6.0 ma
	.32 V	4.9 ma
	.33 V	4.9 ma
4700 A°	.35 V	6.9 ma
	.26 V	4.2 ma
	.22 V	4.3 ma
5400 A°	.37 V	10.8 ma
	.33 V	9.3 ma
	.32 V	6.0 ma
6100 A°	.37 V	8.4 ma
	.37 V	7.0 ma
	.36 V	10.3 ma
6900 A°	.38 V	8.7 ma
	.37 V	8.6 ma
	.37 V	6.8 ma
7200 A°	.40 V	7.0 ma
	.39 V	6.4 ma
	.30 V	8.0 ma

All cells were 1 cm^2 measured with 100 mw/cm^2 of tungsten

The determination of the actual minimum thickness of the n-type layer has not as yet been accomplished, although, as can be seen from Table 1, reasonable response can be obtained with cells as thin as 4000 A°. Response in the few millivolts range has been recorded with cells whose n-type layer was less than 1000 A° thick, and a cell (.1 cm^2) whose n-type layer was 1500 A° thick gave an output of 0.3 milliamps, at 60 millivolts when irradiated with 100 mw/cm^2 tungsten. The major difficulty involved here is attempting to show that it is the thickness of the n-type layer which is acting as the controlling factor.

The spectral response of a back wall (irradiation incident upon the n-type layer) cell can possibly be used as an experimental means for determining minimum n-type film thickness. It can be seen in

Figure 1 that the photovoltaic response (plotted on log scale to emphasize the response at short wavelengths) at wavelengths shorter than 500 mμ (within the absorption edge of the n-type layer) is not evident, until the thickness is less than 6000 A°, and is the same as a front wall cell when the thickness has been reduced to 1500 A°. This follows if the transmission of a film of CdS as a function of thickness is considered, and it is assumed that the junction being formed between the CdS (n-type layer) and the p-type layer penetrates the n-type layer (CdS), only a small percentage of its total thickness. Figure 2 shows the transmission of CdS as a function of thickness. It can be seen that at a thickness of 4000 A° a typical CdS film transmits only 2.5% of the incident energy at 450 mμ, and a film 1500 A° thick transmits only 25% at this same wavelength.

As the thickness of the n-type layer is decreased the interface between the barrier and the n-type layer will receive more and more of the energy, at wavelengths within the absorption band of the n-type layer, until the back wall response should be similar to the front wall response. In this manner the spectral response should be able to indicate the minimum thickness of the n-type layer.

Figure 3 gives the comparison of the two modes in which a thin film cell may operate. Curve A is the photovoltaic spectral response of a front wall cell (irradiation incident on the p-type layer) and curve B is the photovoltaic response of this same cell being used in the back wall cell mode (irradiation incident on the n-type layer). The effect of the bulk transmission of the n-type (CdS) film can be seen by comparing the response present in these two modes at wavelengths shorter than 500 mμ.

The fabrication of moderately (3.0%) efficient photovoltaic cells using a total film thickness (n-type plus p-type) of less than 1 micron on a glass substrate together with transparent electrodes allows this direct comparison of the front and back wall modes for a single cell. The photovoltaic spectral response has been used extensively, throughout the work being reported here, as a measure of what contribution to the total output was made by the various parts of the cell.

As an example, Figure 4 shows four curves which are the response of different cells (back wall mode) on a common substrate, with each of the cells using a different metal as the contact to the p-type layer. Examination of these photovoltaic responses shows an apparent difference depending on the metal used as the p-layer current collector. With another cell also operating in the back wall mode, except that an open grid of silver paint is used as the contact to the p-type layer, it can be shown using different metals as mirrors that the difference in spectral response seen in Figure 4 is due to the spectral reflectivity of the metal used as the electrode and not due to any semiconductor or metal semiconductor phenomena. Thus when interpreting the spectral responses of thin film photovoltaic cells due consideration must be given such things as the spectral reflectivity of the rear electrode and even to the interference phenomena which might be present in a very thin film cell such as the one whose spectral response is shown in Figure 5 and appears to have so much structure.

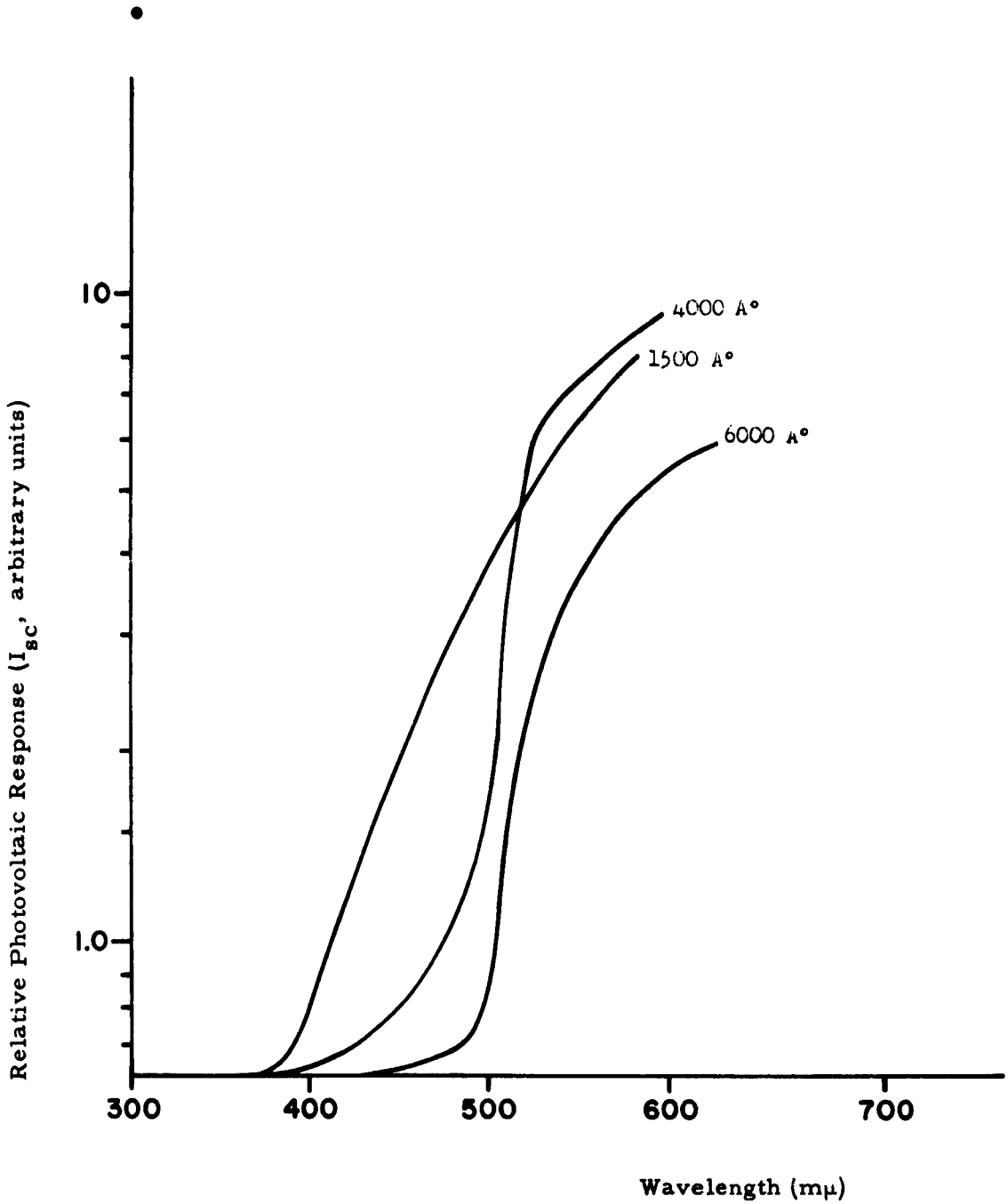

FIGURE 1
Spectral Response of CdS Films of Various Thickness

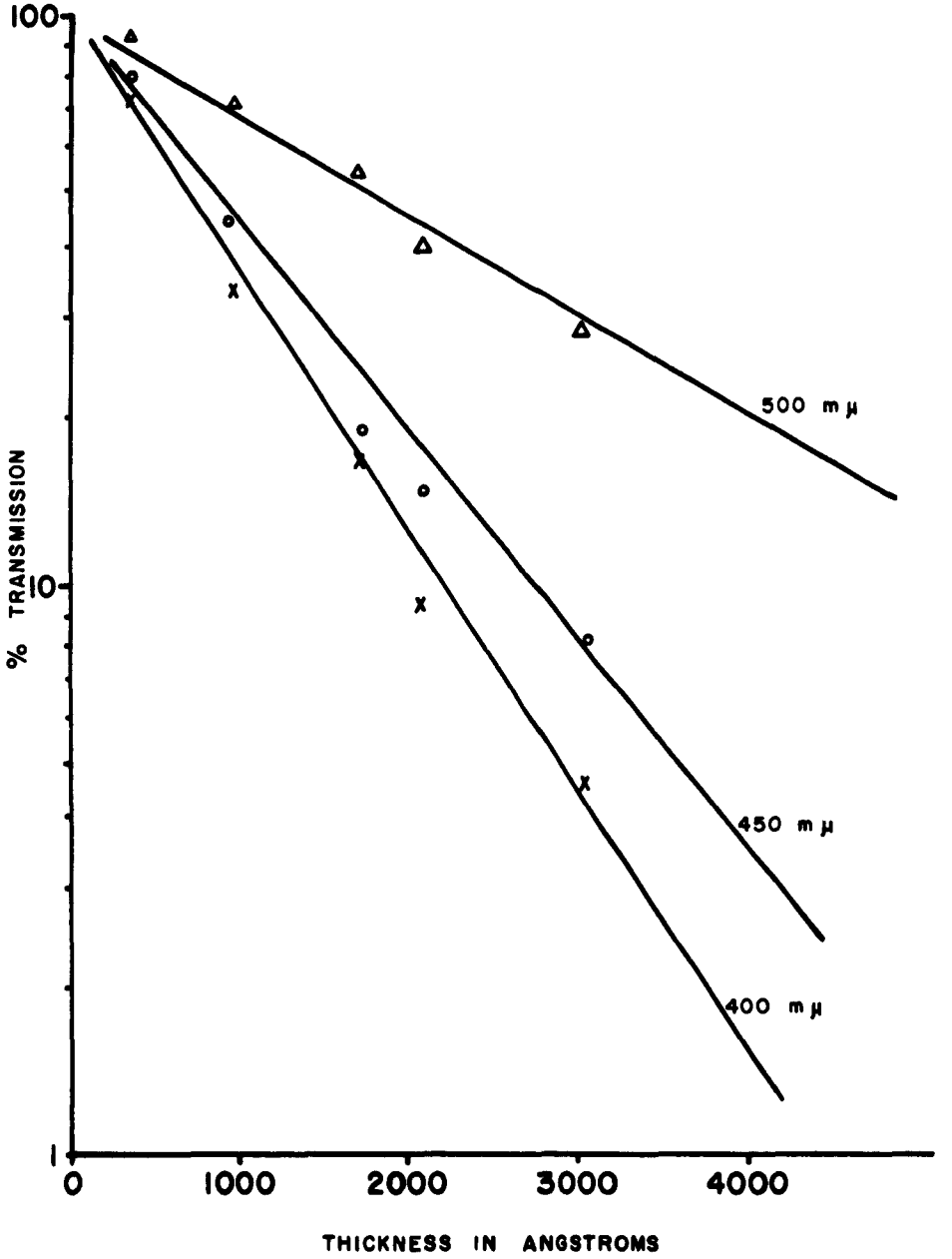

FIGURE 2
Transmission vs Thickness for Chemically Sprayed CdS Films

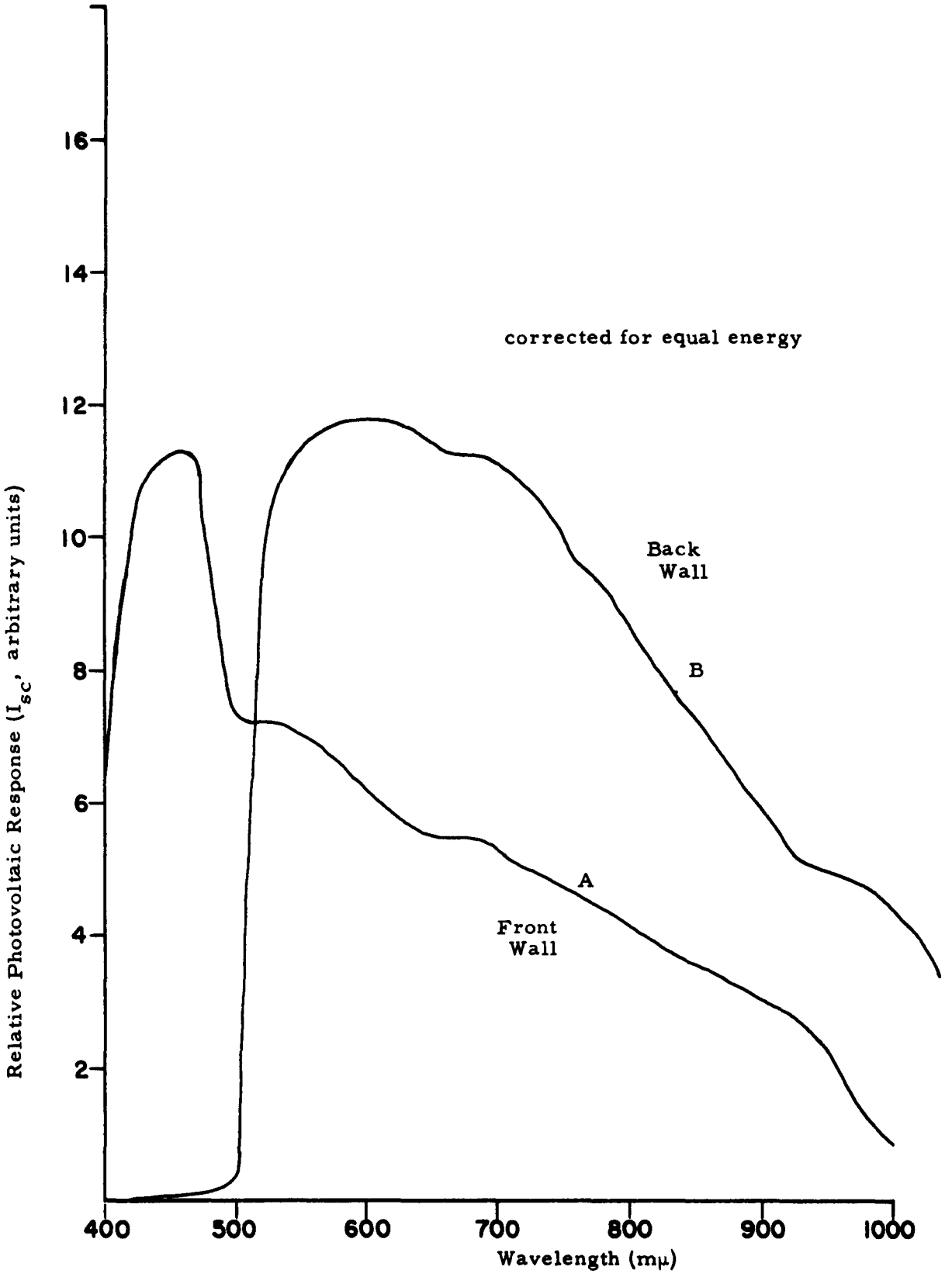

FIGURE 3
Spectral Responses of a CdS Cell

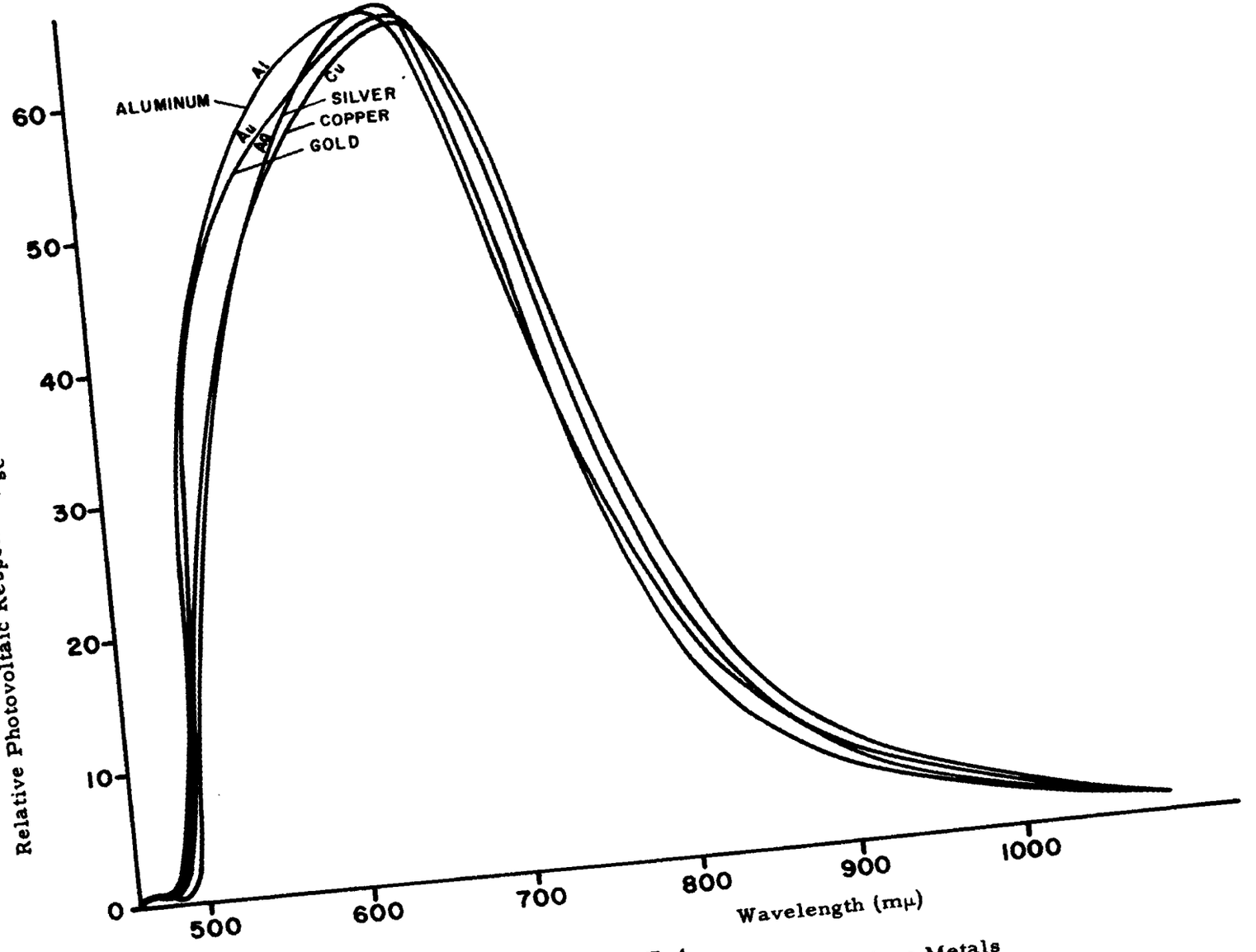

FIGURE 4
Spectral Response of a CdS Cell Electroded with Various Metals

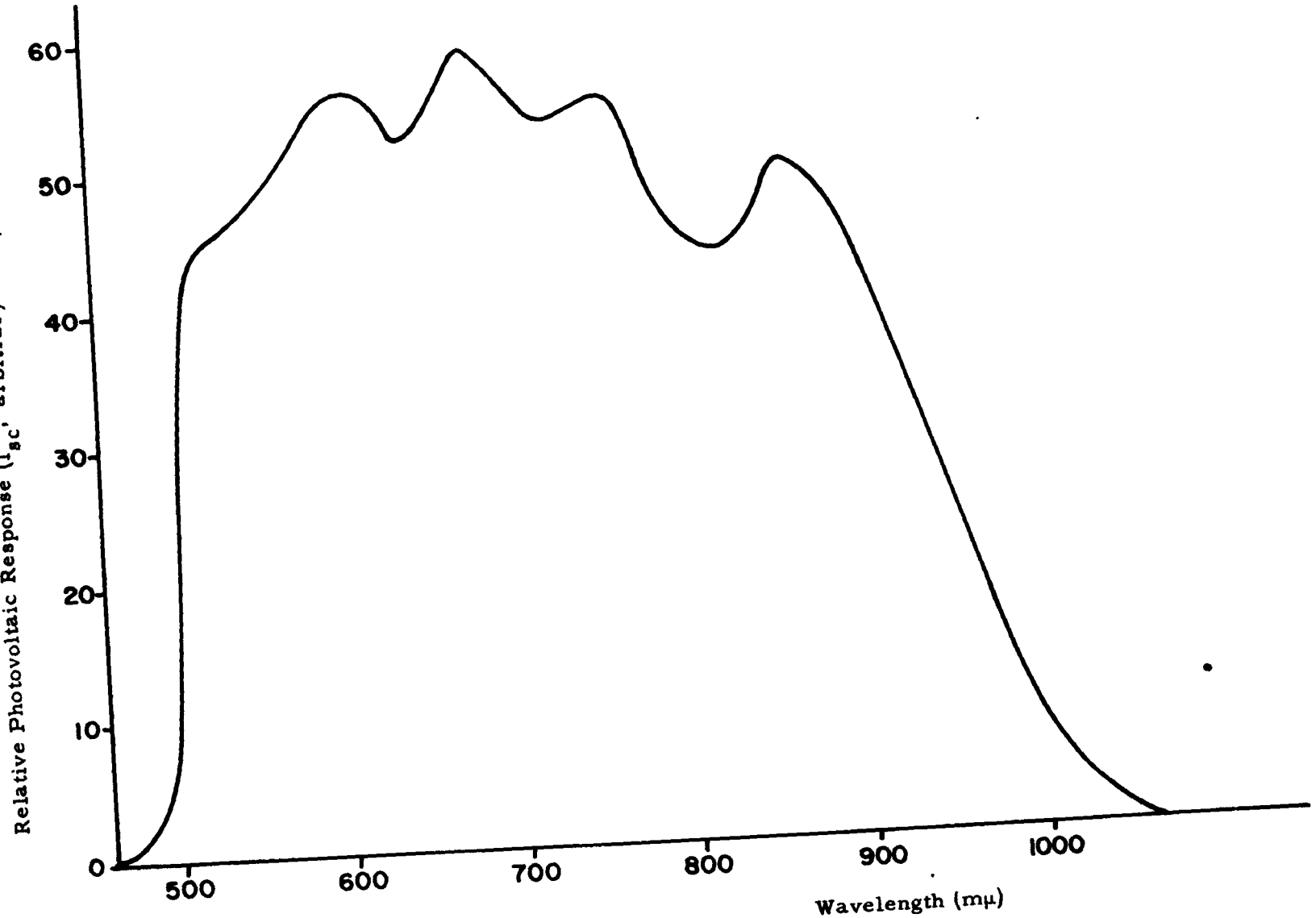

FIGURE 5
Spectral Response of a CdS Cell

The deposition of discrete electrodes on a common substrate was found to be a very valuable means of cell evaluation, especially in comparing the efficiency over the area of a large (4" x 4") cell. This method of forming discrete cells on a common substrate is illustrated in Figure 6, together with illustrations of the front and back wall cell modes.

As this first phase has been primarily concerned with the demonstration of the feasibility of a process, very little effort was available to search for what might be the limiting parameters involved in the structure for which process feasibility has been shown. However, two areas which will be examined in the second phase are evident in Table 1. It can be noted in this table that the open circuit voltage tends to increase with the increase in the thickness of the n-type layer. The theory of homogeneous p-n junctions says that the open circuit voltage should be a function of the carrier concentrations on both sides of the junction; it will require Hall effect measurements to determine if this holds true in the case of heterogeneous junctions, and if so, why the open circuit voltage appears to be dependent on the thickness of the n-type layer. It can also be seen from Table 1 that the short circuit current in this series of cells seems to peak between 5000 A° and 6000 A°. It is obvious from the standpoint of transmission that more of the incident energy should be available at the junction the thinner the cell, and in this series with the p-type layer parameters being held constant, one would expect that the current would be inversely dependent on thickness. Thus some measurement or systems of measurements must be found which can be shown to be characteristic of that which determines the short circuit current. The success of the present experimental effort to produce efficiencies greater than 3.5% in CdS photovoltaic converters in which the CdS layer is less than 1 micron in thickness is due in part to the film deposition process, and in part to the formation of a junction or barrier between two distinct and separately deposited films, one n-type and one p-type.

Although several thin film combinations were developed, the system on which the majority of the effort was expended during the period covered by this report, and the one for which feasibility was shown, is a combination of a thin film of cadmium sulfide (.4-1 μ) and a thin film of copper sulfide (.04-.09 μ), where the cadmium sulfide is an undoped n-type film and the copper sulfide a p-type film of the digenite type. The digenite form of copper sulfide is a stable non-stoichiometric form usually of the $Cu_{9-x}S_y$ or the $Cu_{1.8}S$ type and will be referred to in the remainder of this report as Cu_xS_y.

2. CdS Photovoltaic Converters

The CdS-Cu_xS_y structure which has been developed under this contract is not especially unique in its spectral response or output, but is unique in the distinct heterojunction between the CdS and Cu_xS_y films and the thickness of these films. If a watts per pound determination was to be made on the basis of some efficiency per square, the CdS-Cu_xS_y layers would contribute only 1/200 of the total weight if a substrate such as .002" Mo is used.

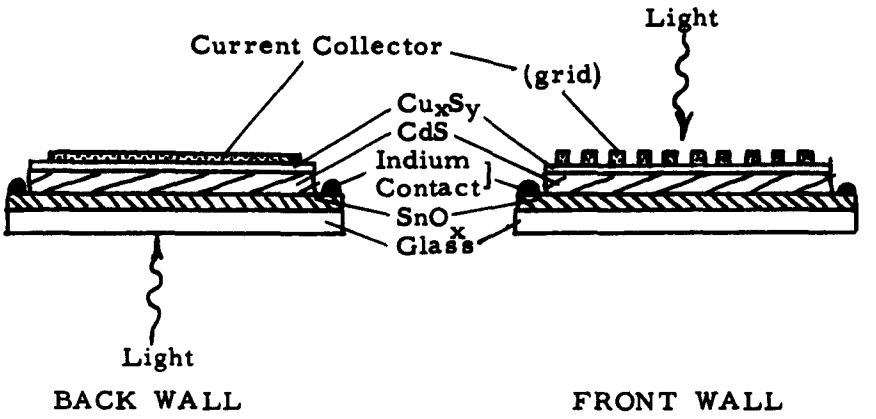

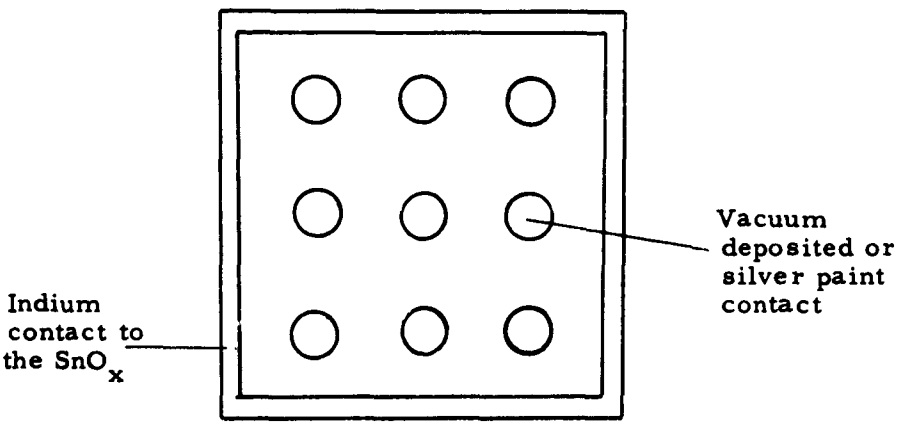

FIGURE 6
Front and Back Wall Constructions and a Multiple Electrode Configuration

Figures 7 through 10 give the photovoltaic spectral response and relative quantum yield of a large (16 inch^2) area and a small (1 cm^2) area CdS-Cu_xS_y cell.

The yield of these cells is defined as relative quantum yield because an experimental apparatus is not yet set up which will adequately account for the energy which is reflected and the energy which is transmitted through the cell at each wavelength.

3. CdSe, Cd(S, Se) and CdS-CdSe Photovoltaic Converters

The compounds listed in the title of this sub-section are the n-type layer of the photovoltaic structure.

Initial work with CdSe resulted in a few very inefficient cells which were interesting only in their spectral response, which is given in Figure 11. It will be noted that the polarity of one of (B) these cells is the reverse of two others (C and D) and the polarity of one (A) cell is wavelength dependent. This series of spectral responses together with their polarities suggests the possibility that a barrier exists between the n-type CdSe and a more n-type SnO_x.

Later improvements in the deposition of Cu_xS_y have resulted in 12 inch^2 CdSe cells which were .01% efficient. Figures 12 and 13 give the photovoltaic spectral response and the relative quantum efficiency of typical CdSe-Cu_xS_y cells. Even though a CdSe-Cu_xSe_y structure has to date been unsuccessful, it is believed that it should yield cells with efficiencies similar to that now possible with CdS-Cu_xS_y.

Because of the difficulties in the formation of a good barrier with CdSe two other approaches were tried; one was a combination of the CdS and CdSe processes to deposit a solid solution of Cd(S, Se) where the sulfur and selenium are in approximately equal percentage. The crystallographic examination of this solid solution is given in Section II. It was found that responsive cells could be obtained with this solid solution and Cu_xS_y more easily than with CdSe alone but with no greater efficiencies. Figure 14 gives the photovoltaic spectral response of a typical solid solution cell. Note that the response peaks between the CdS and the CdSe absorption edge.

As the other approach to utilization of CdSe, a structure consisting of a first film of CdSe and a second film of CdS as the n-type layer was made. Cu_xS_y was subsequently deposited on the CdS to form the junction. These cells, while more efficient than the CdSe or the Cd(S, Se) cells, were not nearly as efficient as the CdS-Cu_xS_y combination. Figure 15 gives the front and back wall mode response for a multiple layer film, and Figure 16 the relative quantum yield.

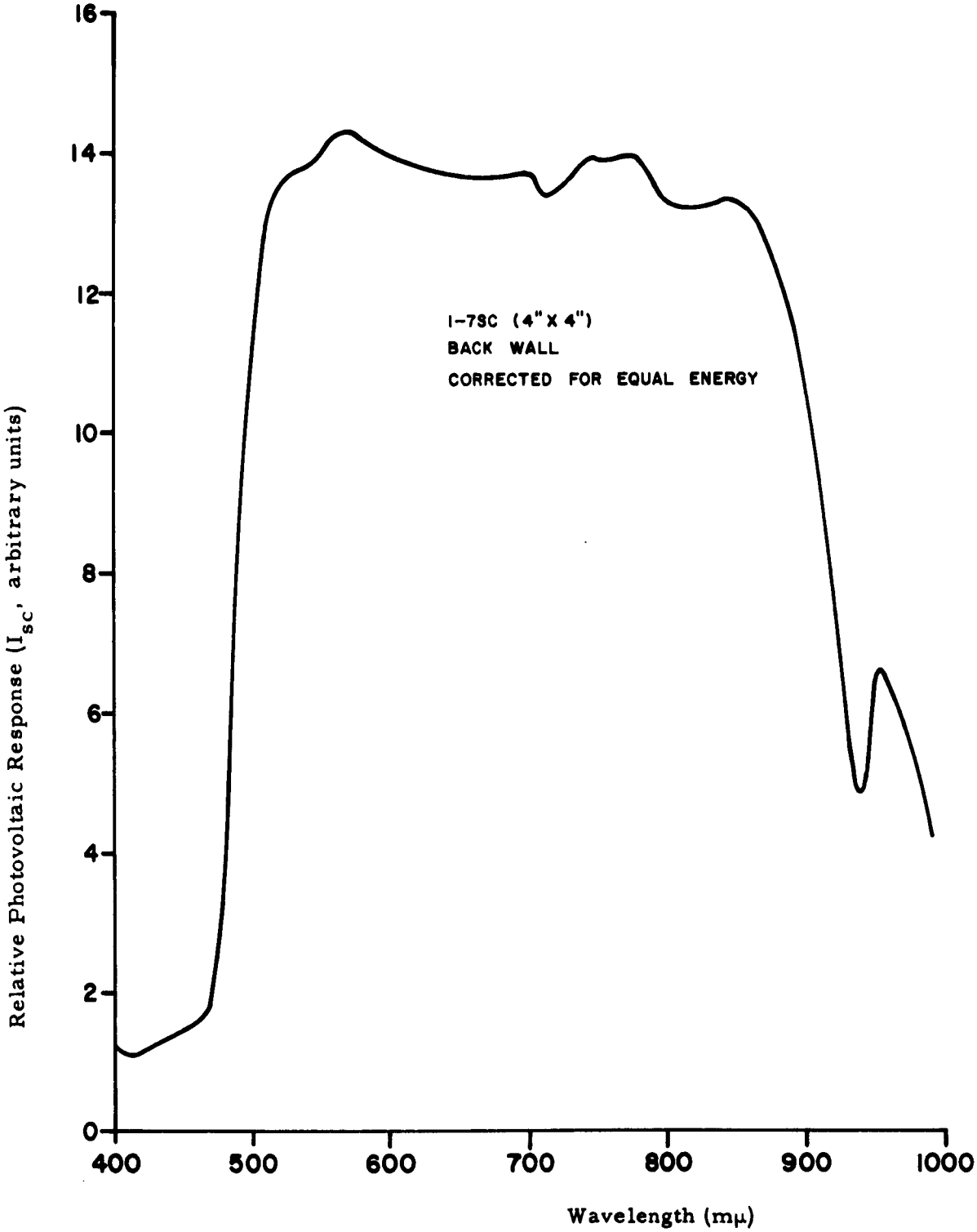

FIGURE 7
Spectral Response of a Back Wall 4" x 4" CdS Cell

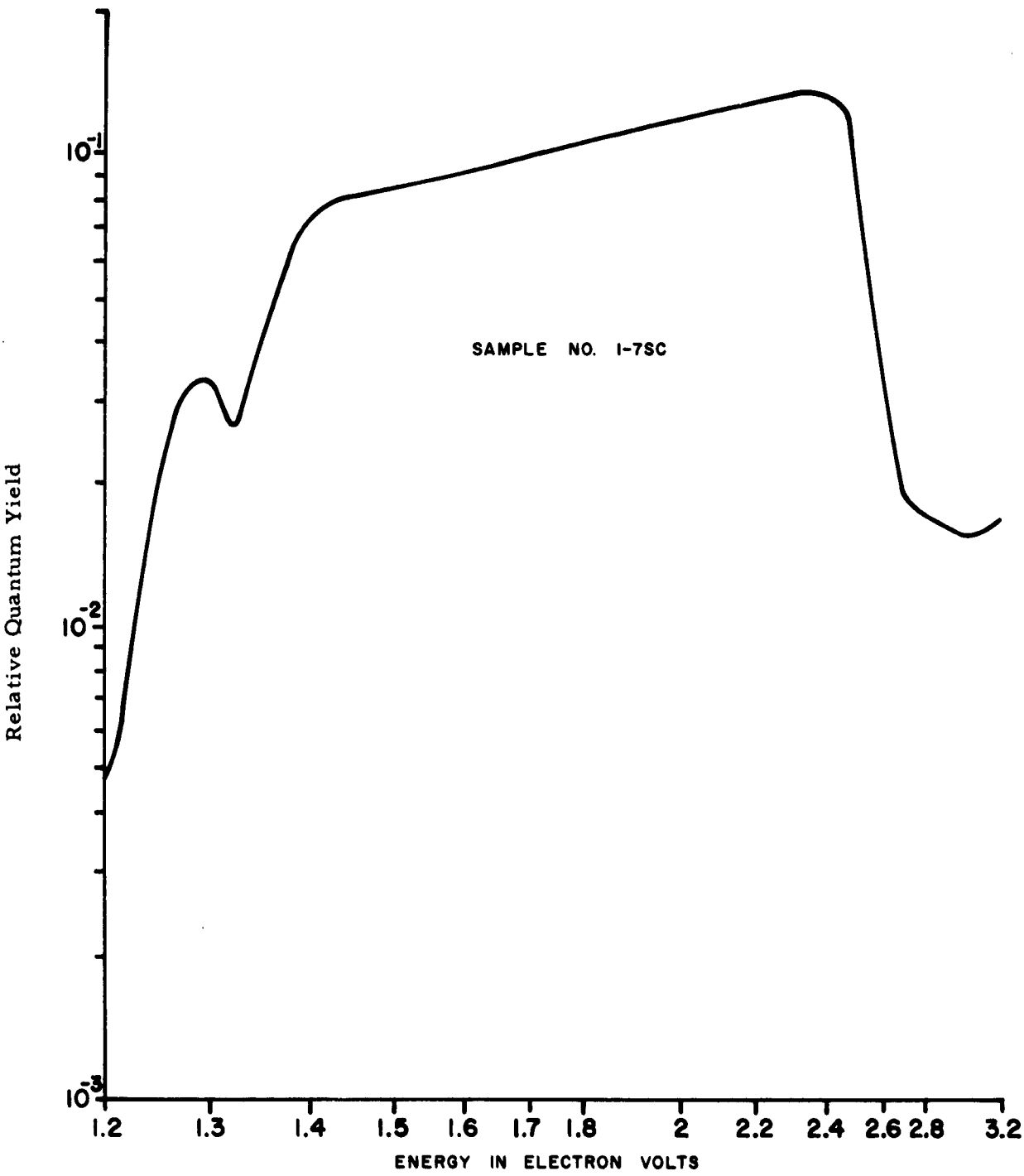

FIGURE 8
Relative Quantum Yield of a Back Wall 4" x 4" CdS Cell

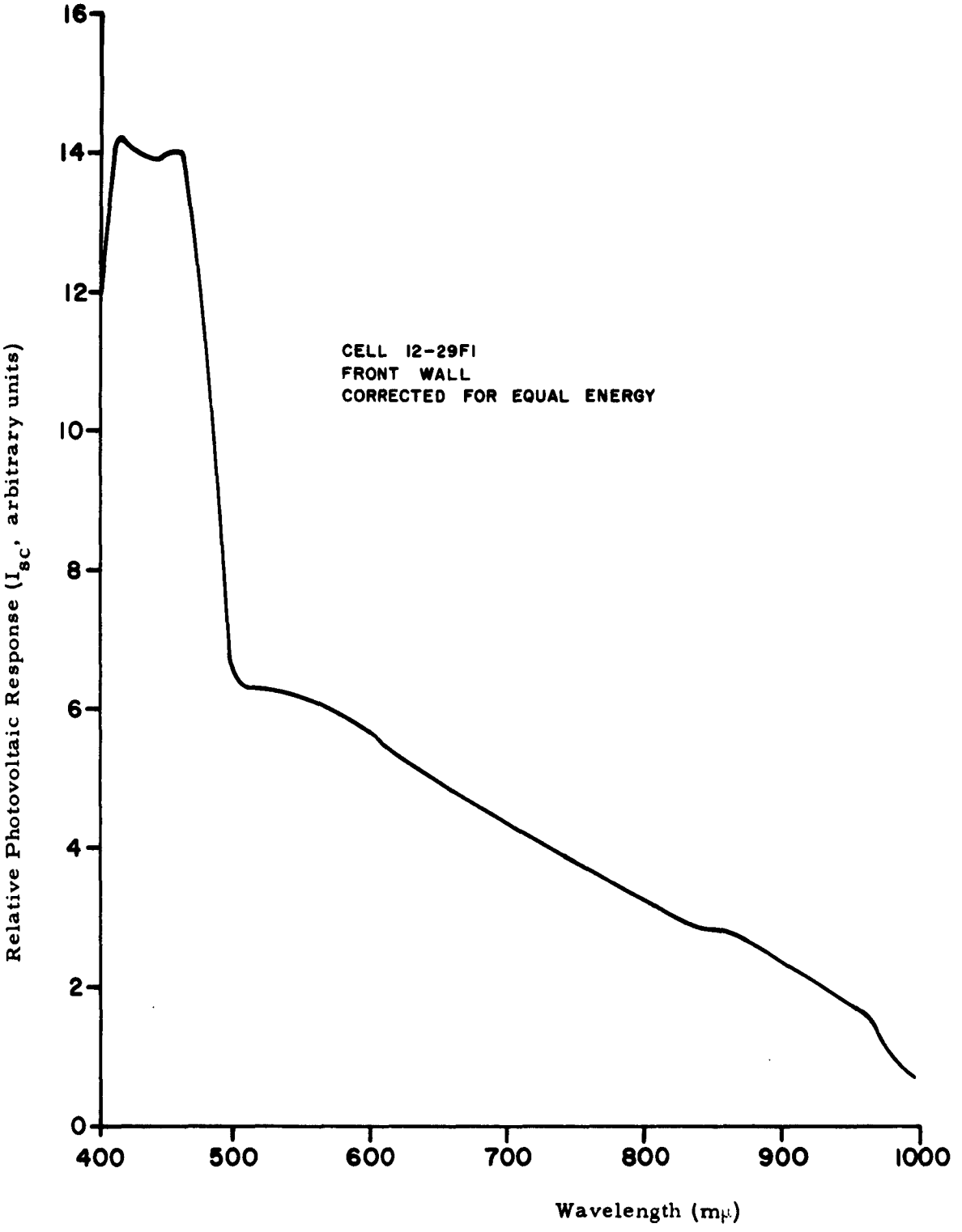

FIGURE 9
Spectral Response of a Front Wall 1 cm^2 CdS Cell

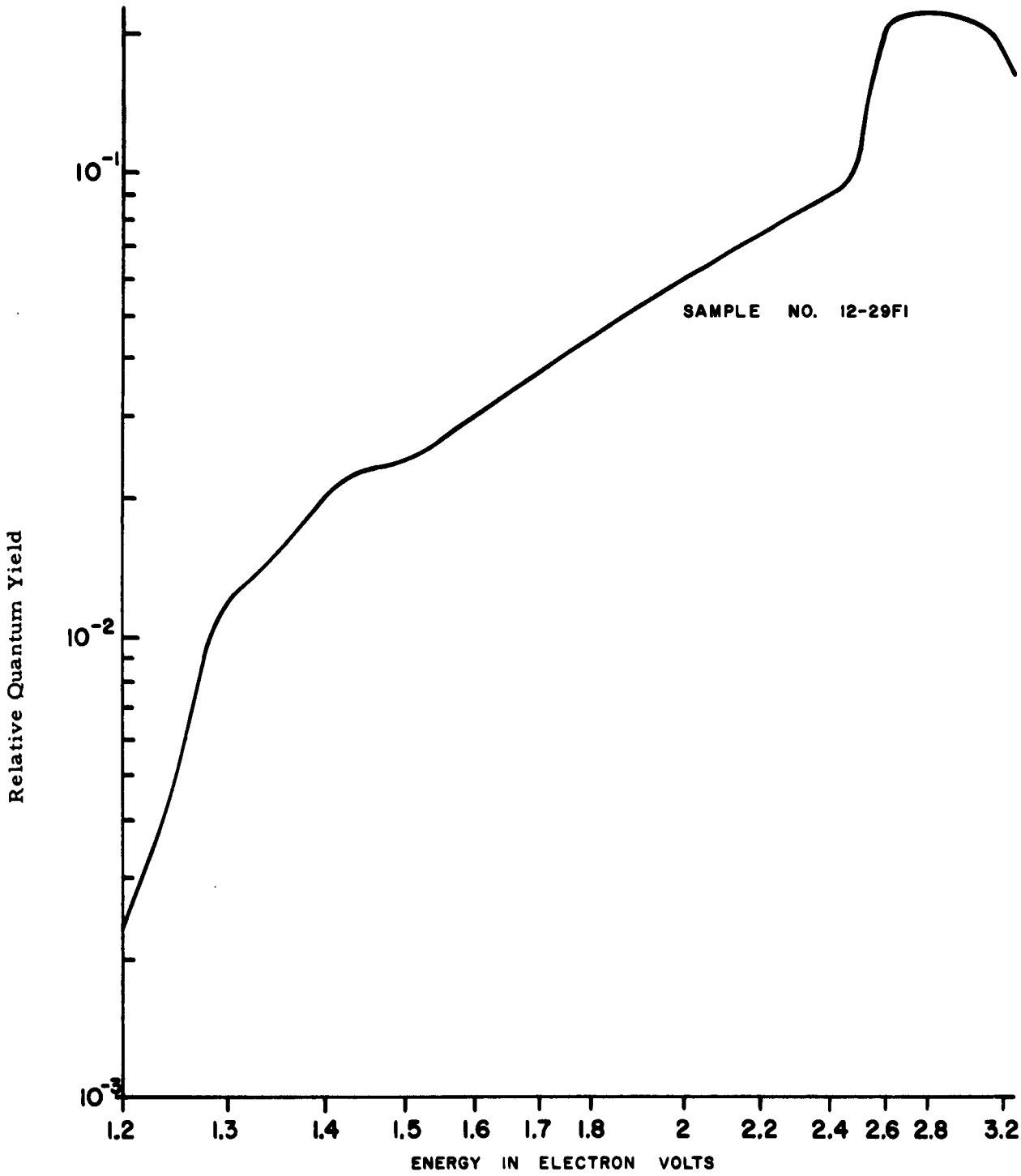

FIGURE 10
Relative Quantum Yield of a Front Wall 1 cm^2 CdS Cell

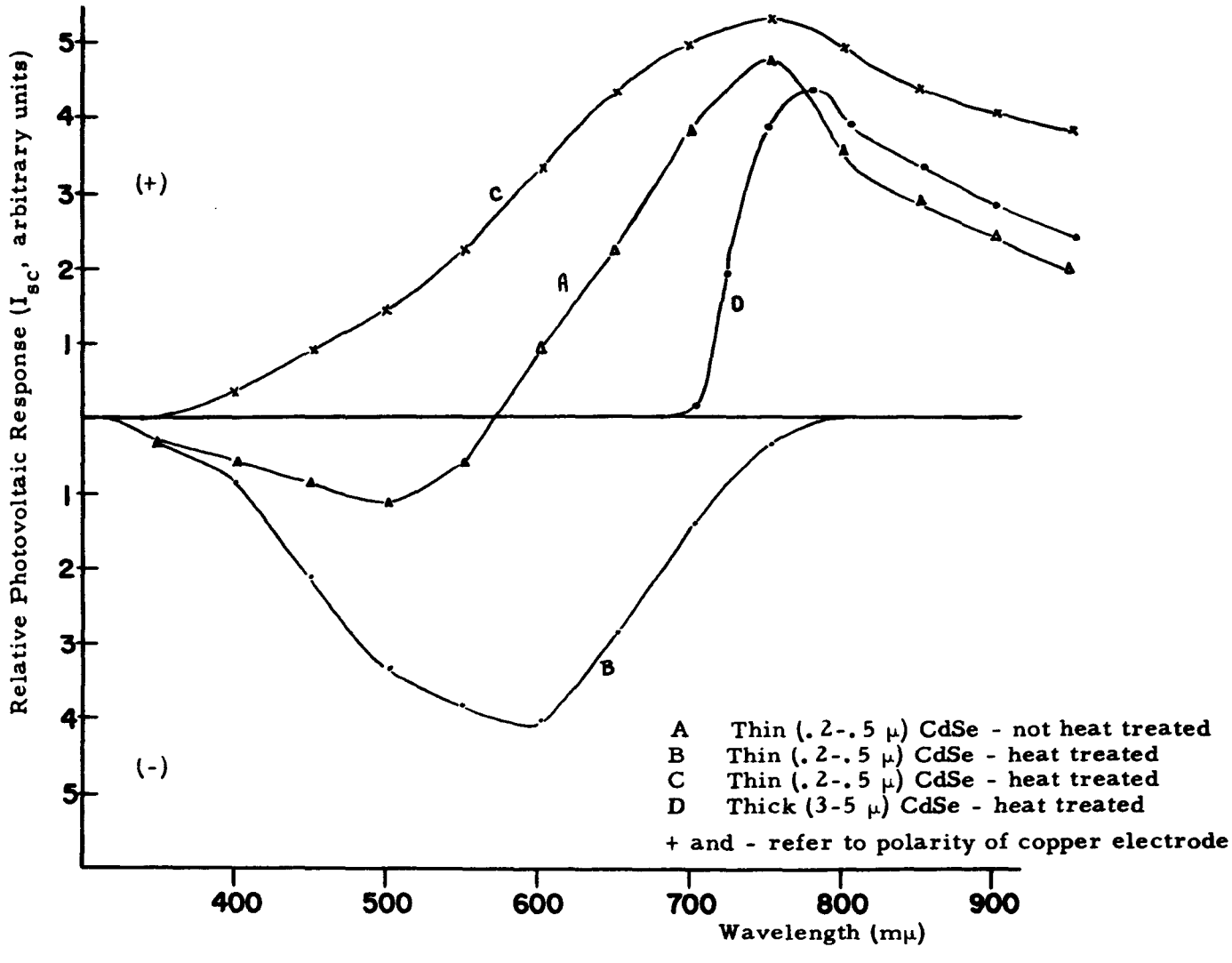

FIGURE 11
Spectral Responses of Several CdSe Cells

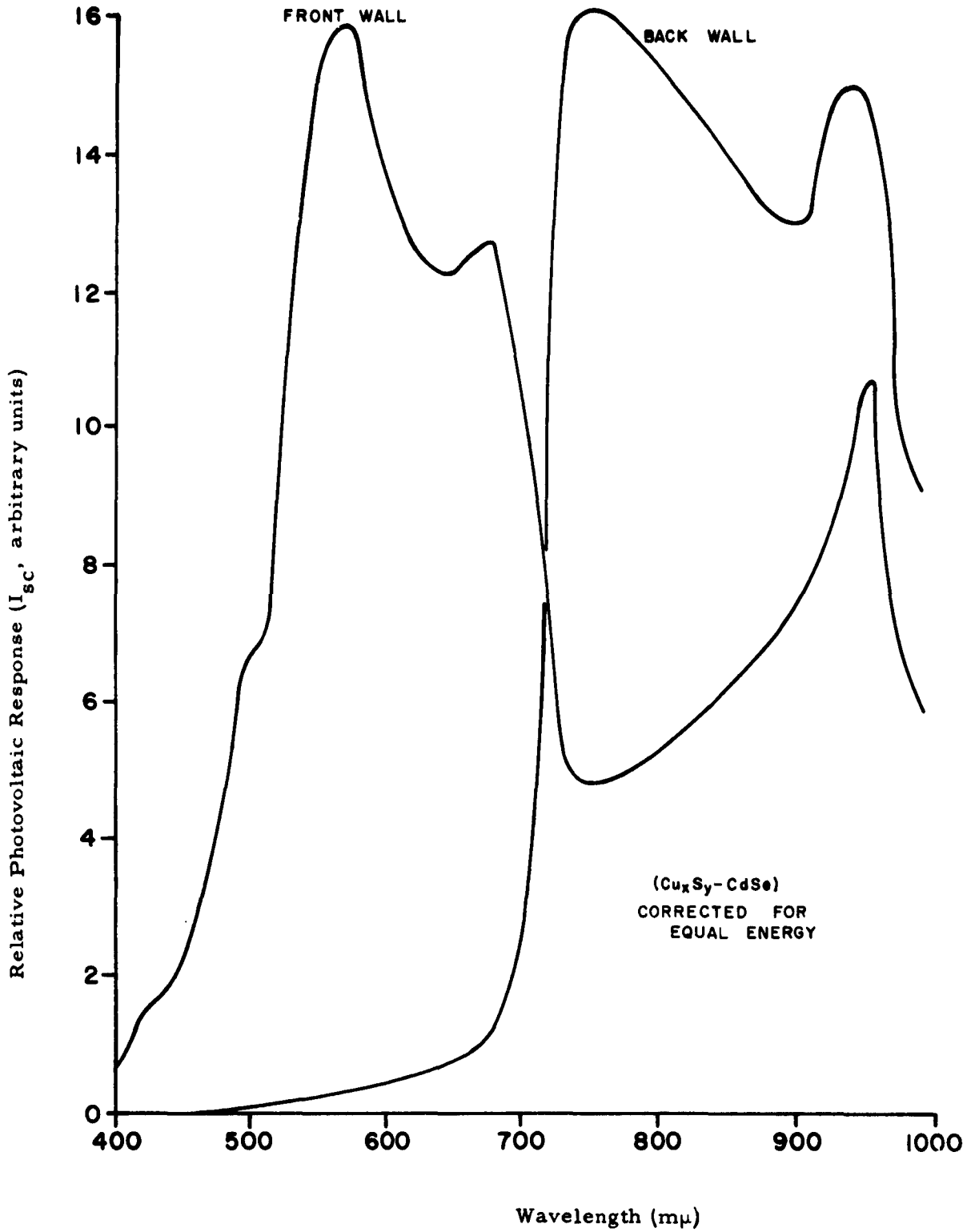

FIGURE 12
Spectral Response of a CdSe Cell

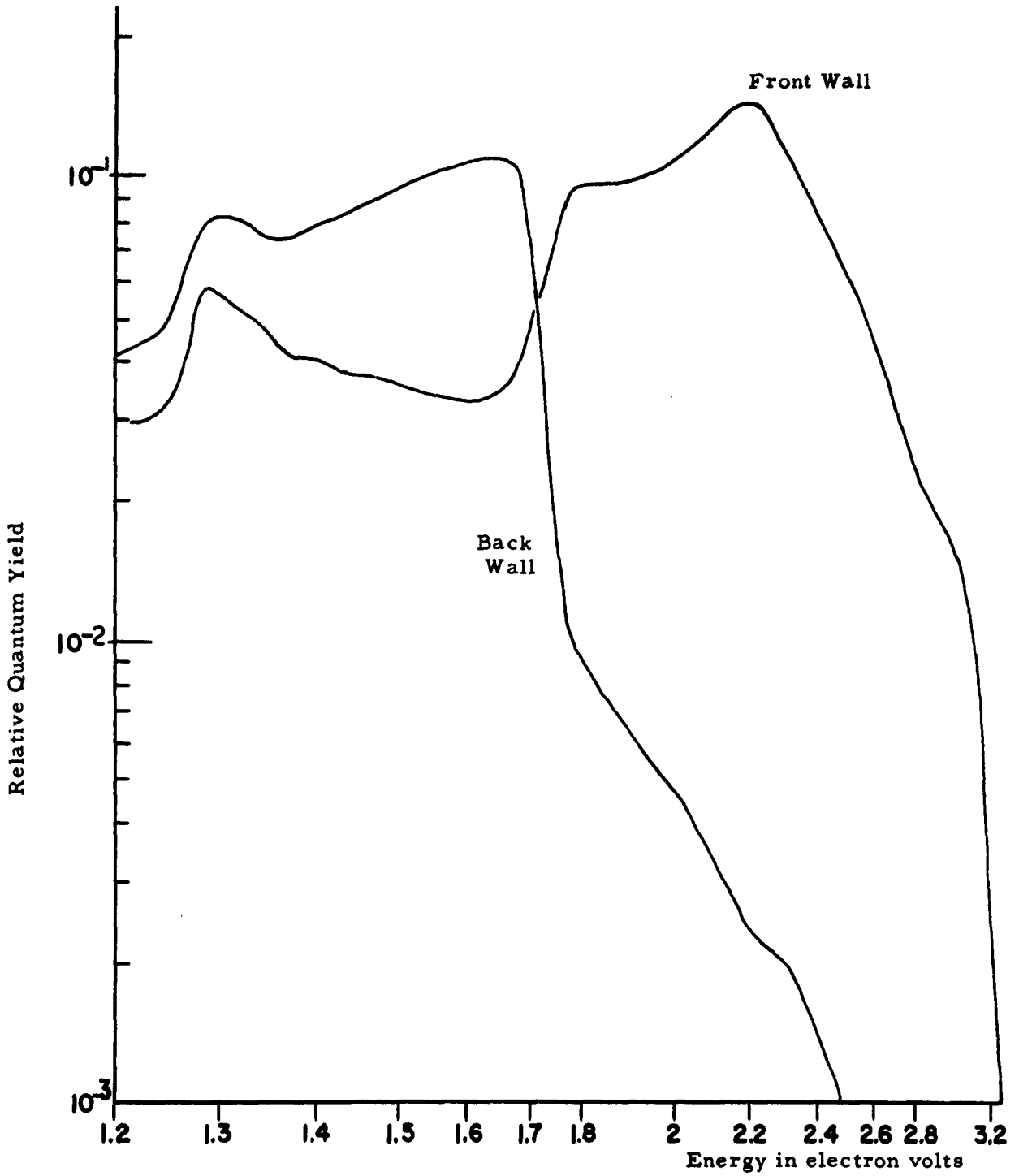

FIGURE 13
Relative Quantum Yield of a CdSe Cell

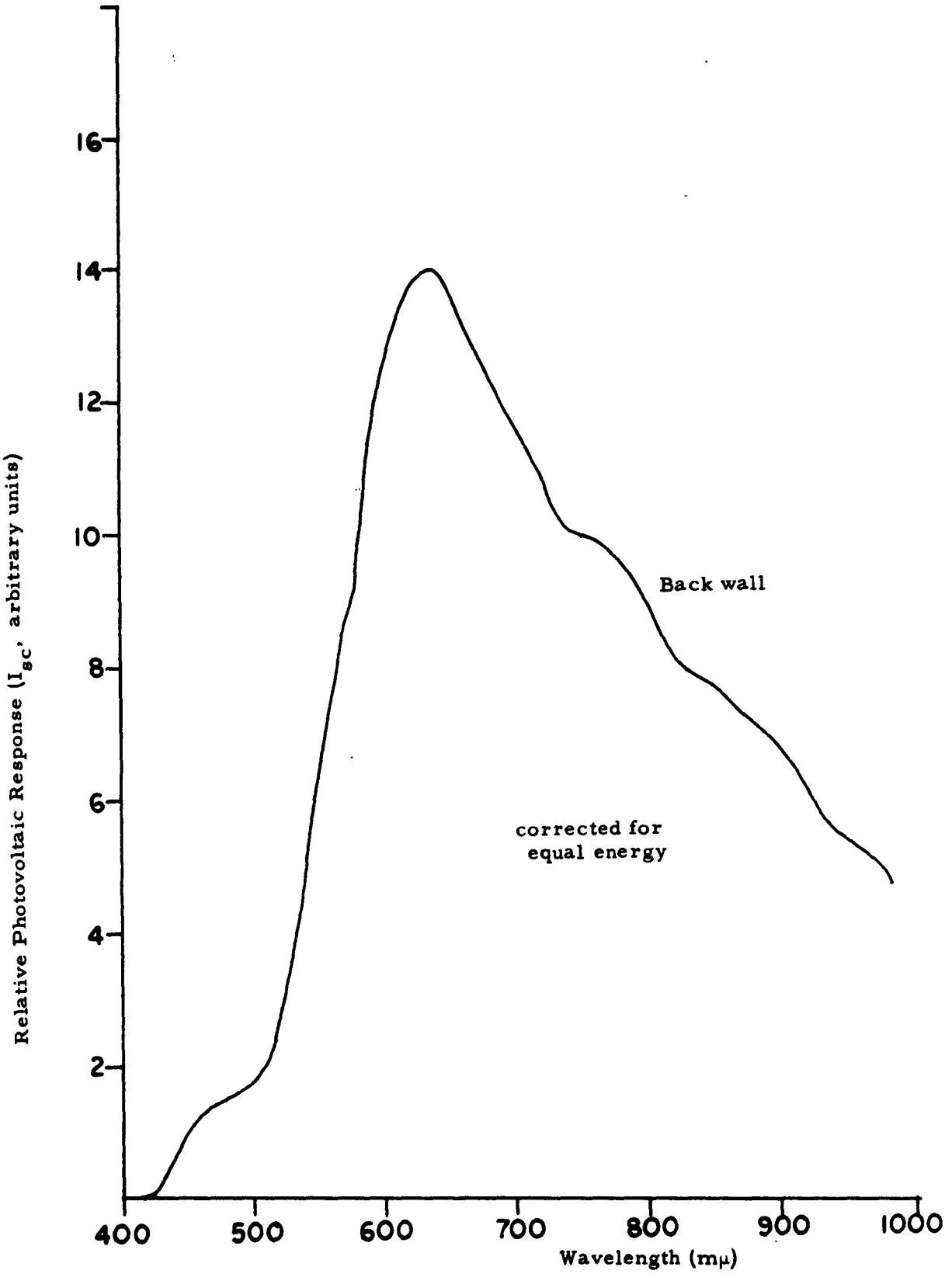

FIGURE 14
Spectral Response of a Cu_xS_y-Cd(S, Se) Cell

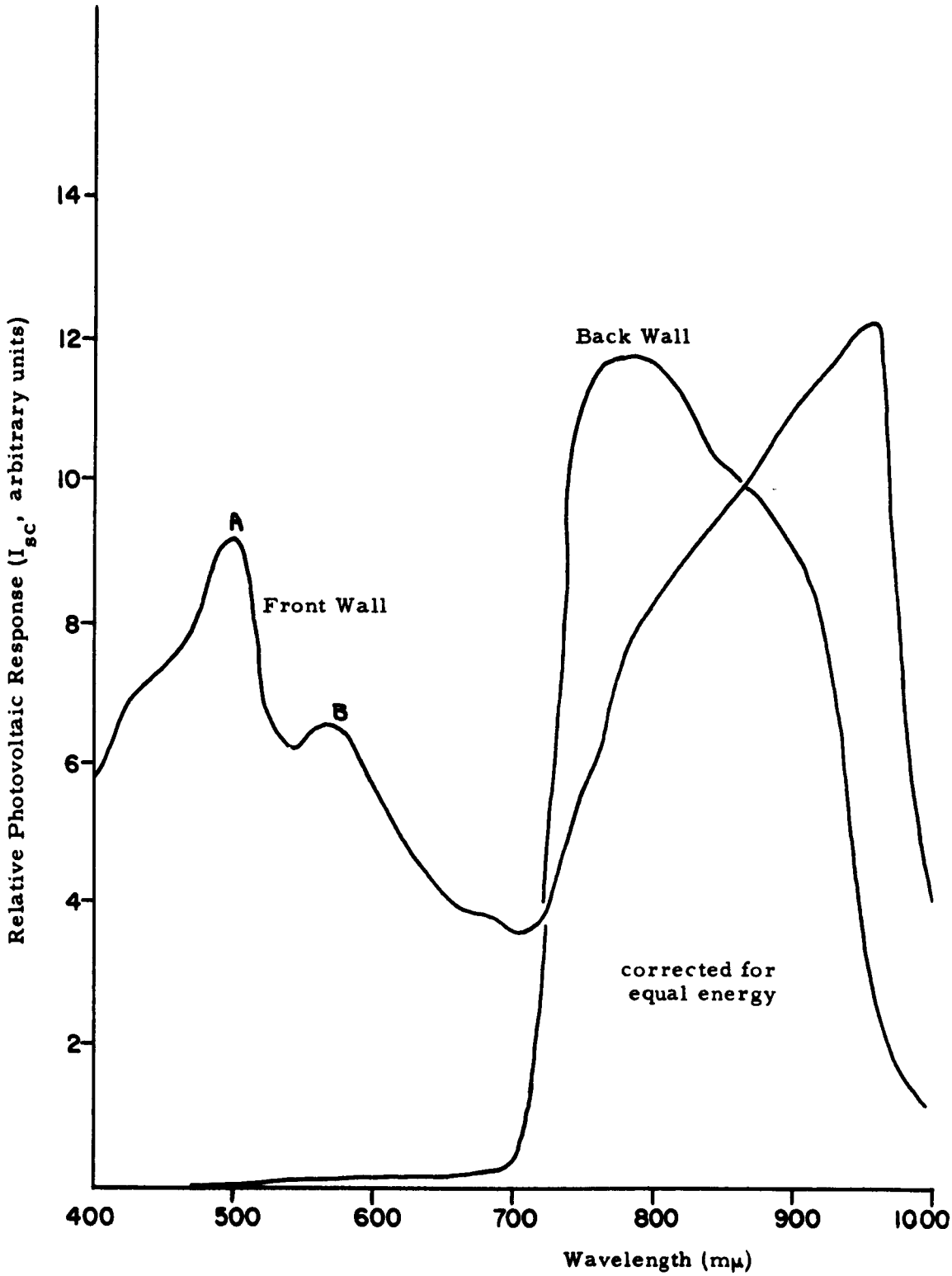

FIGURE 15
Spectral Response of a Multiple Layer CdS-CdSe Cell

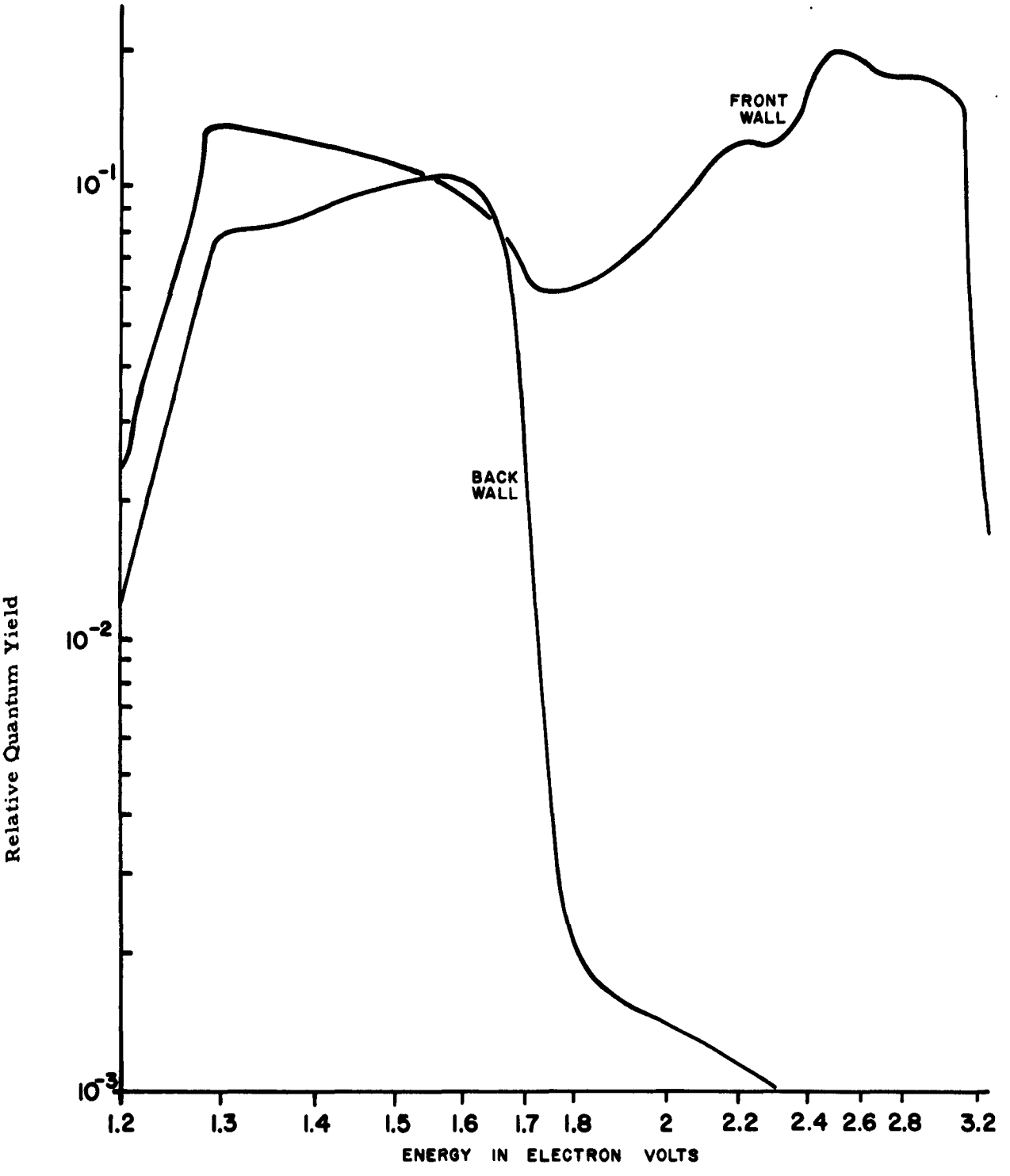

FIGURE 16
Relative Quantum Yield of a Multiple Layer CdS-CdSe Cell

4. Barrier Type Determination

As stated in a previous sub-section, photovoltaic cells have been fabricated using two separate films, one n-type such as CdS and one p-type such as Cu_xS_y. These films are separately deposited and the junction or barrier is formed by a short (15 minutes at 300° C) heat treatment.

The junction or barrier region, as formed in CdS photovoltaic cells made by other organizations, is the result of heat treating a CdS film in physical contact with the metallic copper. Vacuum and slurry deposition of Cu_2S have been done previously [1] with very limited success. However, the identification of a distinct heterojunction between CdS and Cu_2S was not shown. This identification is now possible with the cells which have been made using films of CdS and Cu_xS_y. Figure 15 shows in part the front wall mode spectral response of a photovoltaic cell using a silver paint grid as the top electrode. The peaks which are marked as A and B match those which would be due to materials with absorption edges of .52 μ and .58 μ (See Figure 17). These values match the optical characteristics of CdS and Cu_xS_y respectively. The response on the long wavelength side of 700 mμ is due to the CdSe layer of this photovoltaic cell. The apparent peak at 960 mμ has not yet been adequately accounted for.

It should be noted that the proposed junction is due to the heat treatment of a layer of CdS and a physically continuous layer of Cu_xS_y, and not due to any deposition and/or diffusion of metallic copper. As shown in Section IV, vacuum deposited copper as an electrode is used only from the convenience standpoint and not as a source of copper. Figure 4 gives further support to the fact that the metallic electrode is only acting as a current collector.

Another indication that a distinct heterojunction is being formed between n and p-type films is the spectral response which is obtained with a Cu_xS_y-CdSe photovoltaic cell. This spectral response is shown in Figure 12; as can be seen, a very distinct peak is present at about 580 mμ and when the cell is irradiated in the front wall mode. There can be little doubt that this peak at 580 mμ is due to the Cu_xS_y layer and not due to some "unusual" doping of the CdSe layer.

It can be shown that no gross change occurs in the surface of the Cu_xS_y film during heat treat, and that an etch of dilute KCN or a mild abrasion which apparently removes only the Cu_xS_y film does remove all evidence of photovoltaic response.

There are many other compounds in addition to copper sulfide which have been shown as p-type [7] and could conceivably be used to form a photovoltaic converter with an n-type film such as CdS. Examples would be silver sulfide and copper selenide. These materials deposited as thin films, together with films of copper sulfide, have been shown to be p-type using the thermoelectric probe technique [8].

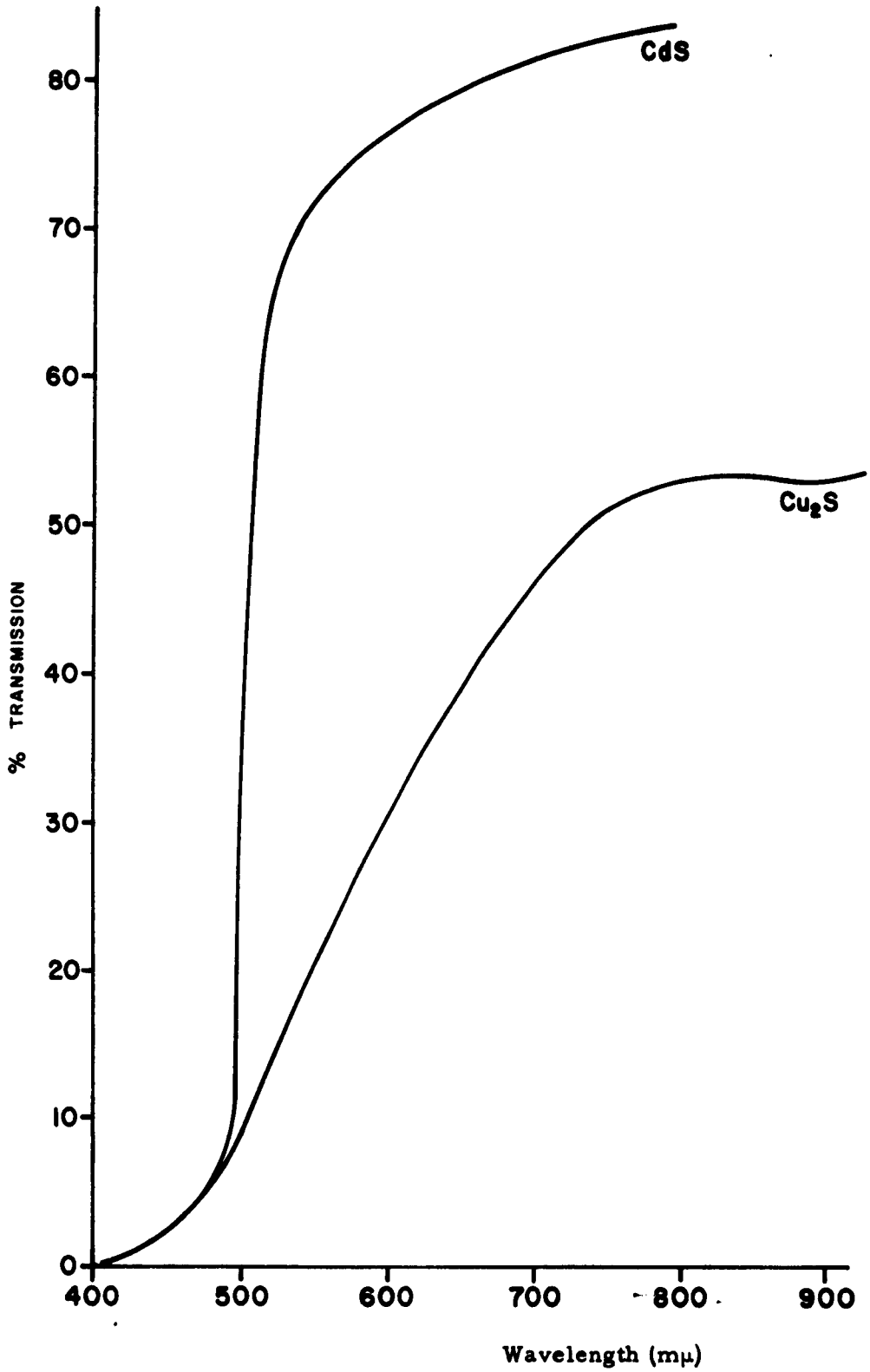

FIGURE 17
Optical Transmission of CdS and Cu_2S

Figure 18 is the spectral response of a photovoltaic cell formed using CdS and Ag_xS_y. Of note here is the peak at about 530 mμ which corresponds to the absorption edge of silver sulfide. Figure 19 is the spectral response of a photovoltaic cell using Cu_xSe_y as the p-type layer and a solid solution of CdS and CdSe as the n-type layer.

These combinations by no means exhaust the list of p and n-type film combinations which might be combined and used to make an efficient photovoltaic converter. Each combination, however, would probably require a separate research effort to produce a cell which has an efficiency of greater than 1.0%.

SUMMARY AND CONCLUSIONS ON PHOTOVOLTAIC MATERIALS

The chemical spray process is suitable for the fabrication of very thin film CdS photovoltaic converters. These thin film cells show characteristics similar to CdS cells which are made by vacuum deposition.

A distinct heterojunction between the n-type CdS layer and a p-type Cu_xS_y layer has been proposed.

Several new (CdSe, Cd(S, Se) and CdS-CdSe) thin film photovoltaic converters have been fabricated and their spectral responses measured.

These new thin film converters together with the demonstration of the barrier formation using such p-type films as Ag_2S and Cu_xSe_y open a wide field for further investigation.

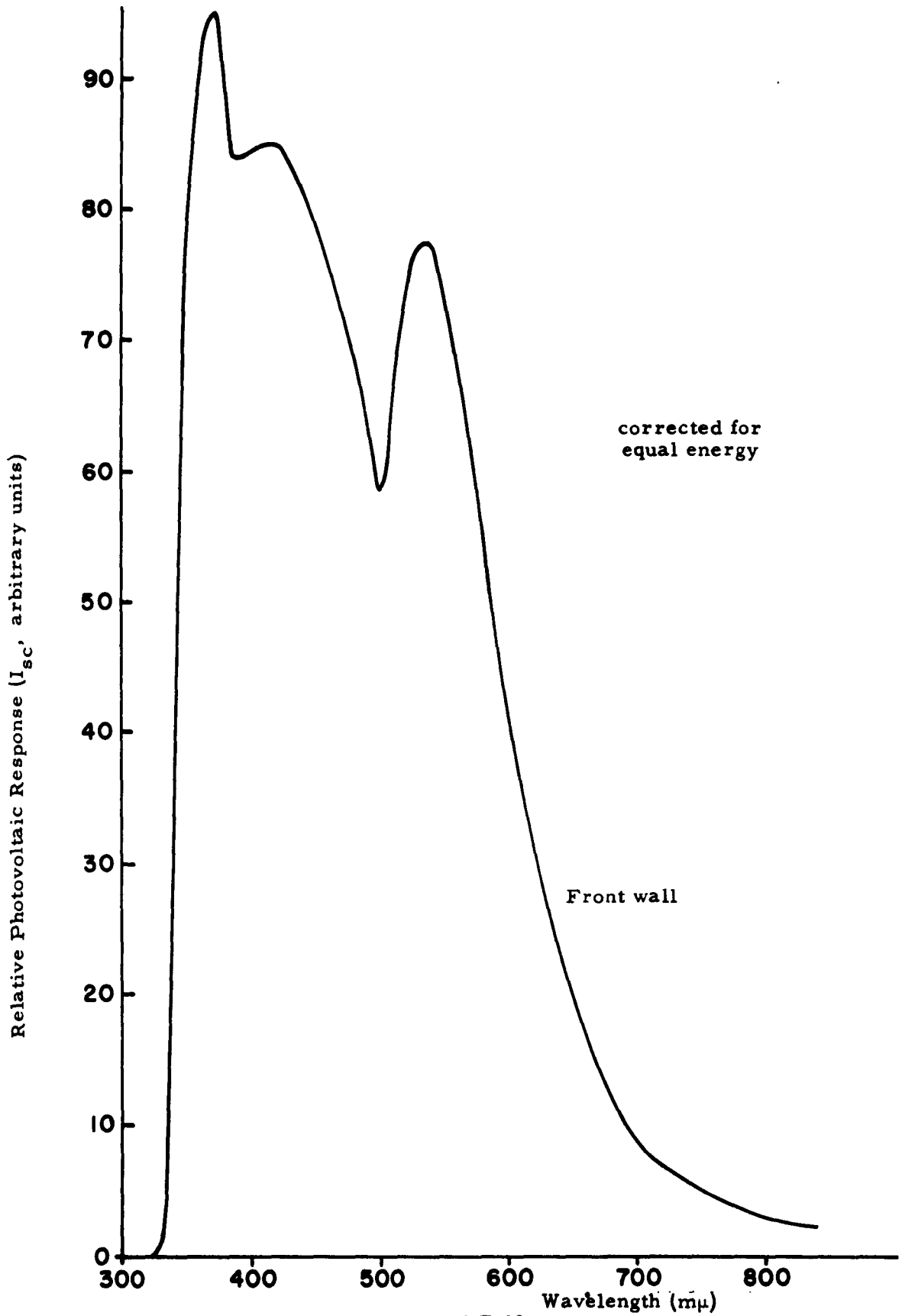

FIGURE 18
Spectral Response of a CdS-Ag_xS_y Cell

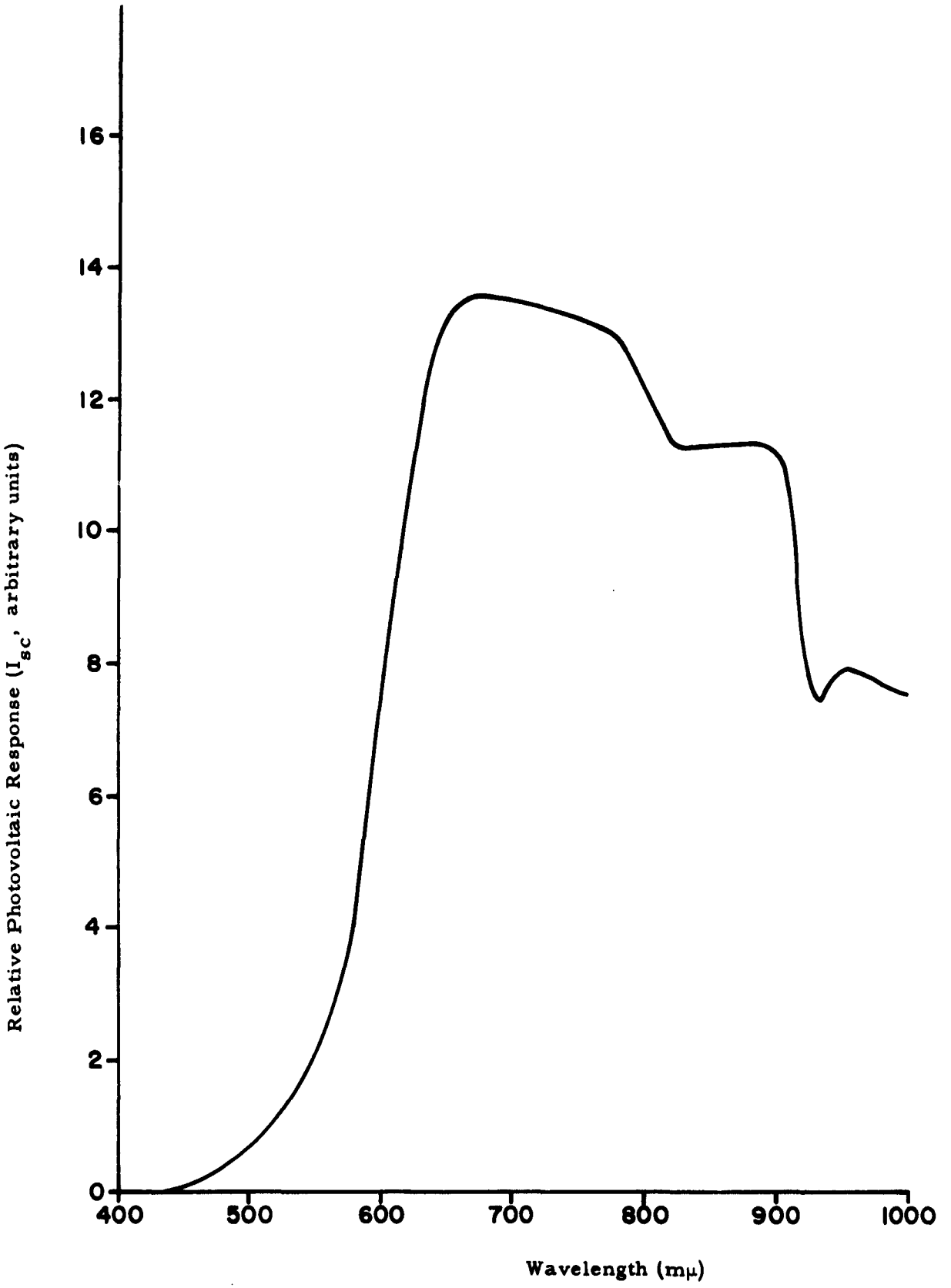

FIGURE 19
Spectral Response of a Cd(S, Se) -Cu_2S Cell

II. FILM STUDIES

INTRODUCTION

Hexagonal cadmium sulfide, the mineral greenockite, has the crystallographic space group symmetry of $P6_3mc$. To one not familiar with this notation, and yet interested in stimulated response, the important significance is that one end of the c crystallographic axis is not like the other end. This is exemplified by the external morphology of the crystal where the terminations at each end are different, as in the Figure below. The axis is said to be heteropolar.

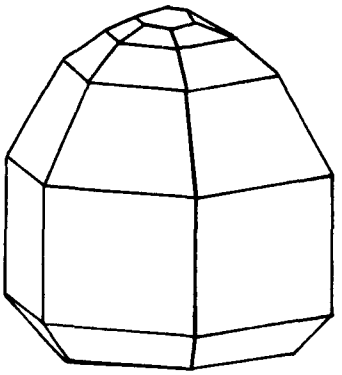

FIGURE 20

Hexagonal Crystal Model

The heteropolar nature of the c axis gives rise to piezoelectricity when stress is applied parallel to this axis and to pyroelectricity when the crystal is heated and the potential is measured along this axis. These stimulated electric responses are definitely dependent on the orientation of the crystal with respect to the stimulating action.

Although the investigation at hand does not include single crystals, per se, but thin films of polycrystalline aggregates, the gross orientation of these films, theoretically, will have a definite effect on the induced stimulated response. Also having an effect on the response will be the "degree of crystallinity" of the thin films. The response phenomenon being due to the heteropolar structure of the cadmium sulfide, the thin films must be fairly crystalline to make this phenomenon possible.

Determination of the orientation and crystallinity of cadmium sulfide films is the objective of the x-ray diffraction phase of this project. The x-ray studies are primarily comparative in nature and do not include absolute measurements. Correlation with the response data is not attempted in this section, but is to be found in Section IV of this report.

TECHNICAL DISCUSSION

1. Crystalline Orientation Study Techniques

The x-ray diffraction data obtained from thin film cadmium sulfide deposited on glass tends to classify the deposits into one of four categories, (1) amorphous to x-radiation, (2) random, little or no orientation, (3) oriented parallel to $(10\bar{1}1)$, and (4) oriented parallel to (0002). The latter orientation, (0002), is the most prevalent, and, by our findings, results in the best cell when all other experimental parameters are equal.

Pole figures of three samples were made to obtain semi-quantitative data about the nature of the thin films with respect to the substrates. Figures 21 , 22 and 23 are diffractograms of the three samples and represent diffraction only from those crystallographic planes parallel to the substrate. The samples differ markedly in intensity of diffraction for the three planes, $(10\bar{1}0)$, (0002), and $(10\bar{1}1)$. This suggests that a difference in primary orientation exists.

Figure 24 is the resulting pole figure for the (0002) plane of sample PH 720 (Figure 21). The pole diagram indicates that most of the normals to the (0002) planes are normal to the substrate. Figure 25 depicts the pole diagram for sample PH 724 (Figure 22) for the planes $(10\bar{1}1)$. This sample has a slight orientation parallel to the $(10\bar{1}1)$, but as can be seen from the broadness of the most intense area, this sample has an almost random orientation with respect to the substrate. This observation is confirmed by the relative intensity data to be found later in the text.

The last two pole figures are of the same sample, PH 723 (Figure 23). In some respects this sample is more interesting, academically, than the preceeding two samples. The figures are less symmetrical than the foregoing, especially Figure 27 , the (0002) planes. Another feature of note is that the strongest intensities of diffraction for each plane are at an angle to the substrate normal. This angle is in the range of 45 to 55° for the (0002) and 10 to 35° for the $(10\bar{1}1)$. The angle between the most intense areas for the (0002) and the $(10\bar{1}1)$ is roughly 60 to 70°, which is in accord with optical goniometric measurements which report the angle between (0002) and $(10\bar{1}1)$ as 61° 54'. [11]

The three samples do have in common one aspect. All show one degree of orientation, a randomness in the plane of the sample, i. e. there is no lineation or apparent direction observed in the plane of the substrate.

FIGURE 21

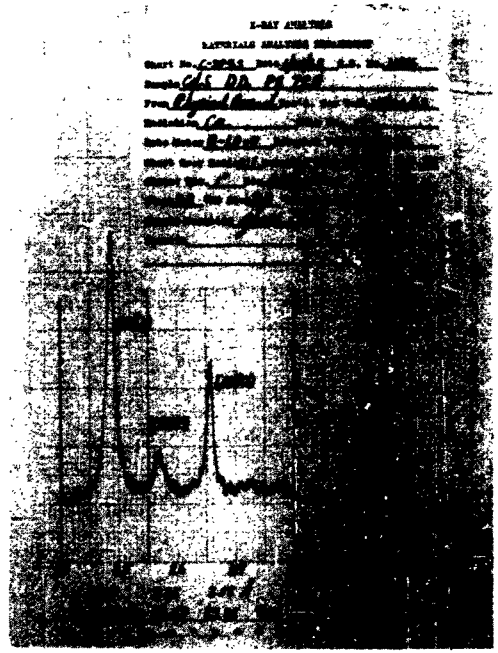

FIGURE 22

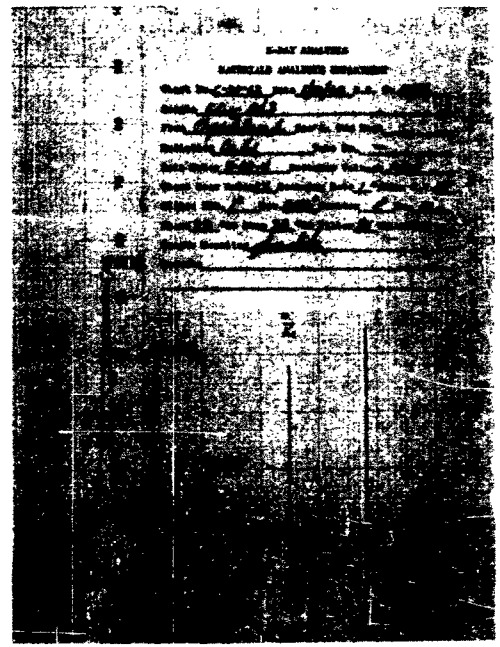

FIGURE 23

X-ray Diffractographs of CdS Films

Sample AA PH-720
CdS (0002)

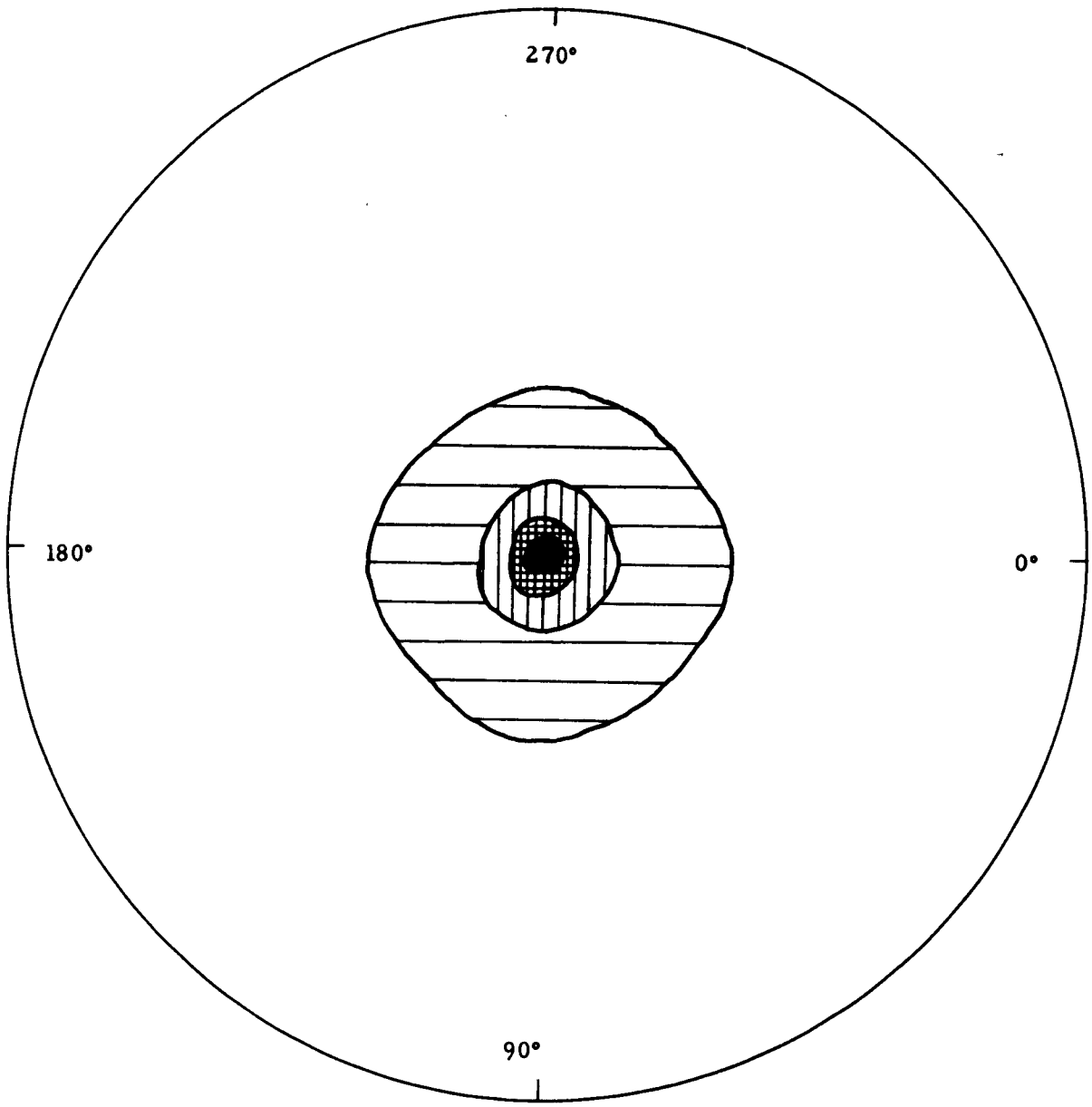

FIGURE 24
Pole Figures of CdS Films

Sample DD_1 PH-724
CdS ($10\bar{1}1$)

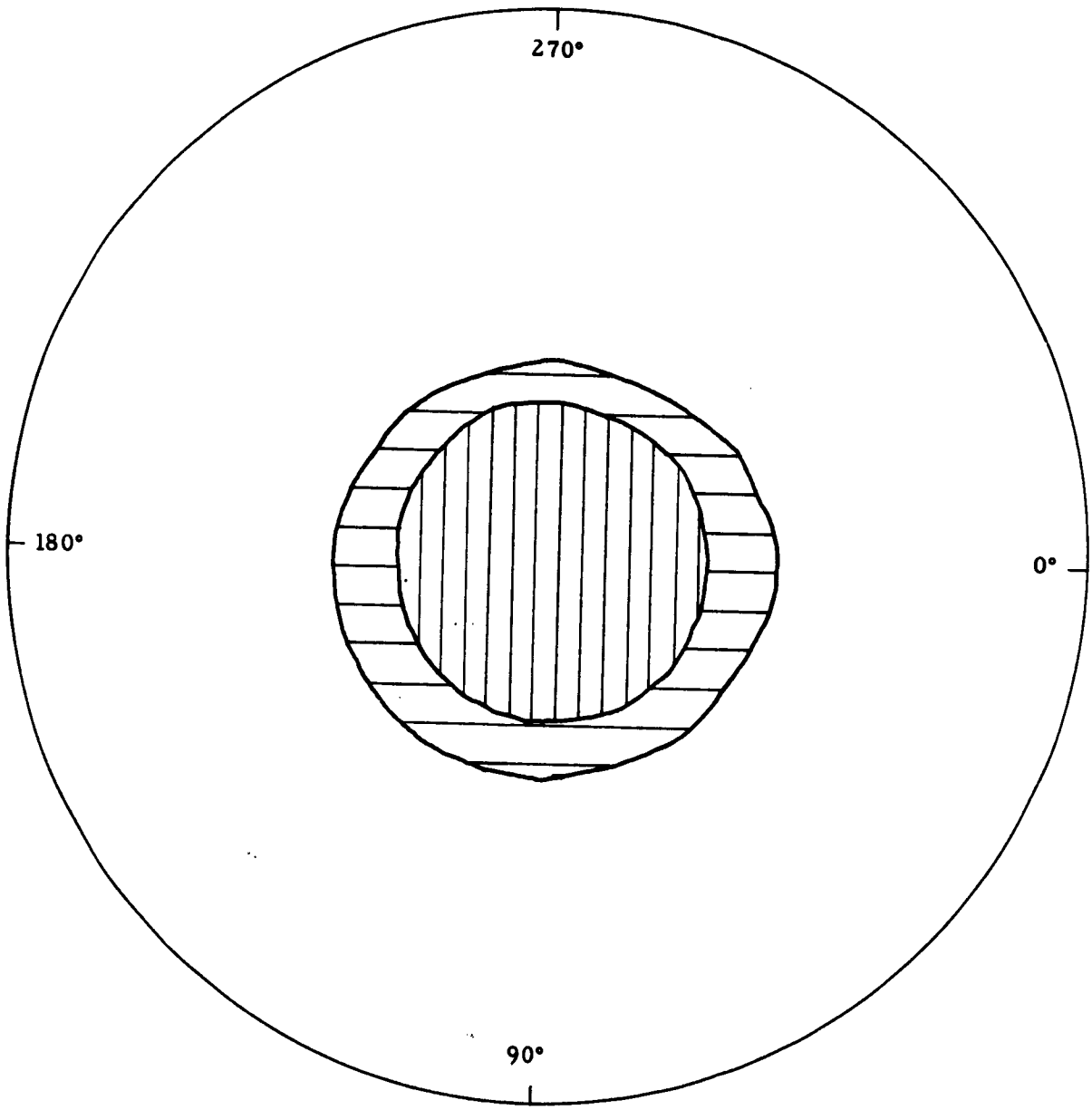

FIGURE 25
Pole Figure of CdS Films

Sample CC_2 PH-723

CdS $(10\bar{1}1)$

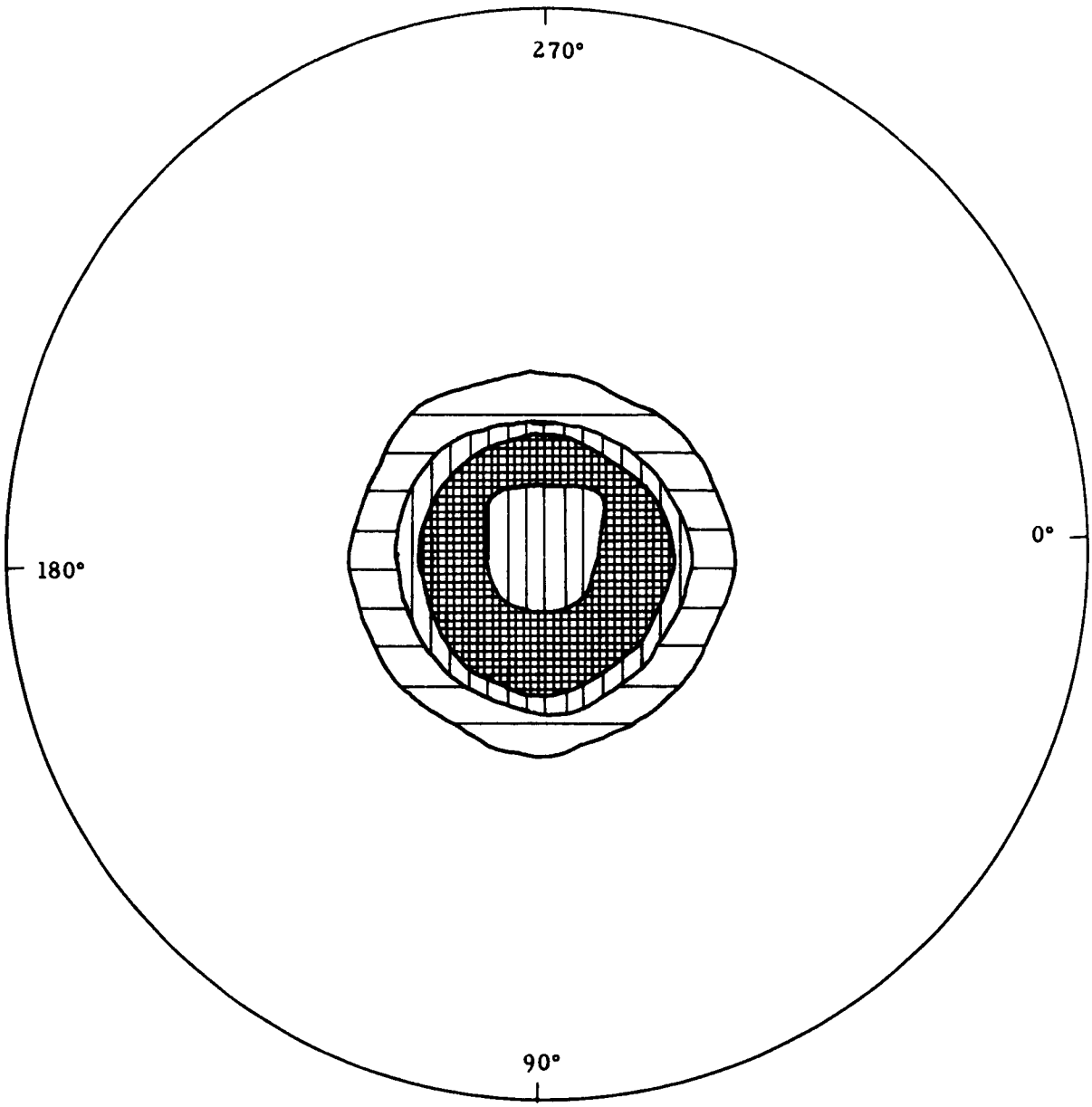

FIGURE 26
Pole Figures of CdS Films

Sample CC_2 PH-723

CdS (0002)

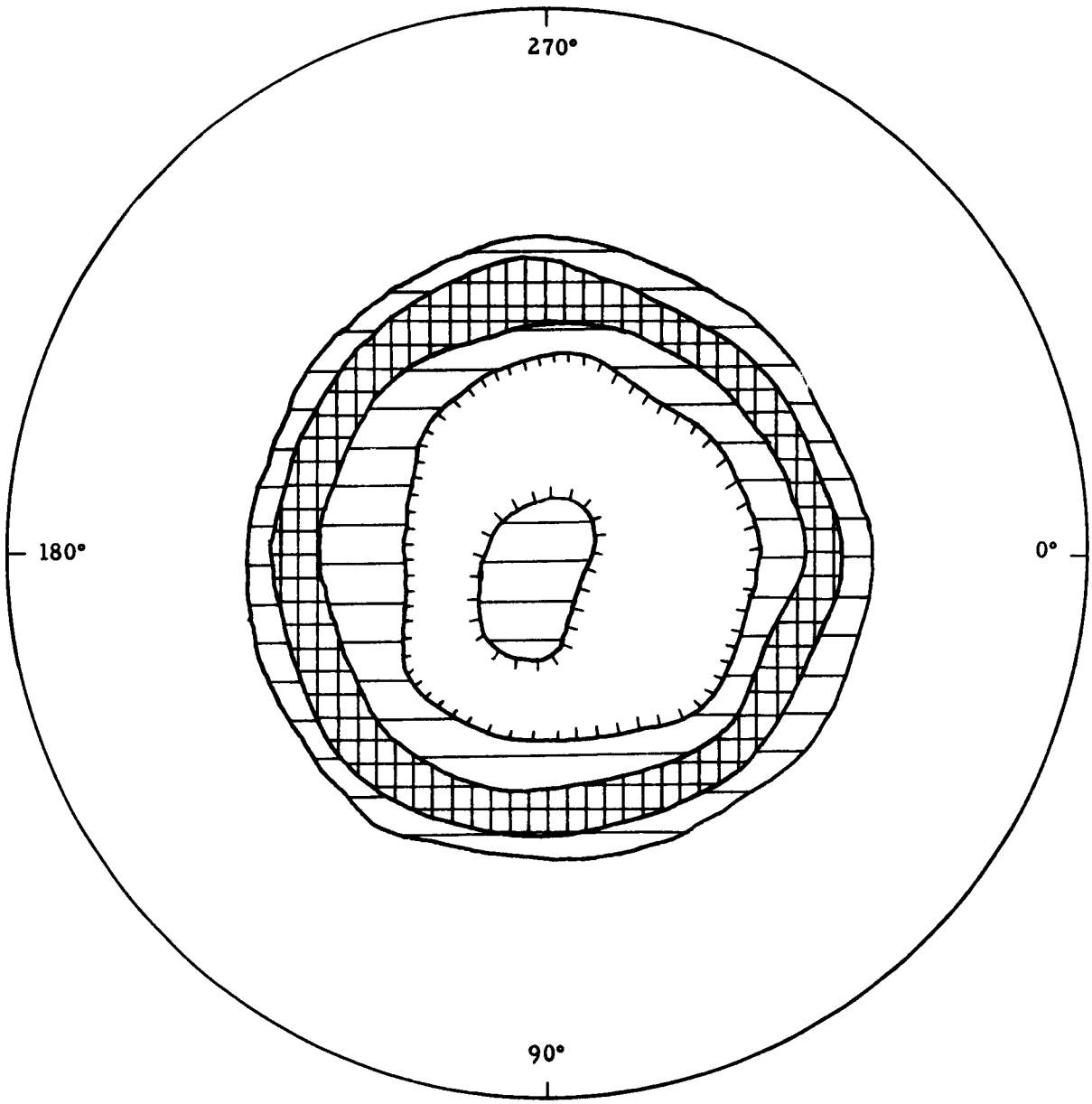

FIGURE 27
Pole Figure of CdS Films

Pole figure determinations are time consuming and cannot be prepared for every sample of interest. A simpler and quicker, although less satisfactory, method for gaining some insight as to the orientation of the thin films is the method of relative intensities. Table 2 gives the relative intensities for two standard diffraction patterns of hexagonal cadmium sulfide and for the three samples above. Listed are the relative intensities for the $(10\bar{1}0)$, (0002) and the $(10\bar{1}1)$ peaks.

TABLE 2

	Standard Random Powder		PH 720	PH 723	PH 724
$(10\bar{1}0)$	75	78*	40	12	38
(0002)	59	45	450	54	16
$(10\bar{1}1)$	100	100	100	100	100

The figures are based on the diffracted intensity of the $(10\bar{1}1)$ plane, which in a random powder specimen of CdS* is the strongest reflection.

Using this method of comparison of relative intensities, it is possible to determine the primary orientation, but nothing about the sample in the plane of the substrate.

For sample PH 724 the intensities of diffraction are in the same order as that of the standard, $(0002) < (10\bar{1}0) < (10\bar{1}1)$. It is to be noted, however, that the (0002) and $(10\bar{1}0)$ are reduced when compared with the standard. The interpretation of this data would be that the sample is almost random in nature, but does have a slight orientation parallel to the $(10\bar{1}1)$. This compares favorably with the interpretation of the pole figure for this specimen. Sample PH 720 shows the (0002) peak intensity to be very strong. Only one interpretation can be accorded to this specimen, that the (0002) plane is oriented parallel to the substrate and has very little angular departure.

The interpretation for sample PH 723 is not as satisfactory as for the two other samples. The data shows a reversal of intensities for the (0002) and $(10\bar{1}0)$ and a slight increase in intensity for the (0002). One would expect a moderate orientation of (0002) for this sample which the pole figure indicates, but one could not ascertain the angular departure of the poles of the (0002) and the $(10\bar{1}1)$ planes for the substrate normal.

* Prepared at The National Cash Register Company and used as the primary standard.

For the interpretation of the relative intensity data, the standard pattern prepared in our own laboratory was used. Our pattern differs slightly in intensities when compared with that prepared at the National Bureau of Standards [12]. A tabulation of intensities for the first twelve peaks is given in Table .

TABLE 3

	N. C. R.	N. B. S.
$(10\bar{1}0)$	78	75
(0002)	45	59
$(10\bar{1}1)$	100	100
$(10\bar{1}2)$	26	25
$(11\bar{2}0)$	44	57
$(10\bar{3}0)$	41	42
$(20\bar{2}0)$	11	17
$(11\bar{2}2)$	31	45
$(20\bar{2}1)$	16	18
(0004)	6	4
$(20\bar{2}2)$	6	7
$(10\bar{1}4)$	2	5

The peak intensities agree essentially except in three instances, the (0002), $(11\bar{2}0)$ and the $(11\bar{2}2)$. These apparent discrepancies may be the result of many factors, such as specimen preparation, disordered sample, machine variations, scanning speed, etc.

For this particular investigation the standard sample prepared in our own laboratories made interpretation of the diffraction data more satisfactory.

2. Effect of Substrates on Orientation and Crystallinity

The question as to the extent of influence a substrate has on the orientation and crystalline nature of a subsequent deposited layer requires an involved investigation of compatibility of structure and unit cell parameters, surface smoothness, surface cleanliness, habit of the deposited layer and different environmental conditions, etc. It is not within the scope of this investigation to answer this general question, but a limited amount of data obtained by x-ray diffraction studies is presented.

Figures 28 and 29 are diffractograms of cadmium sulfide deposited on various substrates. These samples were processed at the same

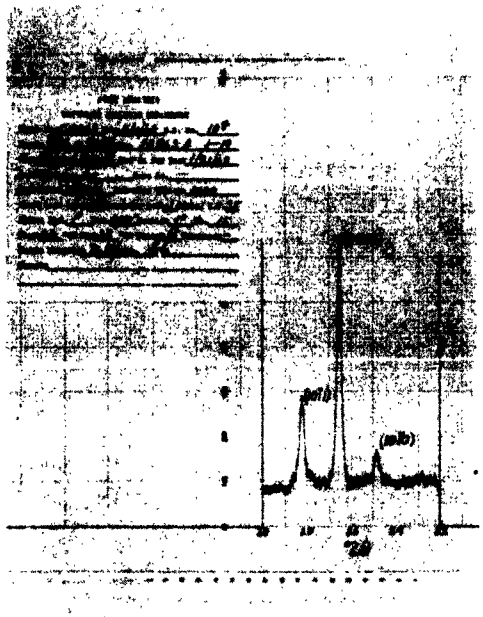

FIGURE 28a

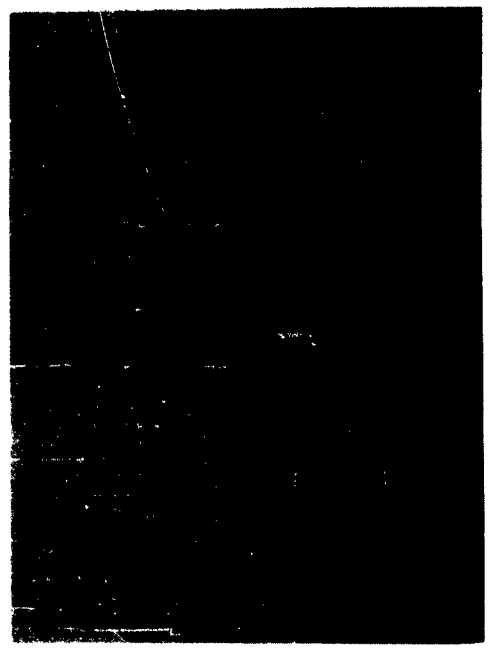

FIGURE 28b

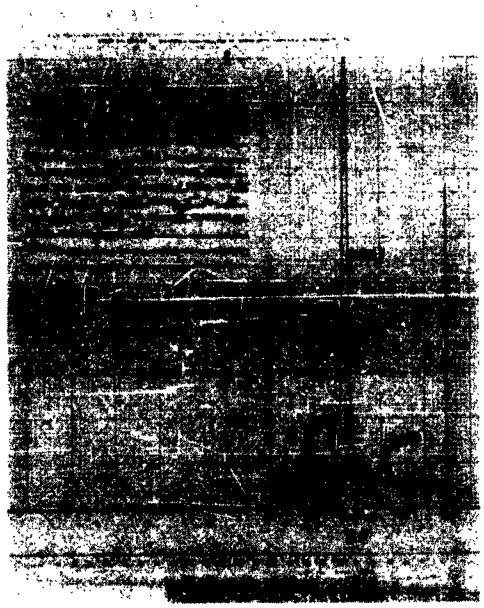

FIGURE 28c

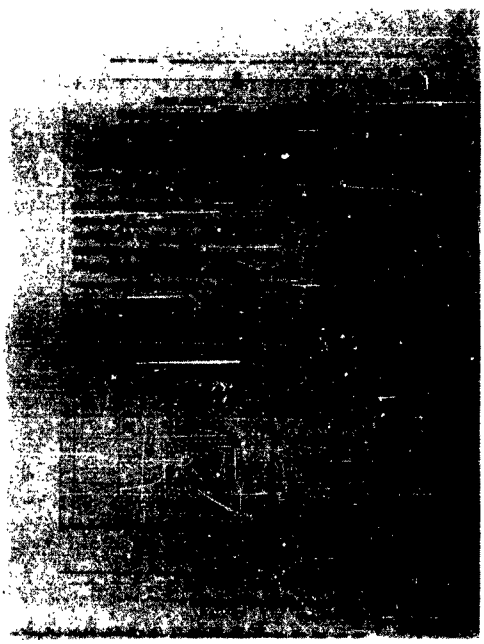

FIGURE 28d

X-ray Diffractographs of CdS Films

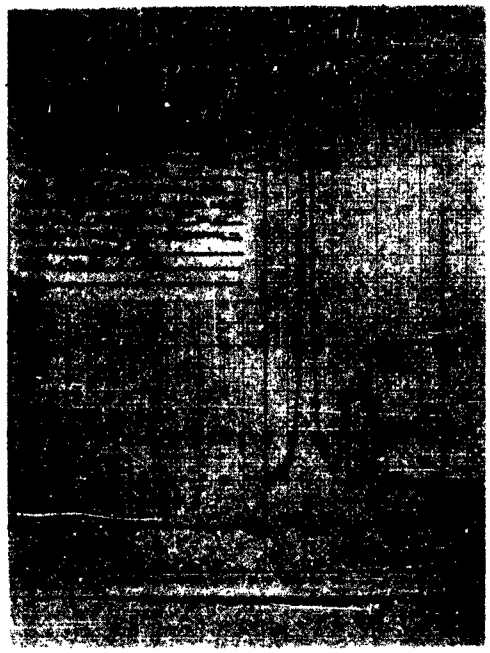

FIGURE 28e

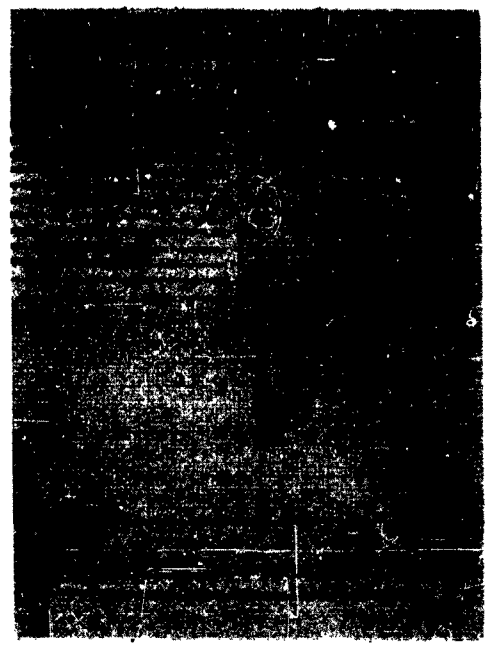

FIGURE 28f

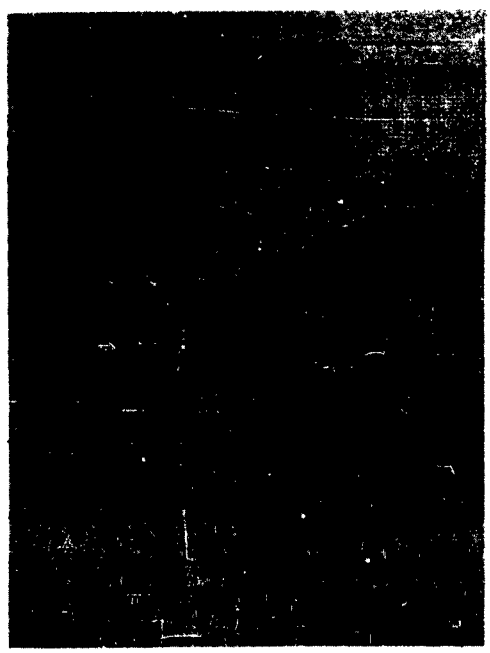

FIGURE 28g

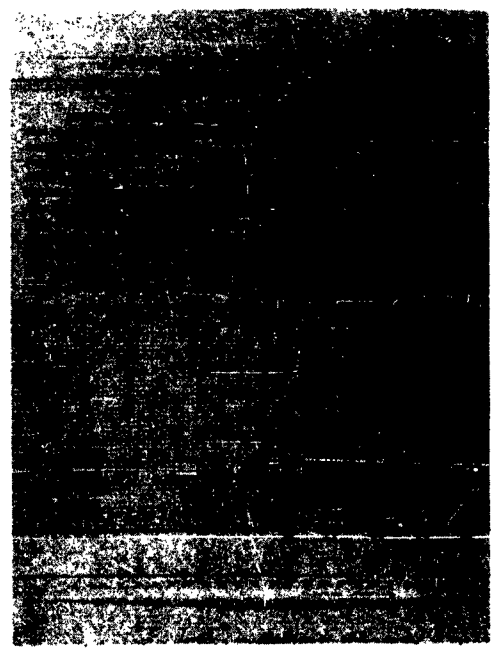

FIGURE 28h

X-ray Diffractographs of CdS Films

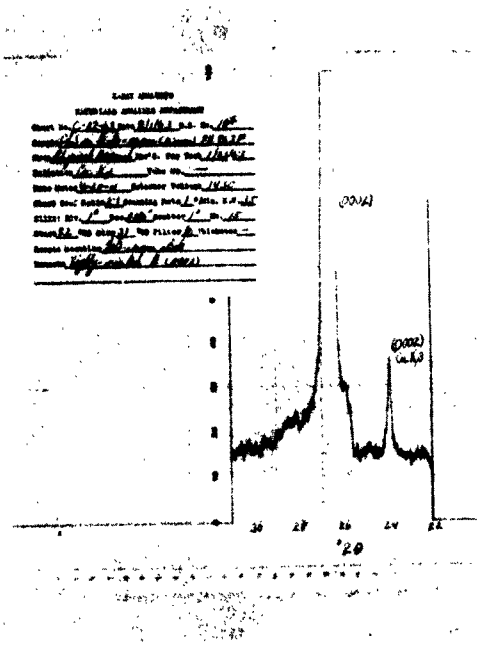

FIGURE 28i

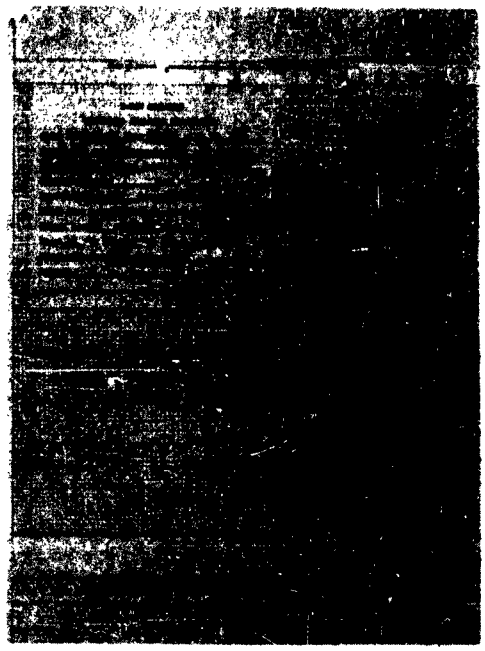

FIGURE 28j

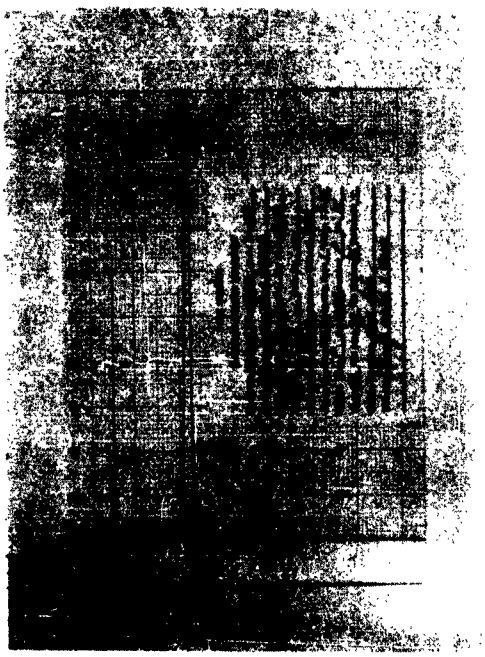

FIGURE 29a

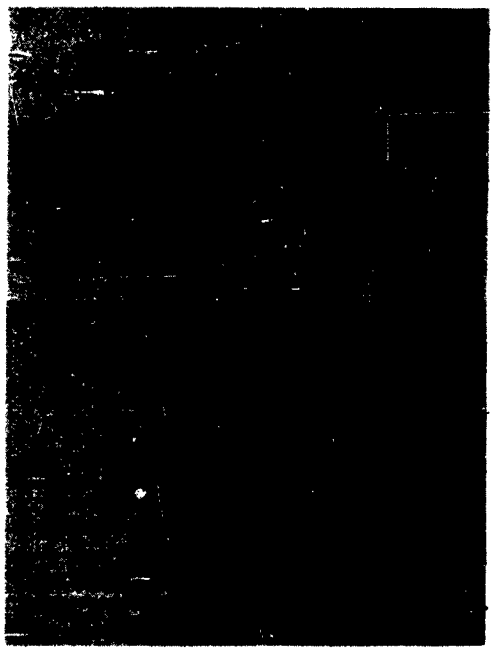

FIGURE 29b

X-ray Diffractographs of CdS Films

time and under like experimental conditions. The diffractograms marked group "A" were prepared using the same x-ray unit conditions. The group "A" charts can be compared directly as to intensities of diffraction and apparent orientation. Group "B" charts are diffractograms of the more intense patterns (above) at approximately 1/64 of the above amplifications. These particular samples are very strongly oriented and have good crystallinity. Table 4 summarizes the data obtained for both groups.

The x-ray patterns of the thin films on metallic and non-metallic substrates lead one to some very interesting results and speculations:

1. CdS sprayed onto pyrex glass, a vitreous non-crystalline substrate, produces a very crystalline and highly oriented layer. This sample also gives the highest diffraction intensity noted to date.

2. CdS sprayed onto molybdenum, a very crystalline and oriented substrate, produces a layer amorphous to x-radiation.

3. CdS sprayed onto a molybdenum substrate precoated with a non-crystalline CdS layer, produces a crystalline layer of CdS.

4. CdS sprayed onto various substrates which are composed of mixtures of crystalline and vitreous materials produces layers having various orientations and diffraction intensities. The specific substrates involved were tite white on univit, Foto ceram, Foto form, Pyroceram, and Multiform.

5. CdS sprayed onto Diamonite (crystalline) produces a poorly crystallized layer of low diffraction intensity.

6. SnO_x may have influenced the orientation of CdS on tite white on univit. The sample having no SnO_x is oriented parallel to the $(10\bar{1}1)$, the sample having the SnO_x is oriented parallel to the (0002).

The observed data is limited in scope and does not lead to any definite conclusions, but does point out an area of investigation that should be explored for chemically sprayed deposits.

The photovoltaic structures fabricated and tested to date have used tin oxide coated pyrex plate glass as a substrate. Although very thin glass is available and could be used to increase a watts per pound ratio, it does not lend itself for use in any reasonable type of flexible array. Since the physical characteristics (brittleness and inflexibility) limit the application of front wall (or even back wall cells) which are made with a glass substrate, a search was started to find a metal which can be obtained in foil form that would be

TABLE 4

Substrate	Primary Orientation	Comparative Intensity
Multiform[1]	(0002)	low
"Black glass"[2] coated steel	(0002)	high
SnO_x coated Tite[3] white on Univit[4]	(0002)	medium
Pyrex[5] glass	(0002)	extremely high
"Brown" Foto Ceram[6]	(0002)	very high
Tite white on Univit	$(10\bar{1}1)$	very high
Pyroceram[7]	(0002)	very high
Diamonite[8]	$(0002)>(10\bar{1}1)>(10\bar{1}0)$	very low, almost amorphous
Foto Form[9]	$(0002)>(10\bar{1}1)$	high
"White" Foto Ceram	$(0002)>(10\bar{1}1)$	high

1, 5, 6, 7, 9	Trade marks of Corning Glass Company
2, 3	Trade names of O. Hommel Company
4	Trade name of Armco Steel Company
8	Trade name of Diamonite Corporation

Crystallite Orientations and X-ray Diffraction Intensities of CdS Films Deposited on Various Substrates

compatible with the chemical spray technique. This film deposition process puts greater restrictions on the physical characteristics of the substrate than does a process such as vacuum evaporation. Table 5 below, together with the notes, gives a summary of the results which were initially obtained with various metal foils.

TABLE 5

Metal	Film Sprayed	Deposited	V_{oc}	Crystallinity	Comments
Al	CdS	CdS	0	poor	Note 1
Mo	CdS	CdS	.4 V	"	Note 2
W	CdS	CdS	0	"	Note 3
Ta	CdS	CdS	0	"	Note 4
Pt	CdS	CdS + PtS	0	"	Note 5
PbSn	CdS	CdS	.44 V	fair	Note 6
Cu	CdS	Cu_2S	0	Note 7	Note 7
Cd	CdS	CdS	0	poor	Note 8
Mo	CdSe	- -	0	Note 9	Note 9
W	CdSe	WO_3	0	poor	Note 10

NOTES:

1. X-ray examination indicated random orientation of the crystallinity of CdS. The aluminum oxide on the aluminum foil apparently prevents electrical contact by the CdS (as evidenced by a vertical resistance in the megohm range).

2. Only currents in the microampere range were detected in cells made of CdS on Mo.

3. Very low (2-10 ohms) vertical resistance with no evidence of rectification at the CdS-W interface.

4. Very low (2-10 ohms) vertical resistance with no evidence of rectification at the CdS-Ta interface.

5. This experiment was particularly interesting in that a sufficient reaction took place with the foil, so that platinum sulfide was formed and with sufficient thickness and crystallinity to be detected by x-ray. Figure 30 shows a copy of the x-ray goniometer tracing.

6. A lead-tin alloy gave the best results, with cells which were in the 0.1% efficiency range. A low melting point placed a severe

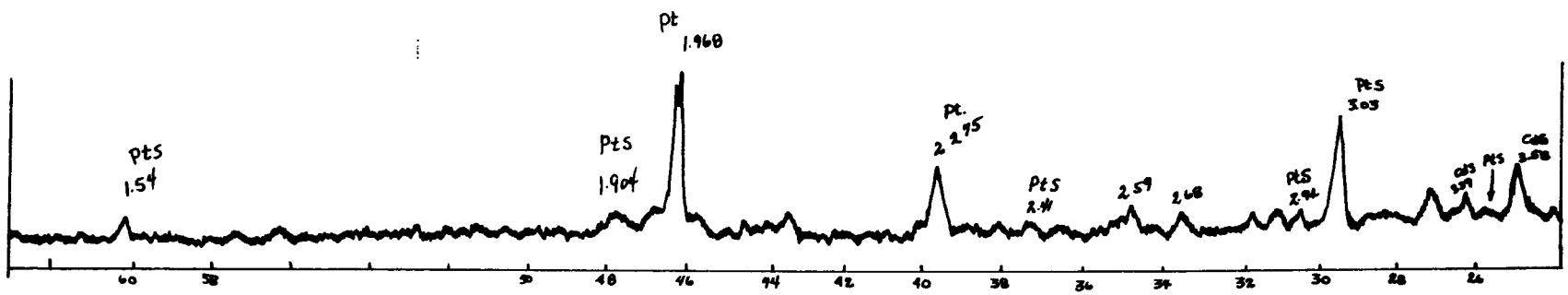

FIGURE 30
X-ray Diffractograph of a CdS Film on Pt Foil

limitation on the crystallinity which could be obtained while depositing the CdS film and also on any post heat treatment that could be done.

7. The copper oxide which was formed was quite thick (0.5 microns) but was amorphous to the x-ray goniometer; an x-ray powder camera run was necessary to identify the copper oxide and determine that no cadmium sulfide could be detected.

8. Cadmium was plated on copper and this combination yielded a CdS film with good optical appearance; x-ray examination showed it to be almost amorphous. No response was obtained regardless of post treatment.

9. X-ray examination of films deposited on Mo, where CdSe was the intended film, showed only that the film was amorphous to x-rays and thus not identified. No photovoltaic response was ever obtained.

10. Here we have another situation like CdS on Cu which as yet cannot be explained. The formation of an oxide during or just at the start of a deposition (here of CdS or CdSe) by the chemical spray process is in part understandable, but unexplainable is the lack of intended film at the end of the deposition time.

Figure 31 shows the diffractogram of a film of CdS on a lead-tin alloy. All other films of CdS deposited on other metals, during these first attempts to use metal as a substrate, were amorphous to x-ray examination.

Late in this first phase of the contract x-ray studies indicated that an amorphous film predeposited at a low temperature on a metal foil such as Mo might prevent any unwanted reaction with the substrate and provide an ideal base for a crystalline layer of CdS deposited at a high temperature. This system has been tried and Figure 32 shows the diffractogram of the result. As can be seen good crystallinity was obtained. The photovoltaic response of these first crystalline films on Mo indicates that at least the problems of CdS deposition on metal are solved.

3. Effect of Doping, Deposition Parameters and Heat Treatment

a. Doping

Table 6 gives a tabulation of the effect of the impurity upon the crystal orientation in the CdS film. It can be seen that a "doping" level of 10,000 ppm of gallium was needed before any effect was detected. In contrast only 10 ppm of indium caused a change in the preferred orientation, normally, an (0002) orientation is expected in a film of CdS which is deposited on an uncoated hard glass substrate. If one considers the atomic radii of the indium and gallium atoms in light of the effect of their addition on the orientation of a CdS film, it appears reasonable to suggest that the indium goes substitutionally into the CdS lattice and the gallium goes in interstitially. The electrical characteristics of these films are covered in Section IV.

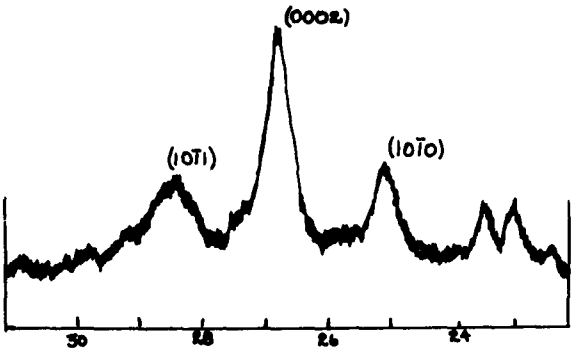

FIGURE 31
X-ray Diffractograph of a CdS Film on Pb-Sn Foil

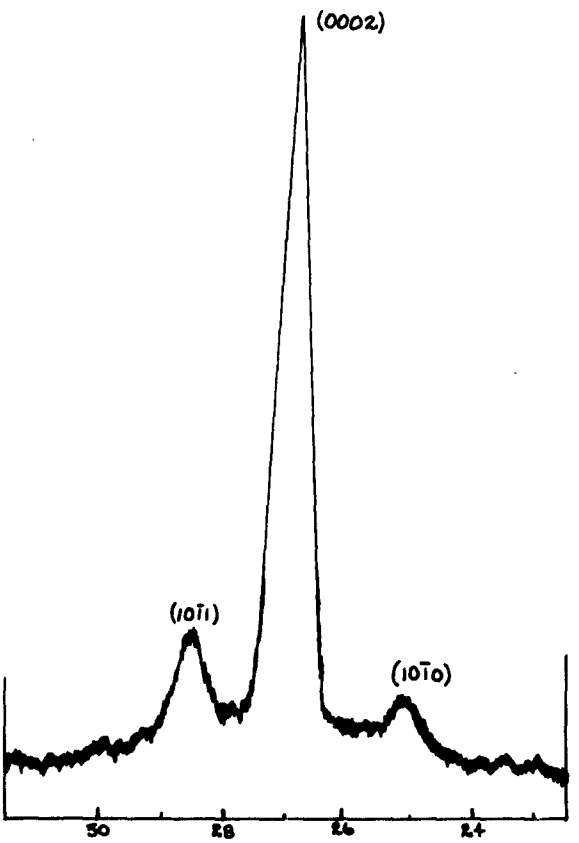

FIGURE 32
X-ray Diffractograph of a CdS Film on Mo Foil

TABLE 6a

Ga ppm	Orientation	Comments
10	(0002)	
100	(0002)	
1000	(0002)	Some other small diffraction peaks observed
10 K	(0002)	Some other small diffraction peaks observed

An increase of diffraction intensity is observed on addition of $GaCl_3$ from 10 ppm to 10 K with the 10 K ppm giving the greatest diffraction intensity.

Effect of impurity concentrations on the crystal orientation of thin CdS films deposited on glass.

TABLE 6b

In ppm	Orientation	Relative Intensities	
10	(0002) >> $(11\bar{2}2)$ > $(10\bar{1}1)$	Good	3
100	(0002) >> $(11\bar{2}2)$ > $(10\bar{1}1)$	Good	2
1000	$(11\bar{2}2)$ > (0002) > $(10\bar{1}1)$	Reduced	4
10 K	(0002) >> $(11\bar{2}2)$ > $(10\bar{1}1)$	Good	1

Effect of impurity concentrations on the crystal orientation of thin CdS films deposited on glass.

Examinations were conducted using x-ray fluorescence equipment to determine if the impurity concentration used in the starting materials was in fact included in the same relative concentration in the deposited film. It was determined by these examinations that indium did not appear in the film as far as x-ray fluorescence was concerned until a concentration of 100,000 ppm was used even though x-ray diffraction showed an effect with just 10 ppm of indium. Likewise gallium was not clearly detectable until a concentration of 10,000 ppm was reached. (It had not been intended that "doping" levels of 100,000 ppm be used but films with these concentrations were made when x-ray fluorescence was unable to detect the lower concentrations.) Table 7 gives the results of x-ray diffraction examination of doped CdS films which were deposited on SnO_x coated pyrex plate glass. The modification in the crystal orientation of the CdS film due to the SnO_x is different depending upon whether an additional modifier such as indium is also present.

b. Deposition Parameters

Figures 33 through 41 show the x-ray goniometer tracings of typical orientations which are possible by varying deposition parameters. Figures 33 through 35 are of thin (.3μ) films which were deposited at successively higher deposition temperatures. Figures 36 through 38 are of films (.7 - .8μ) which were also deposited with temperature as the parameter, with Figure 38 showing the results of the highest temperature. Figures 39 through 41 are the x-ray goniometer tracings of films whose physical (e.g. rate and heat) deposition parameters were the same but for which the ratio of the cadmium to sulfur was changed in the starting material, with Figure 39 showing the result of a stoichiometric mixture, Figure 40 the result of excess sulfur, and Figure 41 the result of excess cadmium in the starting materials. It is not intended that these x-ray goniometer tracings (Figures 39 - 41) be interpreted as any measure of how stoichiometric the resulting film may be.

c. Heat Treatment

Figures 42 and 43 show the x-ray goniometer tracing of two films of almost equal thickness which were heated for equal time (15 minutes at 540° C) and then re-examined by x-ray diffraction. Figures 44 and 45 show the results of this heat treatment. It can be seen (Figure 45) that with this heat treatment a film which has a preferred orientation of (0002) will show a slight increase in its degree of crystallinity with a little sharpening of other orientations, but no appreciable change in their intensity. This result with films which have a high degree of preferred orientation has been true in each case where influence of post treatment on the crystallinity has been examined, even where seeding [3] of the film has been attempted.

When a film starts with less crystallinity and almost random orientation, heat treat has a much more pronounced effect, as can be seen by comparing Figures 42 and 44. Here all three major peaks increase in intensity and in sharpness, with some change in their relative heights.

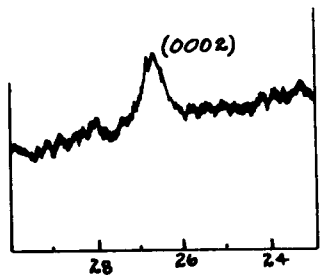

FIGURE 33

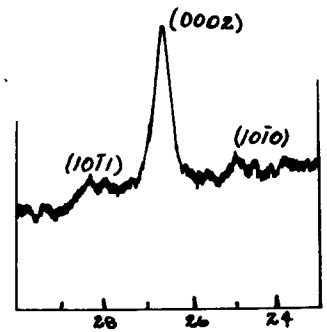

FIGURE 34

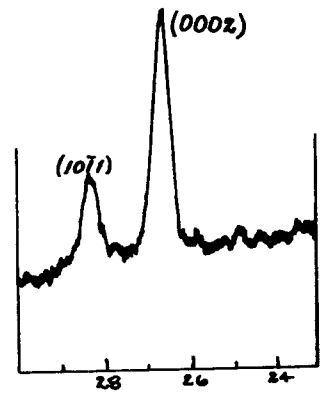

FIGURE 35

X-ray Diffractographs of CdS Films Deposited at Different Temperature

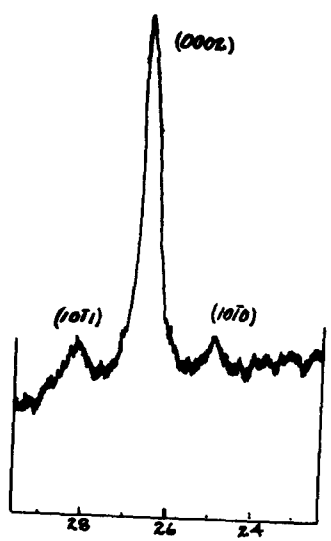

FIGURE 36

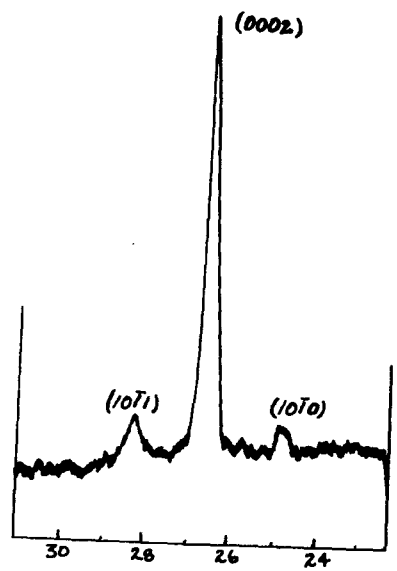

FIGURE 37

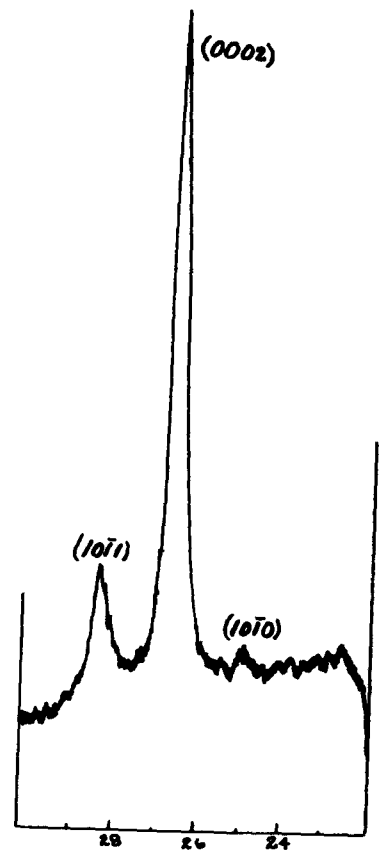

FIGURE 38

X-ray Diffractographs of CdS Films Deposited at Different Temperature

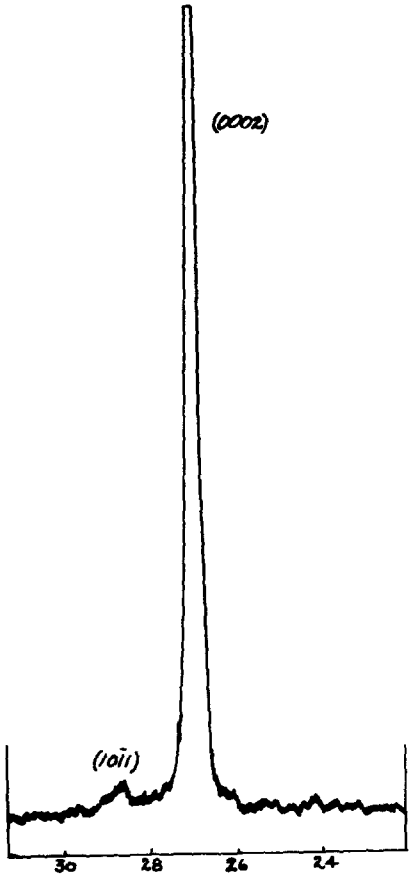

FIGURE 39

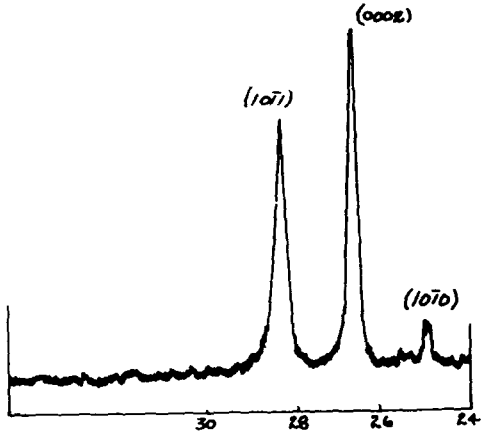

FIGURE 40

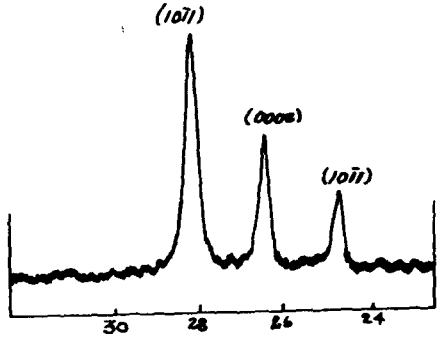

FIGURE 41

X-ray Diffractograph of a CdS Film Deposited from Mixtures of Different Stoichiometric Ratios

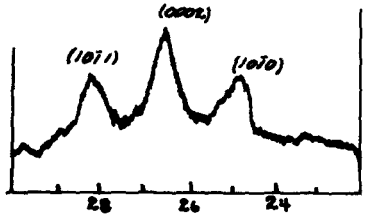

FIGURE 42

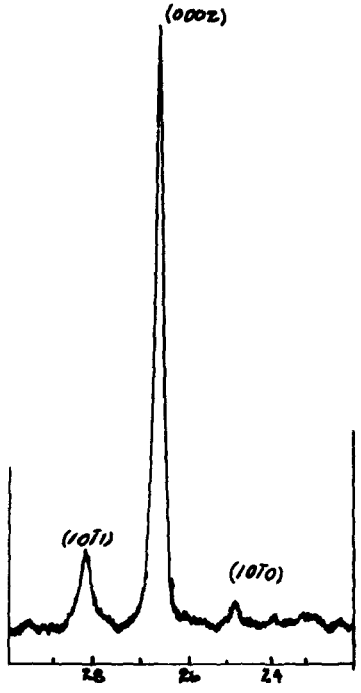

FIGURE 43

X-ray Diffractographs of Two CdS Films before Heat Treat

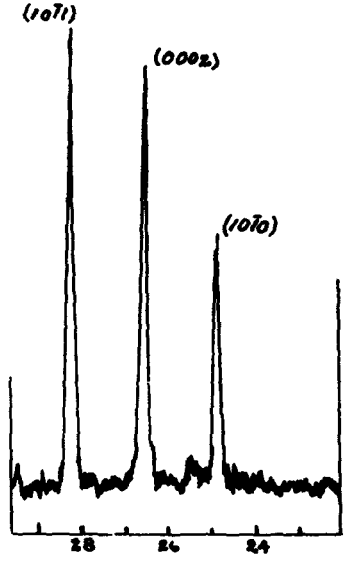

FIGURE 44

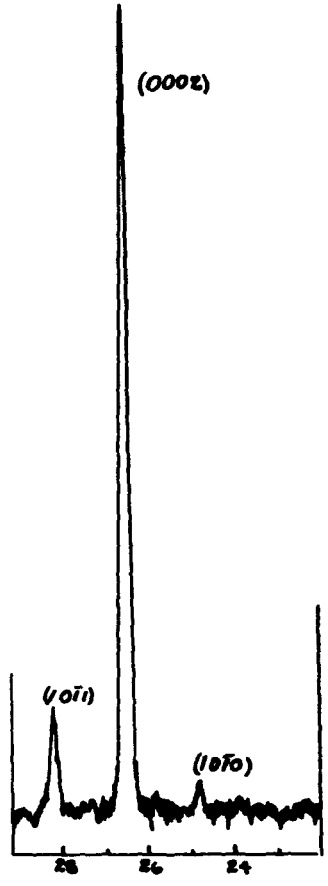

FIGURE 45

X-ray Diffractographs of Two CdS Films after Heat Treat

TABLE 7a

Ga ppm	Orientation	Comments
10	(0002) >> (10$\bar{1}$1)	
100	(0002) >> (10$\bar{1}$1)	
1000	(0002) >> (10$\bar{1}$1)	
10 K	(0002) >> (10$\bar{1}$1)	Reduced intensity of diffraction

The samples containing 10, 100 and 1,000 ppm $GaCl_3$ gave relatively the same diffraction intensities.

Effect of impurity concentrations on the crystal orientation of thin CdS films deposited on SnO_x coated glass substrates.

TABLE 7b

In ppm	Orientation	Relative Intensities	
10	(0002) > (10$\bar{1}$1)	Low	3
100	(0002) > (10$\bar{1}$1) > (11$\bar{2}$2)	Good	2
1000	(11$\bar{2}$2) > (10$\bar{1}$1) >> ($\bar{1}$1$\bar{2}$2)	Reduced	4
10 K	(0002) >> (10$\bar{1}$1) > (0002)	Good	1

Effect of impurity concentrations on the crystal orientation of thin CdS Films Deposited on SnO_x coated glass substrates

There usually appears to be some growth of one orientation at the expense of another, although the large change which takes place in the crystallinity may best be accounted for by assuming that micro-crystallites of the same orientation are growing together to form larger crystallites. It was found that a temperature near 420° C was necessary to cause any appreciable change in a film's crystallinity as measured by x-ray diffraction methods. Figure 46 shows the x-ray goniometer tracing for an untreated film, Figure 47 shows the results of 15 hours at 300° C and Figure 48, 1 hour at 420° C.

4. Examinations of CdSe and Cd(S, Se)

Cadmium selenide films have been prepared by much the same method as for CdS. In general the CdSe films are not as crystalline nor is the diffraction of x-rays as intense as for CdS. Figure 49 is a diffractogram of CdSe on SnO_x coated glass.

CdS-CdSe solid solutions have been prepared as single crystals[14]. At the present time no reference of the solid solution prepared as thin films has been found in the literature. With the chemical spray process the solid solution has been deposited as thin films and by application of Vegard's law the approximate atomic percent has been calculated. Figure 50 is a graphical representation of the change in unit cell parameters of Cd(S, Se) with composition. The points plotted are for the sample Cd(S, Se), PH 803. Table 8 gives the mole percentages as calculated from the x-ray data.

TABLE 8

% Composition Cd(S, Se) Solid Solutions

	Mole % CdSe
$(10\bar{1}0)$ average of 4 calculations	50.3
$(11\bar{2}0)$ 1 calculation	46.0
(0002) 1 calculation	48.5

The composition of the sample is close to that of $Cd(S_{1/2} \cdot Se_{1/2})$. Figure 51 is the diffractogram of this particular sample.

5. Surface Morphology

Figures 52 through 52f are electromicrographs of surface replications for various thin films. There is a definite correlation of the surface morphology and the resulting diffraction patterns. Figure 52a, 52b, and 52c depict very fine grain surface structure with no apparent crystallites present. The diffraction patterns show an amorphous deposit for the sample of Cu_xS_y and nearly amorphous patterns for CdSe and CdS. In

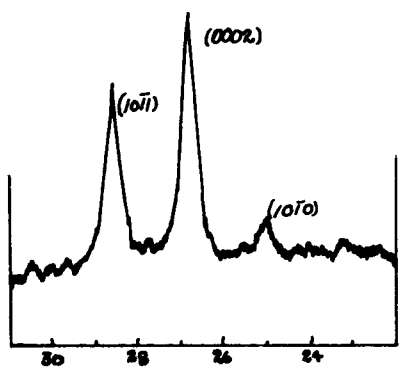

FIGURE 46
CdS Film before Heat Treat

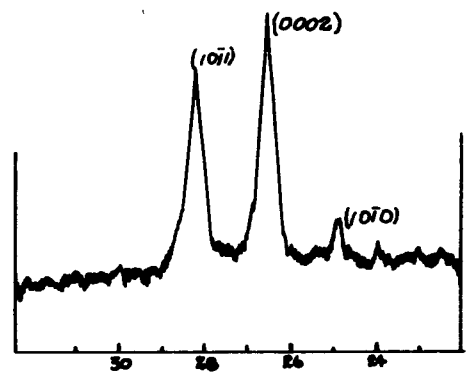

FIGURE 47
CdS Film after Heat Treat

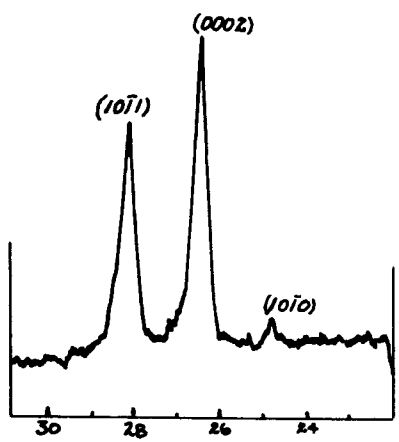

FIGURE 48
CdS Film after Heat Treat

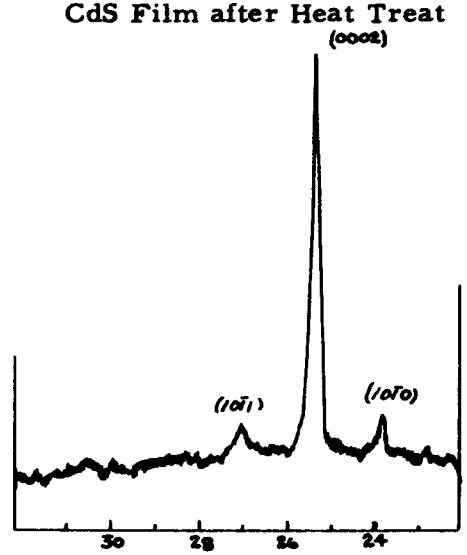

FIGURE 49
CdSe Film on SnO_x Coated Glass

X-RAY DIFFRACTOGRAPHS OF THIN FILMS

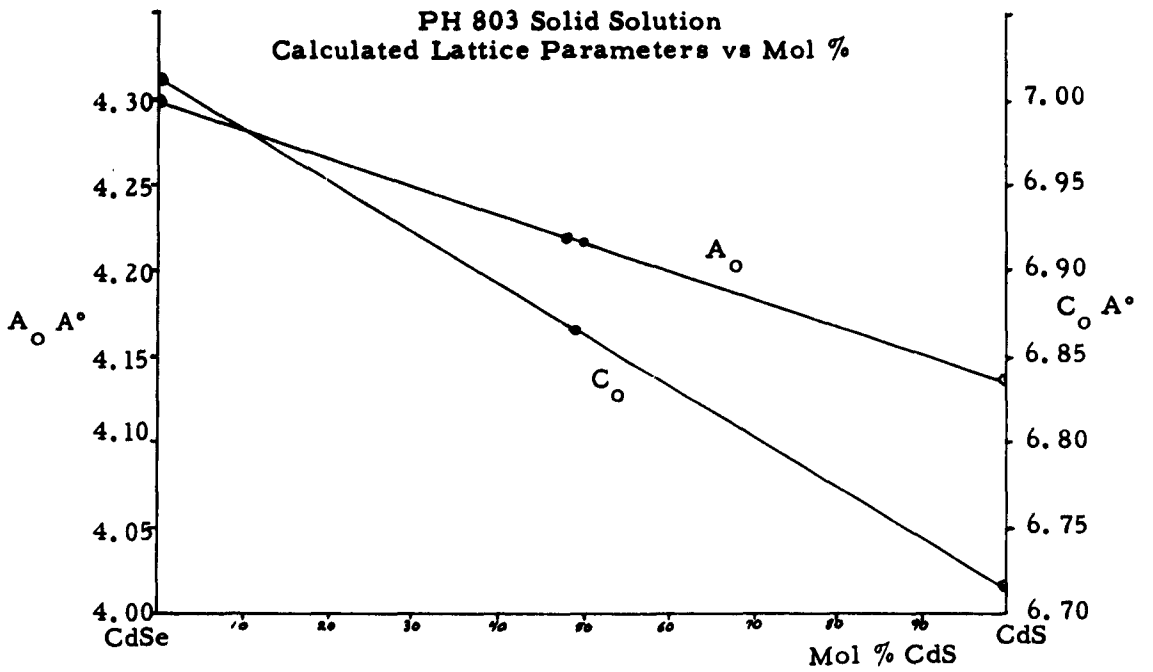

FIGURE 50
Change in Unit Cell Parameters of Cd(S, Se) with Composition

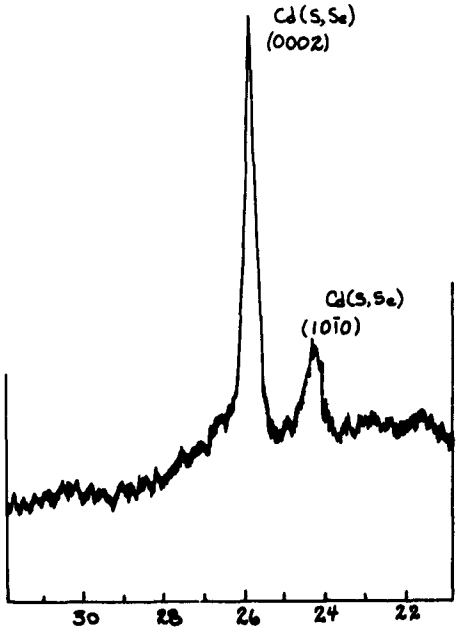

FIGURE 51
X-ray Diffractograph of a Cd(S, Se) Film

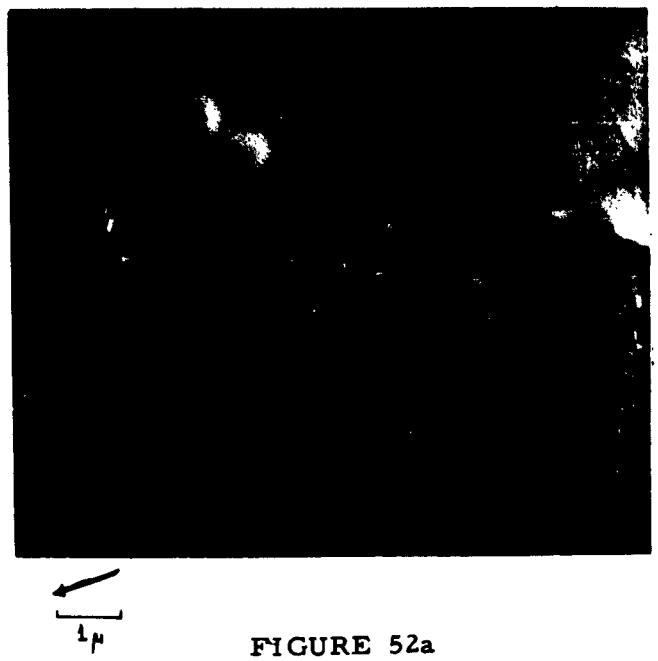

FIGURE 52a

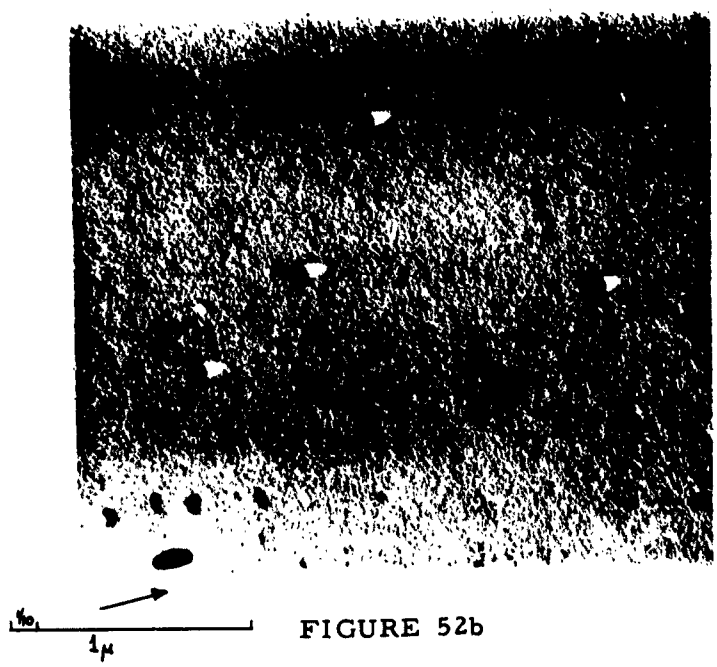

FIGURE 52b

Electronmicrographs of Various Chemically Sprayed Films

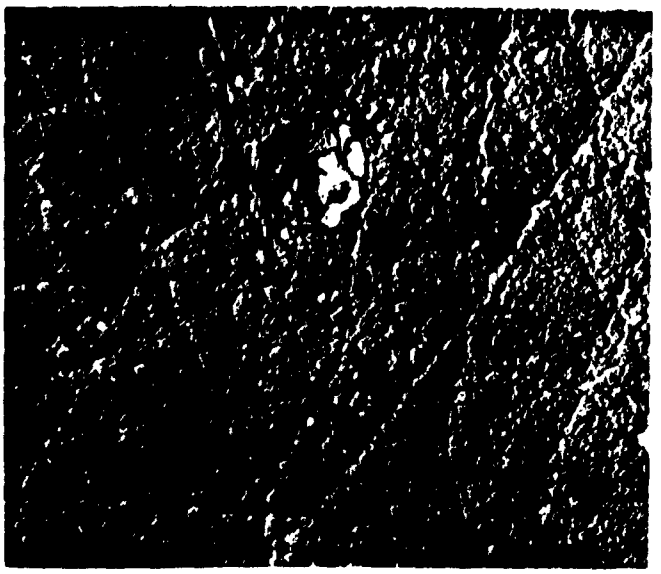

FIGURE 52c

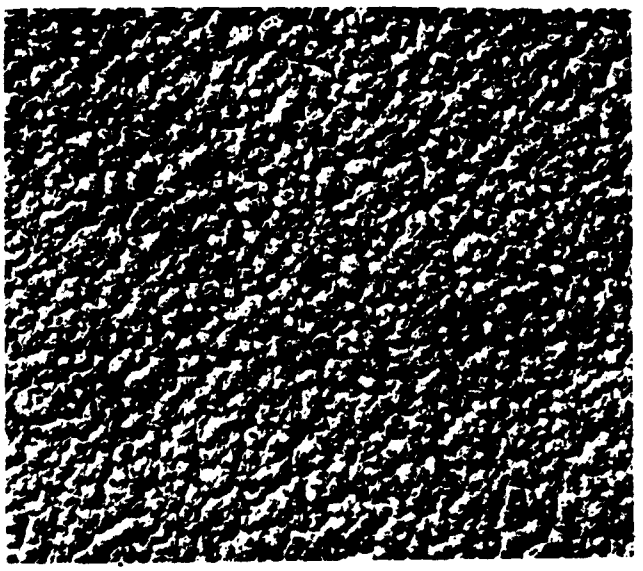

FIGURE 52d

Electronmicrographs of Various Chemically Sprayed Films

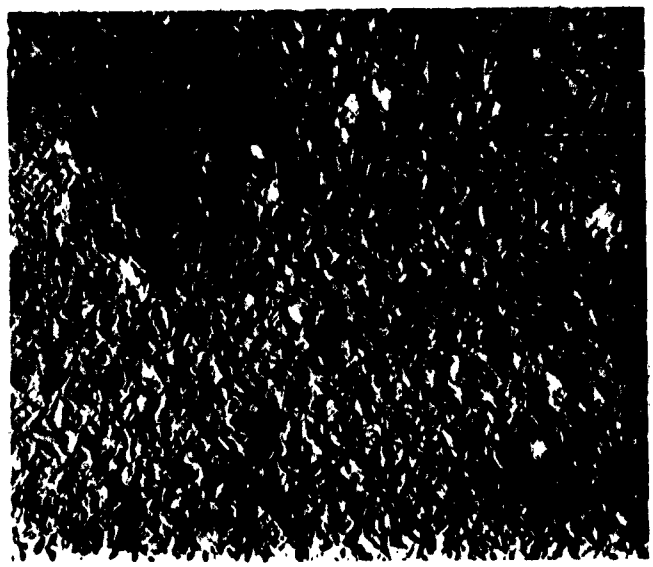

FIGURE 52e

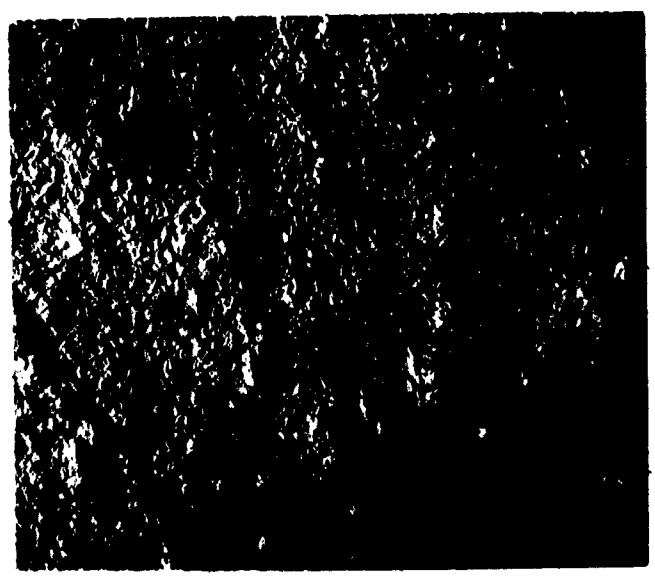

FIGURE 52f

Electronmicrographs of Various Chemically Sprayed Films

Figures 52d, 52e, and 52f discrete outlines of crystallites are present, being more apparent in Figures 52d and 52e than in Figure 52f.

The diffractograms of these samples confirm that a crystalline layer exists and tends to be highly oriented parallel to the (0002) planes while it is not possible to predict the orientation by any interpretation of micrographs, a hint of orientation can be seen in the micrograph of CdS doped with 100 ppm of $GaCl_3$. The pseudo-hexagonal outline of some individual crystallites might lead one to guess that the orientation is (0002).

III. ANTI-REFLECTION COATINGS

INTRODUCTION

The utilization of incident energy in the case of the photovoltaic cell is primarily dependent on the parameters of the semiconducting layers and the subsequently formed barrier. The incidence of the maximum amount of energy at the barrier, however, is primarily dependent on either the surface of the substrate, in the case of the back wall cell (Figure 6), or the surface of the top semiconducting layer, in the case of the front wall cell (Figure 6). In general, the reflectance of either of these surfaces can be modified by coating the surfaces with one or more layers (films) of materials of selected indices of refraction. These procedures can be classified into three major categories:

a. One Thick Film;

"thick" in this context means thickness, d, greater than about one micron. For this case, the maximum decrease in reflectance is 50%, obtainable when the "Strong condition", $n_1 = n^{1/2}$, is satisfied (n_1 = index of refraction of film; n = index of refraction of reflecting material). This approach was rejected since (1) the hard glass used has an index of 1.5 and therefore it is difficult to find materials with refractive indices small enough to satisfy the "Strong condition", and (2) at best only a 50% reduction can be obtained.

b. One Thin Film;

A very effective decrease in reflectance over a wide wavelength range (e.g. the complete visible spectrum) can be obtained by coating the reflecting surface with a film of one quarter wavelength optical thickness ($n_1 d$) whose index of refraction, n_1, satisfies the "Strong condition". This approach was tried in initial experiments but reflectance reduction of only one or two percent was achieved because of the almost impossible task of finding materials which simultaneously satisfy the "Strong condition" and are suitable for coating a hard glass.

c. Two or more Thin Films;

Since the time allocated to this phase of the contract did not permit the extension of this part of the program to multilayer films, only the effect of two films was considered. Two double-film cases are usually considered, (1) both films have optical thicknesses of one quarter wavelength, or (2) the first film (in contact with air) with index n_1 has an optical thickness of one quarter wavelength but the second film, of index n_2, has one half wavelength optical thickness. Analagous, but more complex, "Strong conditions" must be satisfied in both cases. Since MgF_2 ($n_1 = 1.39$) and Sb_2O_3 ($n_2 = 2.02$) had been reported to give a very effective reflectance decrease [6] using the second approach, it

was decided to try this method for reducing the reflectance of the hard glass substrate used for back wall cells. Film thicknesses of 920 A° of MgF_2 and 1260 A° of Sb_2O_3 were selected to obtain minimum reflectance at 5100 A°. (Initial efforts were designed to reproduce previous work in which 5100 A° had been selected as the wavelength for minimum re> flectance.) The calculation of the spectral dependence of reflectance of this system is quite lengthy; however, it can be shown that the resulting reflectance should exhibit two wavelength minima with an intervening maximum and this maximum will be less than that of the clean surface for $n_1 < n$.

TECHNICAL DISCUSSION

1. Apparatus and Evaporation Techniques

All of the experimental work done with vacuum deposited coatings was directed towards possible improvements which could be gained with back wall cells. The anti-reflection coatings were prepared in a Consolidated Vacuum Corporation LCI-18A vacuum system. In-chamber components for substrate heating and shuttering protection against spattering were constructed and installed as recommended in the literature (17, 18).

Heating of the substrate was accomplished by clamping the sample to the underside of a 10" x 10" x 1/8" aluminum plate. A 500 watt Chromalox HKL ring heater was mounted on top of the aluminum plate.

The evaporation source employed for MgF_2 was a slightly modified Allen-Jones Corporation 3901 Molybdenum boat. The modification consisted of extending the boat cross section area 1/2" toward each supporting end. This modification permitted a more uniform temperature distribution over the entire boat depression length.

Since no literature on the methods of evaporation of Sb_2O_3 was available, several methods were tested. Initial evaporations of Sb_2O_3 were made from a molybdenum boat identical to that used for MgF_2. However, the boat surface had a grayish-brown dusty appearance after each evaporation, indicating that the molybdenum and Sb_2O_3 were reacting. Another difficulty encountered in open boat evaporation arose because the Sb_2O_3 apparently doesn't melt but sublimes in burst resulting in loss of material from the boat, thus preventing thickness control by complete evaporation of known starting weights.

To overcome spattering losses and reaction with the boat, the Sb_2O_3 source was changed to a porcelain crucible heated in a tungsten wire basket. With care, the material could be evaporated without spattering loss but the crucible had a dark film covering the upper portions.

Doubt concerning the composition of the porcelain crucible and possible reactions with the Sb_2O_3 as well as the impossibility of visually observing the materials for the first traces of violence, prompted the

fabrication and use of a quartz crucible similar in configuration and size to the porcelain crucible. This crucible also became coated with a dark, bluish film. Since this film was soluble in KOH it was tentatively identified as an oxide or mixture of oxides of tungsten.

Efforts to eliminate this film formation led to the fabrication of a quartz ampoule 1-1/4" long by 5/16" internal diameter with a 1/8" diameter hole sandblasted centrally into the side. This ampoule was heated in a molybdenum boat and located with the orifice aimed approximately at the center of the sample. By taking care not to allow any of the Sb_2O_3 to lie directly beneath the orifice, loss by spattering was completely eliminated and there was no residual film on the inside or outside of the ampoule. The geometric arrangement of the source and sample was a vertical arrangement with the sample 8-1/4" above both the MgF_2 and Sb_2O_3 sources.

Initial attempts to control film thickness were carried out by timed shuttering of the sample. After a few samples were made and the thicknesses measured by a multiple beam interferometric method, described later, it was obvious that the film deposition rate was too high to be reproducibly controlled by shuttering. Adequate reproducibility for the MgF_2 film thickness was finally obtained by evaporating entirely a predetermined weight without shuttering the sample. Thickness control of $\pm$ 5% or better can be achieved by this technique. For our system's geometry, the calibrated MgF_2 thickness was 26.6 A°/mg. Difficulties were encountered initially in controlling the Sb_2O_3 film thickness by this technique. However, the difficulties were found to arise from the thickness measurements. The step at the glass-Sb_2O_3 edge formed by the shutter edge shadow was not as sharp as with the MgF_2. This sloping edge made accurate and reproducible thickness measurements impossible. However, the clamp holding the substrate to the heater formed a very sharp step since it was in intimate contact with the glass. Measurements of Sb_2O_3 film thickness at this step gave reproducible values which made possible a Sb_2O_3 evaporation rate calibration determination of 19.8 A°/mg. The final samples of the series were prepared using 35.7 mg of MgF_2 and 63.6 mg of Sb_2O_3.

The samples were masked so that approximately 1/3 was uncoated glass, 1/3 was coated with MgF_2 superposed in Sb_2O_3 and the remaining 1/3 was a single coating of Sb_2O_3. The sample was then rotated through 90° in the substrate clamp and masked by the shutter to leave a 1/2" strip crossing the previous coatings. This strip was then aluminized for film thickness measurements.

2. Measurement of Film Thickness and Reflectance

Film thickness was measured by a multiple-beam interferometric technique (19). The equipment (see Figure 53) consists of a mercury light, collimating lenses, a 77A Wratten filter and a measuring microscope equipped with a 4X objective and a beam-splitter all mounted on a laboratory optical bench. The sample which was previously aluminized with the aluminum overlapping the film edge such as to form a step with

FIGURE 53
Film Thickness Measuring Equipment

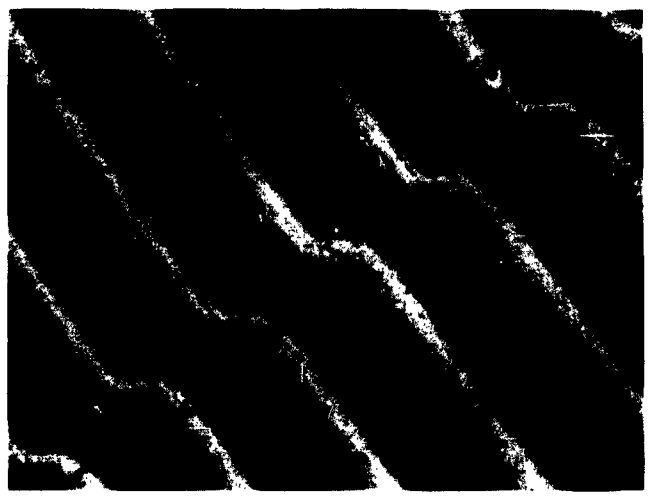

FIGURE 54
Interference Fringes

the substrate was covered with an approximately 90% reflecting aluminized cover glass to generate interference fringes. These fringes were then adjusted (by varying the pressure applied to the cover glass) to be at right angle to the step being measured. Once the fringes had been established, the fringe width, d_2, was measured and the fringe shift distance, d_1, across the step was measured. Film thickness was then calculated from the relation

$$\frac{d_1}{d_2} \times \frac{\lambda}{2} = \text{thickness}$$

λ was 5460 A° (the mercury green line chromatized by the Wratten 77A filter) for all thickness measurements.

Figure 54 shows a typical multiple-beam interference pattern obtained using monochromatic light. From a pattern of this type it is not possible to determine if the fringe shift is a fraction of fringe width or a multiple. To determine just how many fringe shifts are involved in a given measurement, it is necessary only to remove the narrow band pass filter from the light source. A polychromatic light source will produce an interference pattern very similar to that obtained from a monochromatic source except that the fringes are not as sharply defined and every fourth fringe has a reddish-brown color whereas the other fringes are blue. This ability to distinquish every fourth fringe makes it possible to see if a given fringe has shifted 1, 2, 3, or 4 fringe widths. This technique allows the multiple beam interference method to be used on films whose thickness is as great as 2λ, where λ is the monochromatic wavelength.

The reflectance was determined from transmission measurements which were made on a Beckman Model DU spectrophotometer. The percent transmission was measured from 4000 A° to 9000 A° at 500 A° intervals. In wavelength ranges where sharp changes in transmission were encountered, intermediate points were recorded. The reflectivities were calculated from the transmission measurements using the relations below:

$$r_1 = (t_1 / t_0)^{1/2} \qquad (1)$$

and

$$r_0 = 1 - t_0^{1/2} \qquad (2)$$

where

r_1 = reflectivity of glass and film-air interface

r_0 = reflectivity of glass-air interface

t_1 = fraction of incident light transmitted through coated glass

t_0 = fraction of light transmitted through uncoated glass

The results are shown in Figure 55. Two minima (at 5000 A° and 7000 A°) are observed, as expected for a double layer film. Since the selected thicknesses of 920 A° of MgF_2 and 1260 A° of Sb_2O_3 were calculated from the conditions for minimum reflectance at 5100 A°, the minimum at 5000 A° can be regarded as demonstrating qualitative agreement with theory.

3. Front Wall Cell Reflection Characteristics

Solar cells having the front-surface configuration consist of a pyrex substrate coated with approximately 6000 A° of SnO_x, 10,000 A° of CdS and 900 A° of Cu_xS_y. To determine the reflection properties of the CdS and Cu_xS_y films, specimens of hard glass, CdS coated hard glass, Cu_xS_y coated hard glass and CdS-Cu_xS_y coated hard glass were mounted in one of the positions of the three position detector mirror support of a Perkin-Elmer Model 99 monochromator. Energy reflected by the standard mirror and the specimen was detected by a thermocouple whose output was amplified by a Perkin-Elmer Model 107 amplifier. A Hewlett-Packard Model 412A electronic volt-ohm meter was used to measure the amplifier output. The % reflectance was defined to be

$$\frac{Is \times 100}{I_0} = \% R \qquad (3)$$

at each wavelength,

where

Is = fraction of power reflected from sample reaching the thermocouple

I_0 = fraction of power reflected from mirror reaching the thermocouple

The results of these measurements, shown in Figure 56, indicate that improvement on the non-reflectivity of the Cu_xS_y-CdS would be difficult.

SUMMARY OF ANTI-REFLECTION COATINGS

Effective reduction of reflection losses at the glass-air interface of the back wall can be obtained with MgF_2-Sb_2O_3 double-film coatings. Although only one pair of film thicknesses was studied, the spectral dependence of reflectance can be matched to the photovoltaic cell (CdS) spectral response to obtain maximum efficiency through the variation of the film thicknesses. The films obtained appear uniform and homogeneous but their adherence and environmental stability have not been determined.

The gain in output, although small in actual percentage (3.1 mw instead of 3.0 mw when 99% instead of 96% of the incident irradiation is available), could be significant if very large area back wall cell arrays were to be used; however, this gain might be offset by the cost of the vacuum deposition of the double film layer.

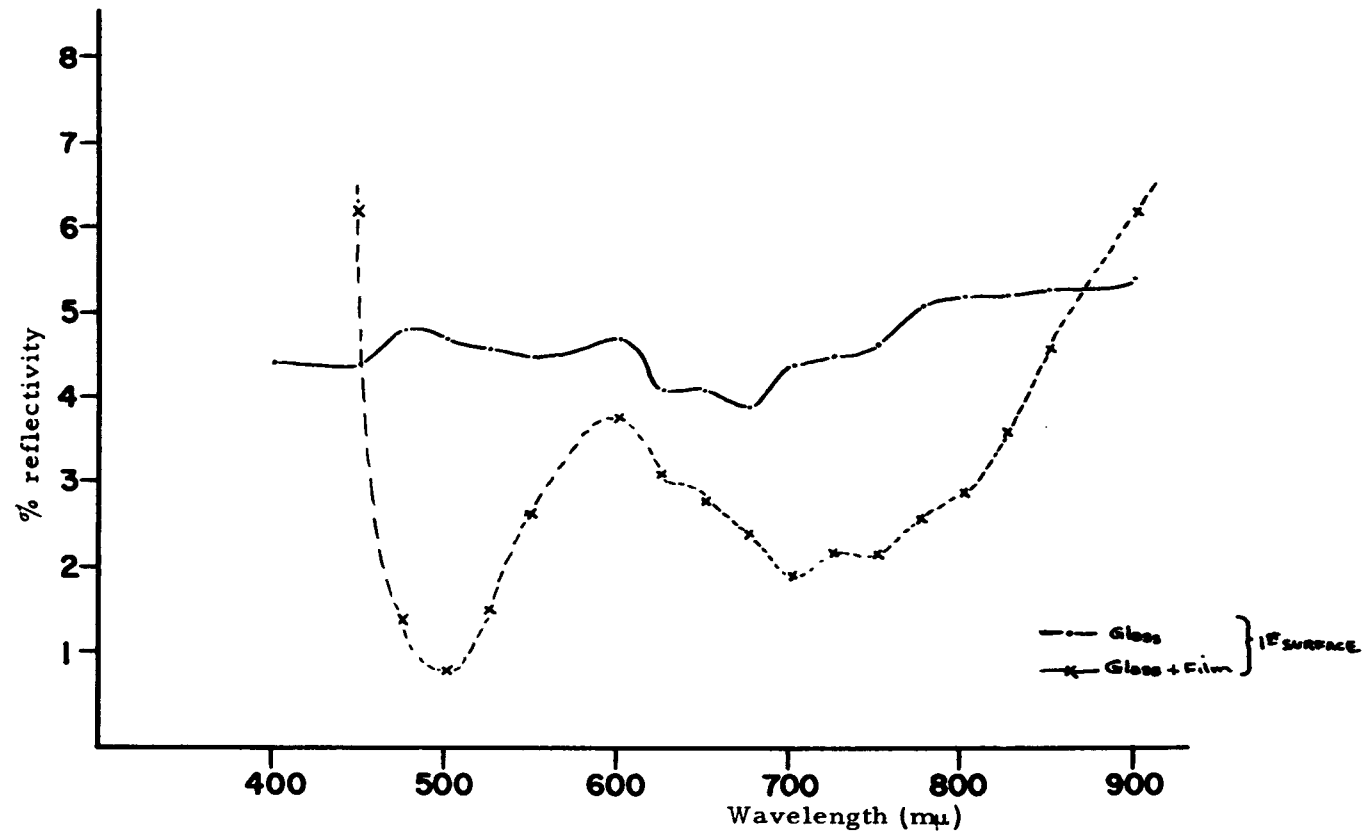

FIGURE 55
Reflection Measurements of Multiple Film Anti-reflection Coating

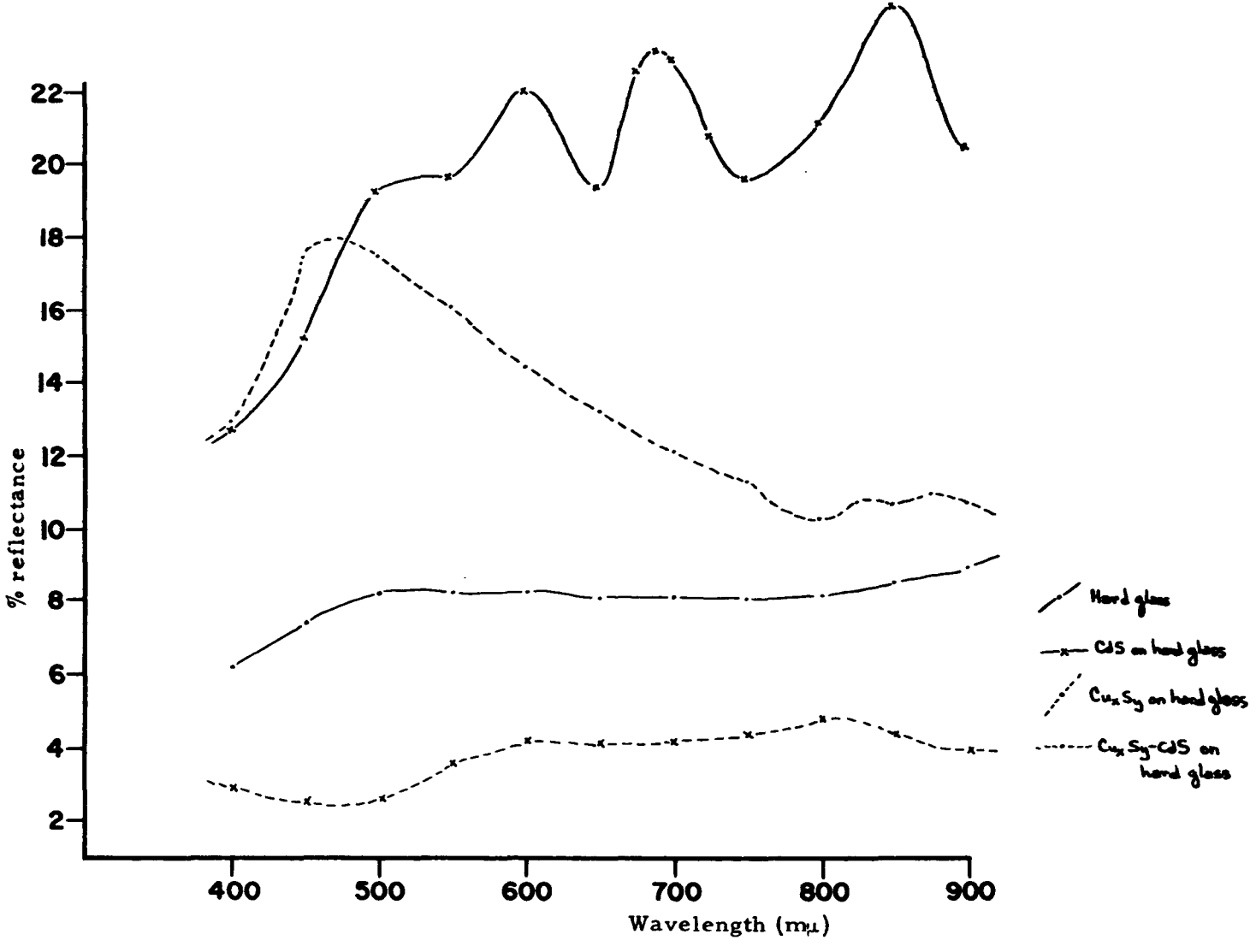

FIGURE 56
Reflection Measurements of CdS Film, Cu_xS_y Film, and of a CdS-Cu_xS_y Combination

Results of reflectance measurements indicate that the Cu_xS_y-CdS combination studied will serve as its own anti-reflection coating with apparently little to be gained with additional films. Whether this will continue to be the case as the front wall configuration is optimized using a metal substrate remains to be determined.

IV. CELL FABRICATION

INTRODUCTION

This section describes the work relating to the fabrication of cells by the chemical spray techniques. The objectives were to attain efficient, large area photovoltaic converters utilizing the technique of chemical spray deposition and to deliver six (6) experimental cells, four (4) of which are composed of CdS and two (2) composed of CdSe.

Initial work on the development of the techniques necessary to produce completed cells was directed toward the attainment of those properties in each of the layers that are part of the unit cell, that would be expected to be desirable. These include the following:

1. Low resistance transparent conductor
2. Strong n-type CdS and CdSe
3. Physically uniform CdS and CdSe films
4. Low resistance metallic electrode for current collection

Techniques for the production of an efficient barrier layer or junction initially followed the procedures used by previous investigators [1, 3]. Lack of efficiency, control and reproducibility using these techniques led to the spraying of the barrier layer. The barrier layer on the delivered cells is a chemically sprayed layer of Cu_xS_y.

TECHNICAL DISCUSSION

1. Transparent Conducting Electrode

The transparent conducting coating on the glass substrates which is used for the fabrication of a back wall photovoltaic cell must be chemically inert, capable of withstanding the temperature reached during the fabrication of the rest of the cell, and must also be transparent to those wavelengths to which the photovoltaic junction is sensitive. Three materials have been considered for this layer and successful deposition of each has been achieved. These materials are SnO_x, CdO, and In_2O_3 : Sn.

a. SnO_x

SnO_x is deposited by spraying a solution of 18.0 molar $SnCl_4 \cdot 5H_2O$ and 10 ml of formaldehyde to every 150 ml of solution onto a glass substrate that is heated to about 500° C. The thickness of the SnO_x is determined by its interference color which is monitored during the spray process. The spray is stopped when the fourth-order red (corresponding to a thickness of about 5400 A°) is reached. The resistance of such a film is about 50 ohms/square.

b. In_2O_3:Sn

In_2O_3:Sn is deposited in a manner similar to SnO_x. The solution consists of 20 molar In_2Cl_3 to which 1.0% $SnCl_4$ has been added. Formaldehyde is again added in the same quantity as in the SnO_x solution to prevent premature oxidization. The solution is sprayed onto glass substrates which are heated to at least 350° C. The thickness is determined by the interference color and is only allowed to reach the third-order red (3850 A°). If the spray is allowed to continue beyond this thickness the film becomes clouded and the transparency rapidly decreases. The average resistance of a third order film is about 40 ohms/square.

Although the thickness of smooth surfaced thin films can be accurately measured by multiple interference [19], the interference colors which can be observed by the unaided eye are much more useful, since thickness can be measured without interruption of the deposition, and require only a knowledge of the order which is being viewed. Figure 57 gives a CIE chart with a plot of the interference color (using illuminant C) for various thicknesses of a dielectric film which has an index of refraction of 2.5. The calculations used to plot this curve were based on a table of values calculated by Hiroshi Kubota [20].

c. CdO

CdO films have been prepared by spraying a highly atomized solution of 0.01 molar cadmium formate with the addition of one part in ten of 30% hydrogen peroxide. The spray is periodically stopped to allow the film to completely oxidize. The substrate is maintained at 325° C during deposition. The films produced in this manner are of optical quality with resistance of about 80 ohms/square.

Each of the materials (CdO, SnO_x, In_2O_3:Sn) seem to offer some advantage; SnO_x is very stable, resisting attack by most acids and alkalis and can be deposited with a resistance of 25 ohms per square (Figure 58 gives typical values) while maintaining a transmission value of almost 70%. The tin-oxide deposited here usually had a slightly preferred orientation of (301) >(211); In_2O_3:Sn likewise is a very stable film and has resistance characteristics equivalent to SnO_x. This material has the advantage of depositing at a slightly lower temperature and the starting solution of $InCl_3$ is less corrosive than the $SnCl_4$. However, the optical clarity of the In_2O_3:Sn film is much harder to control than that of the SnO_x. Small imperfections in the glass appear to be amplified by the deposition of a In_2O_3 film; CdO can be deposited at a much lower temperature (about 325° C compared to 500° C) than either In_2O_3 or SnO_x. This advantage, however, is offset by the longer wavelength of its absorption edge and its susceptibility to attack by mild acids. The transmission characteristics of these three materials are shown in Figure 59. As can be seen, SnO_x and In_2O_3 have the widest transmittance "window". In_2O_3 and CdO were originally considered because of the reverse voltage often seen (the SnO_x being positive) in

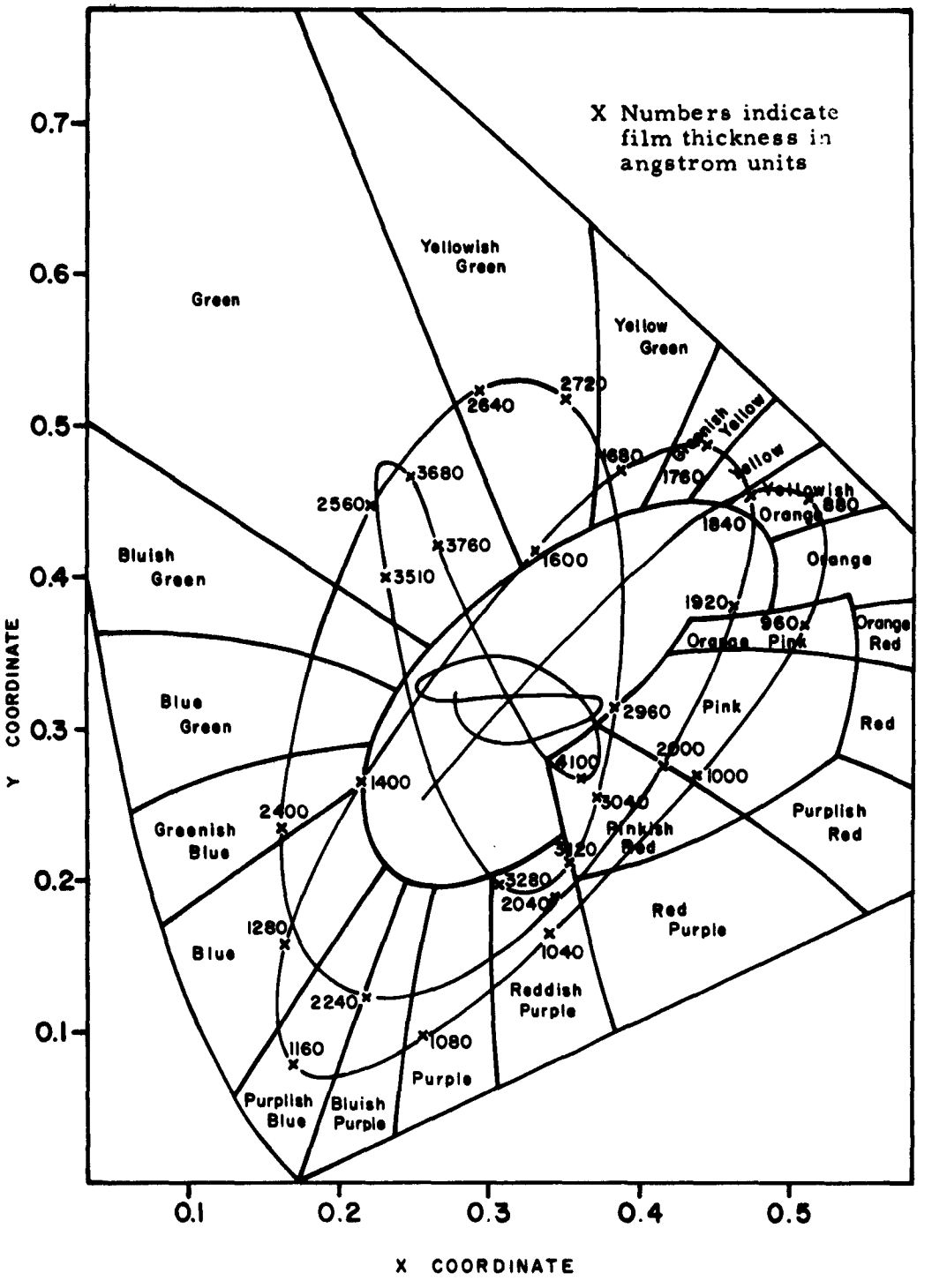

FIGURE 57

Plot of Interference Colors (using illuminant "C") for a Dielectric Film with an Index of Refraction of 2.5

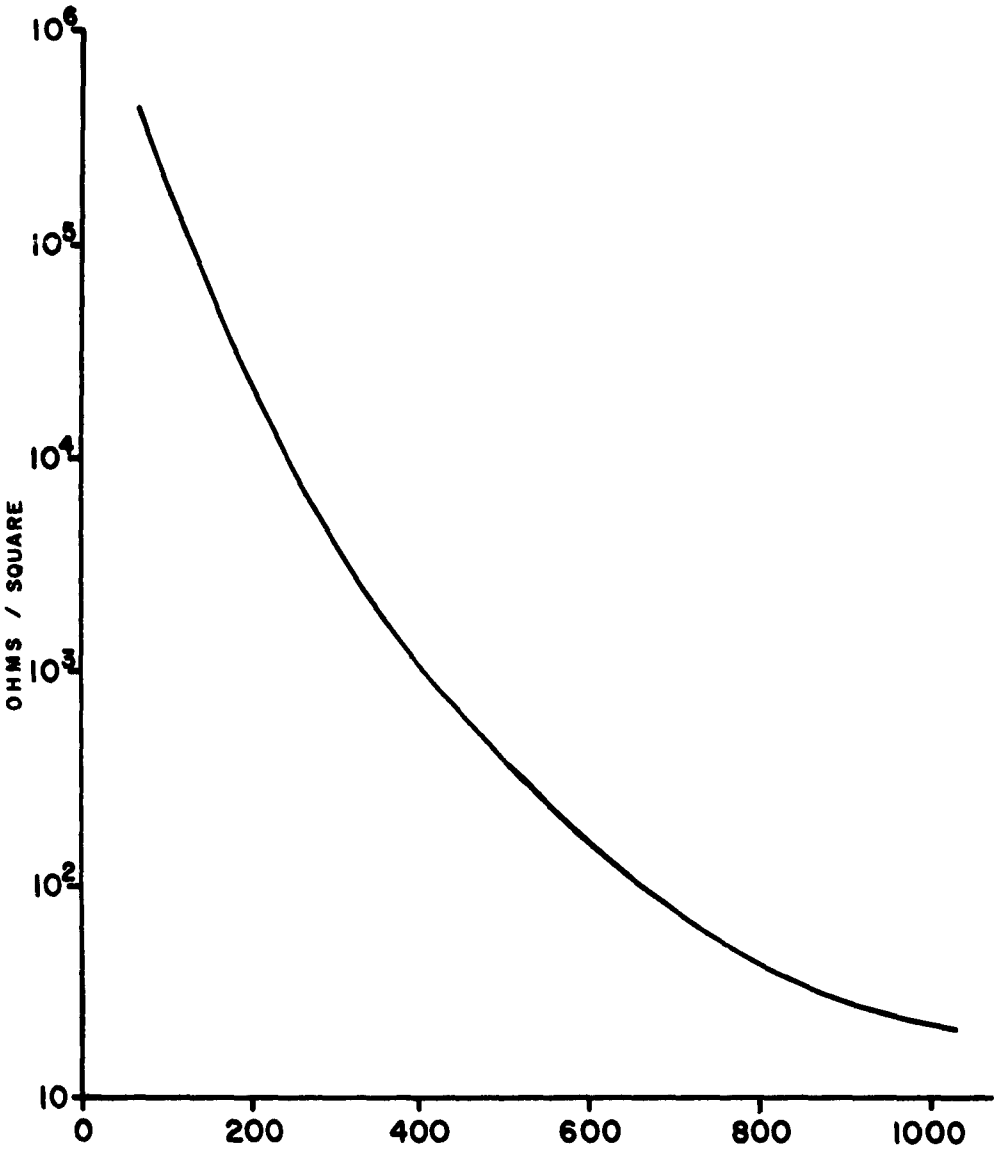

FIGURE 58
Resistance of SnO_x Film vs Thickness

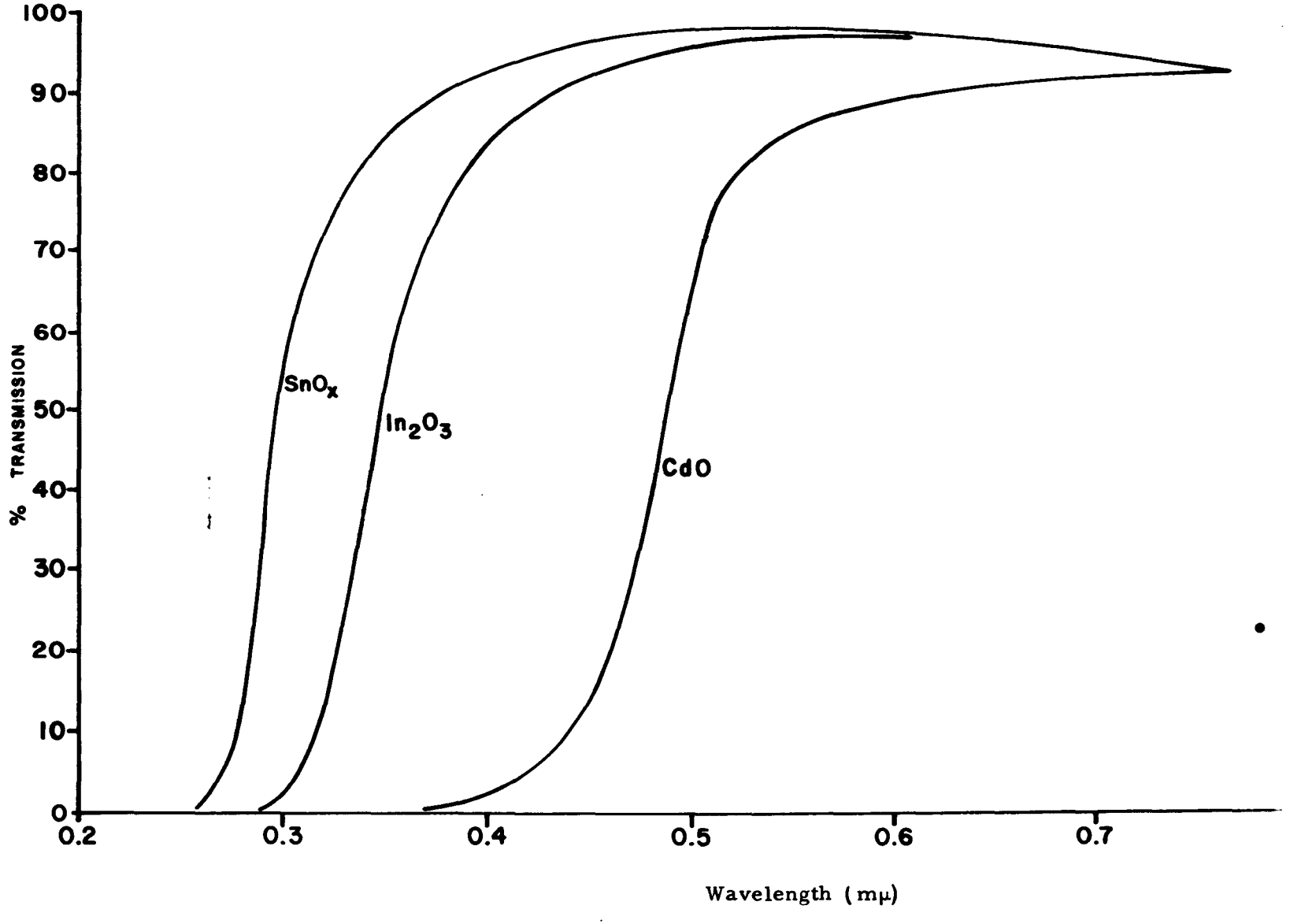

FIGURE 59
Optical Transmission of CdO, SnO_x and In_2O_3:Sn

cells of the SnO_x-CdS-Cu system; it was proposed that a more nearly ohmic contact would be made between the CdS and either In_2O_3 or CdO. Proof of the more nearly ohmic contact was expected to take the form of higher open circuit voltages (greater than 450 millivolts). However, this was not the case; In_2O_3 and CdO tend to yield cells with lower (320-360 millivolts) open circuit voltages but free of reverse voltages. The decrease in open circuit voltage might be due to the influence of the different crystallinity of the In_2O_3:Sn and CdO on the crystal structure of the CdS layer. Cells prepared during the last two quarters of this contract were of the SnO_x-CdS-Cu_xS_y-Cu type and the problem of reverse voltage was not encountered in this type cell.

2. CdS and CdSe Layer

a. Film Deposition

Films of CdS and CdSe were deposited by the chemical spray technique in a wide range of thicknesses to evaluate the physical continuity, electrical uniformity, optical clarity, reproducibility and maximum thickness. Examination of these films resulted in the following conclusions:

1. Maximum film thickness of up to 5 to 10 microns is possible while retaining physical uniformity and reproducibility.

2. Films are free from pinholes when deposition is done under clean conditions on a smooth substrate.

3. Films may be produced which range from glass-like to opaque, dependent on spray parameters (primarily rate) and substrate surface condition (whether smooth, polished or etched).

b. Doping

A series of films of CdS was deposited on both SnO_x coated and uncoated hard glass using various concentrations of indium and gallium as the dopant. The results of optical and electrical measurements on these films are summarized in Tables 8 and 9. Of particular interest are the resistivity values which were obtained for the various impurity levels. Previous workers have reported resistivity values much lower (1-70 ohm-cm) for both single crystals and evaporated films. It is believed likely that in their cases non-stoichiometry in the bulk CdS was the real contributing factor. This conclusion can only be indirectly supported since methods are not available to determine the ratio of cadmium to sulfur in CdS with sufficient precision (x-ray fluorescence is capable at best of 1%), however, x-ray diffraction examination (see Table 6) of the crystal orientation of this series of doped CdS films gives good evidence, in the case of indium, that the impurity was, even at a doping level of 10 ppm, present in the final film and was affecting at least its physical structure.

The observation that both doping and substrate conditions could affect a change in the crystallite orientation and percentage of crystallinity

TABLE 9a

Effect of Indium Doping on Electrical Characteristics of CdS Films

Indium Doping Conc.	Thickness	Transmission 4000 A°	Transmission 6000 A°	Reflection 4000 A°	Reflection 6000 A°	Resistivity
10K ppm	1,100 A°	22	81	17	14	1.65×10^5 ohm-cm
10K ppm	1,300 A°	13	86	29	10	5.2×10^4 ohm-cm
10K ppm	2,400 A°	3.8	78	24	20	3.8×10^4 ohm-cm
1K ppm	1,600 A°	11	76	20	23	2.4×10^5 ohm-cm
1K ppm	2,400 A°	2.4	72	20	23	5.8×10^5 ohm-cm
1K ppm	2,850 A°	.40	63	17	28	1.8×10^5 ohm-cm
10^2 ppm	680 A°	41	72	31	29	6.8×10^4 ohm-cm
10^2 ppm	1,220 A°	10.5	76	20	22	3.6×10^4 ohm-cm
10^2 ppm	2,900 A°	2.1	74	21	25	8.1×10^4 ohm-cm
10 ppm	900 A°	36	74	19	24	1.9×10^6 ohm-cm
10 ppm	1,850 A°	3.5	81	21	14.5	1.8×10^5 ohm-cm
10 ppm	2,000 A°	1.5	78	20	21	5×10^4 ohm-cm

TABLE 9b

Effect of Gallium Doping on Electrical Characteristics of CdS Films

Gallium Doping Conc.	Thickness	Transmission 4000 A°	Transmission 6000 A°	Reflection 4000 A°	Reflection 6000 A°	Resistivity
10K ppm	630 A°	44	72	32	28	3.1×10^{7} ohm-cm
10K ppm	1,270 A°	27	81	20	18	1.8×10^{8} ohm-cm
10K ppm	1,600 A°	9.8	71	22	30	5.6×10^{9} ohm-cm
1K ppm	720 A°	44	72	33	24	1.1×10^{7} ohm-cm
1K ppm	1,200 A°	20	91	23	8	5.4×10^{6} ohm-cm
1K ppm	1,550 A°	7.3	74	12	24	8.5×10^{6} ohm-cm
10^2 ppm	1,050 A°	43	76	28	24	2.3×10^{7} ohm-cm
10^2 ppm	1,250 A°	23	80	18	20	9.6×10^{6} ohm-cm
10^2 ppm	1,900 A°	8.8	74	18	26	5.7×10^{6} ohm-cm
10 ppm	100 A°	91	97	9	3	1.2×10^{9} ohm-cm
10 ppm	950 A°	33	71	19	30	5.9×10^{6} ohm-cm
10 ppm	2,020 A°	10	76	16	20	1.1×10^{7} ohm-cm

led to a study of the relation between spray parameters and crystal structure. The samples generated during this study were then used in an attempt to relate crystallinity and orientation to photovoltaic response. The results of the photovoltaic study are covered in the Photovoltaic Structure Experiments section.

3. Barrier Formation

Early efforts to form a barrier on the chemically sprayed CdS films were directed by the techniques developed by others [2, 3]. These various techniques are outlined below:

a. Electro-deposited Copper

It has been shown [2] that if the CdS layer is sufficiently thick (several mils) copper can be successfully electro-deposited, however, as has been started, the chemical spray technique does not lend itself to the deposition of films of this thickness. Consequently, it was not surprising that electrodeposition of copper for the formation of the barrier electrode was not successful with films in the .5 to 1 μ thickness range. However, it was noted that the conditions of the interface between the copper and the CdS vary with the conductivity of the CdS layer. If the conductivity is great enough to allow even deposition of copper without severe damage to a thin CdS layer the copper appears as bright natural copper at the Cu-CdS interface as viewed through the CdS. As the conductivity of the CdS films is decreased and the evenness of the electrodeposited copper layer decreases, the Cu-CdS interface will change from the bright copper color to the rich brown color which has been reported as typical of the interface color after the barrier "activation" heat treatment.

b. Pyrolytic Deposition of Copper

The limitation on the use of electrodeposited copper because of the thinness of the CdS layer led to the development of a technique to deposit copper by the pyrolysis of a copper formate solution. The technique, which is an extension of a previous [19] examination of the pyrolysis of copper formate, consists of spraying a highly atomized solution of 0.8 M copper formate with the solution pH adjusted to about 1 by the addition of formic acid. This solution is sprayed onto a substrate which has been heated to about 650° F with an oxygen-free enclosure. Since nitrogen is used to operate the spray gun in the sealed system, N_2 plus the vapors of the pyrolysis of the copper formate solution will effectively exclude oxygen so that the deposited copper film may be removed from the substrate heater and cooled without the surface oxidizing. This technique for spraying a metal film is similar to, but much simpler than, the carbonyl gaseous metal deposition system and it is believed that this technique can be directly extended to the deposition of many metals through the pyrolysis of solutions of their formates if the pyrolysis occurs in an oxygen-free enclosure.

Application of pyrolytically deposited copper to CdS films unfortunately results in decomposition of the cadmium sulfide and thus proved unsuccessful as a barrier formation technique. The spray solution is strongly acid and at the elevated temperatures necessary for deposition readily attacks the CdS, producing flaking and complete disruption of the originally continuous, adherent film.

c. Vacuum Deposited Metal Barrier

Vacuum deposited films of copper, silver, and gold have been reported to form good barriers with CdS. Efforts to use this technique for the formation of a barrier on chemically sprayed CdS films have all met with little success. The highest efficiency found in any cells produced by vacuum deposition was 0.1% with a .1 cm^2 area. This was a cell made with a vacuum deposited copper barrier that had been heat treated in air for various intervals at 300° C and then re-electroded with silver paint to improve the current collection properties.

d. Sprayed Barrier

It has been shown previously by others [1] that a film of Cu_2S can be used as a barrier layer and that it has been at least tentatively shown [4, 5] that Cu_2S is the essential element in the CdS:Cu photovoltaic cell where the copper is electroplated on the CdS and the cell then is heat treated. The early work with vacuum and slurry deposited Cu_2S resulted, at best, in a few small cells of .75% efficiency. However, the chemical spray process, being well suited to the deposition of copper sulfide, has been used to deposit films of copper sulfide on top of CdS films as a means of forming a barrier layer. The films which have been deposited are actually (as previously mentioned) films of $Cu_{9-x}S_5$ or Cu_xS_y (Digenite) rather than Cu_2S (Chalcocite), and are in the thickness range of 300 to 1000 A°.

CuS (Covellite) has also been deposited with the chemical spray process along with CuSe (Klockmannite) and $Cu_{9-x}Se_5$ (Berzelianite). Results from the use of any of these films other than digenite have been almost entirely negative.

Present cells are prepared using digenite (Cu_xS_y) as the barrier layer. Efficiencies as great as 3.9% in a 1 cm^2 cell have been achieved. Because of the success achieved using this system and the greater control afforded by the spray process it was decided that future cells would be made with Cu_xS_y as the barrier material.

4. Contacting Techniques

Several metals have been deposited by vacuum evaporation techniques onto SnO_x-CdS-Cu_xS_y cells. The most promising of the metals used are silver, tin, copper, and gold. Table 10 lists the O.C.V. and S.C.C. for a series of cells that use these metals as current collectors. From these experiments it would appear that copper gives the best open

TABLE 10

Electrode Metal	Cell No.	O. C. V.	S. C. C. *
Silver	1	.39 V	3.1 ma
	2	.39 V	3.5 ma
	3	.37 V	3.2 ma
	4	.37 V	3.0 ma
	5	.37 V	2.8 ma
Tin	1	.35 V	2.0 ma
	2	.36 V	2.2 ma
	3	.36 V	2.1 ma
	4	.36 V	2.0 ma
	5	.36 V	1.9 ma
Copper	1	.41 V	2.3 ma
	2	.40 V	2.4 ma
	3	.40 V	2.4 ma
	4	.41 V	2.4 ma
	5	.41 V	1.8 ma
Gold	1	.34 V	0.40 ma
	2	.35 V	0.43 ma
	3	.36 V	0.41 ma
	4	.35 V	0.39 ma

Photovoltaic Responses for Cell using Different Metals as Current Collectors

* Measurements made with 140 mw/cm^2 tungsten on cells of 12 mm^2 area

circuit voltage but that silver acts as a better current collector. Further experiments were made using evaporated copper and silver current collecting electrodes. The relative merits of these two metals are about equal when small (12 mm^2) areas are being electroded. When larger areas (square centimeters) are being electroded copper is the superior material, if a drop in open circuit voltage of the cell results when a large area is electroded. This superiority is due to the fact that a short heat treat at 300° C in air will often cause the open circuit voltage to return to the typical level of (.40-.46 V), whereas this does not occur when silver is used. Whether this is due to the reaction of the copper with the cell or the oxidizing of small areas of the copper is not yet known.

Contact to the SnO_x electrode is made by ultrasonically soldering a narrow stripe of indium around the periphery of the cell. The copper sulfide is removed (either by mechanical abrasion or chemical etch) from the area near the indium to prevent shorting. The sheet resistance of the SnO_x is not a major factor limiting the current capabilities of the cell. To demonstrate the effect of sheet resistance on the short circuit current the following measurements were made. Four 1 cm^2 CdS-Cu_xS_y cells were deposited on a 4" x 4" SnO_x coated glass substrate. The ultrasonically applied indium connections were made at various points around the periphery of the glass. The locations of the cells and the connections are shown in Figure 60. Table 11 shows the short circuit current from the cells when the connections are made at points that are different distances from the cells. This data shows small variations in the currents due to the distance of the indium connection from the cells, however, the changes are only minor and it can be safely assumed that the short circuit current measured for a back wall cell is, for the most part, dependent on the properties of the semiconducting materials and not on the current collecting capability of the SnO_x.

Only a minimum effort has been expended on the investigation of techniques to make contact to the front wall cell. Measurement of the sheet resistance of the Cu_2S on CdS indicates that the current collecting ability of the Cu_2S can be profitably used in conjunction with a metal grid to produce efficient front wall cells. Resistance in ohms per square and thickness of the Cu_2S is given in Table 12.

On small cells (1 cm^2 or less) the contact to the copper current collector electrode is made by a point probe of gold wire. If the contact is to be made permanent a fine wire is attached either by silver paint or silver laden epoxy cement. Temporary contact to large area cells (1 cm^2 to 4" x 4") is made by a woven soft indium mesh that is pressed onto the copper and held under pressure by a 1/4" layer of spongy polyurethane foam. Permanent contact to large cells is made in the same way as small cells.

5. Photovoltaic Structure Experiments

a. Crystallinity and Orientation of the CdS

Efforts to correlate crystallinity and crystallite orientation with

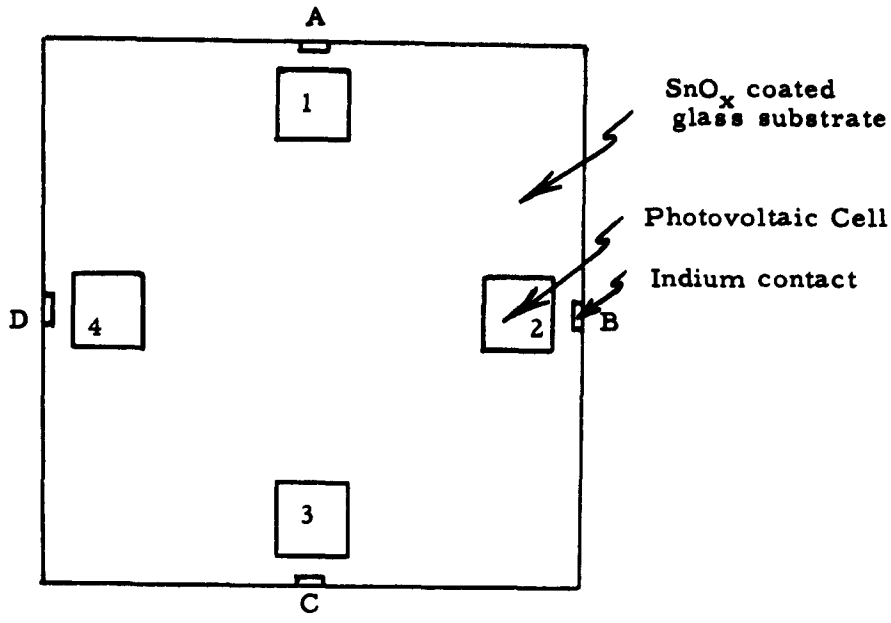

FIGURE 60
Experimental Demonstration of Current Carrying Ability of SnO_x

TABLE 11

Contact	A	B	C	D
Cell No.	S. C. C. ma	S. C. C. ma	S. C. C. ma	S. C. C. ma
1	6.0	5.0	6.0	6.0
2	5.7	5.8	5.7	5.3
3	5.1	6.3	5.9	5.8
4	5.7	6.0	5.2	5.8

TABLE 12

Resistance of Different Thickness Cu_xS_y Films

Thickness	Resistance-No Heat	Resistance after 300° C for 1 minute
260 A°	2×10^5 ohm	6×10^5 ohm
	4×10^5 "	8×10^5 "
	1.2×10^5 ohm	30×10^5 "
520 A°	2.5×10^4 ohm	2×10^4 ohm
	3.8×10^4 "	7×10^4 "
	1.5×10^4 "	4×10^4 "
780 A°	2.4×10^4 ohm	1.5×10^4 ohm
	4.0×10^4 "	1.0×10^4 "
	2.2×10^4 "	0.9×10^4 "
1040 A°	1.4×10^4 ohm	7×10^3 ohm
	3.8×10^4 "	4×10^3 "
	0.9×10^4 "	0.4×10^4 ohm
1300 A°	1.1×10^4 ohm	4×10^3 ohm
	1.3×10^4 "	1.6×10^3 ohm
	$.7 \times 10^4$ "	0.7×10^2 "

photovoltaic response have been partially successful. Figures 61 through 66 show the goniometer tracings which resulted from the x-ray diffraction examination of seven different samples, each of which is the result of a different deposition where some parameter other than thickness was varied. It can be seen that the samples range from almost amorphous (Figure 61) to very crystalline (Figures 65 and 66) to very crystalline with a highly preferred orientation (Figure 67). Table 13 gives the results of using these sample films to fabricate photovoltaic cells using copper sulfide as the barrier forming layer. Each sample was electroded with 1 centimeter squares of vacuum deposited copper with each sample subsequently given a series of short heat treatment (300° C in air) until maximum power point was reached (maximum determined by over-heat treating). It is the maximum power values, of what appear to be the best cells of each sample, that are listed for comparison in Table 13. Comparing the order of the values listed in the table and the order of the goniometer tracings as given, it appears that both crystallinity and preferred orientation can be used as a measure to judge a film prior to using it in the fabrication of a photovoltaic structure and as a means of improving deposition techniques. Samples 3 and 4 do not appear to fit into the sequence of power values in the same way as they apparently fit in the sequence of goniometer tracings; this only points up the difficulty which has been experienced in trying to make comparisons by using as judgment values the V_{oc} and I_{sc} of a completed cell. As yet, not enough is known about the role played by such things as the surface of the CdS, and bulk crystallinity and orientation of the CdS film. The condition of the surface of the CdS might play the major role and is likely the most difficult one to characterize.

b. Barrier Layer of Cu_xS_y

Most of the cells produced this year used a thin film of Cu_xS_y as the barrier layer. The effect of the thickness of the Cu_xS_y layer on the efficiency of the solar cell is evident from Figure 68. However, it is also necessary to consider the diode characteristic dependence on barrier layer thickness. I-V characteristics measured as a function of load resistance indicate that the maximum squareness is achieved for cells where the barrier layer is about 1,000 A° thick. See Figure 69. The fact that the open circuit voltage is relatively constant when the thickness is greater than 260 A° is indicative of the fact that the barrier height is determined by the conditions at the CdS-Cu_xS_y interface and that there are no pin-holes in the Cu_xS_y film to allow shorting of the current collecting electrode to the CdS. The short circuit current increases until the Cu_xS_y is approximately 1,000 A° thick. Greater conversion efficiency has also been achieved by optimization of the temperature at which the Cu_xS_y barrier layer is deposited. Figure 70 shows that at a deposition temperature of 150° C the maximum power output is achieved. I-V curves measured with load resistance as the variable show that at higher temperatures the diode characteristics become soft.

c. Heat Treat

Empirical investigation of the techniques involved in producing an optimum solar cell has indicated that a heat treatment of the cell

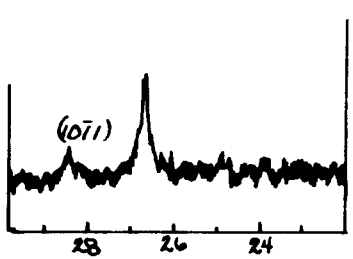

FIGURE 61

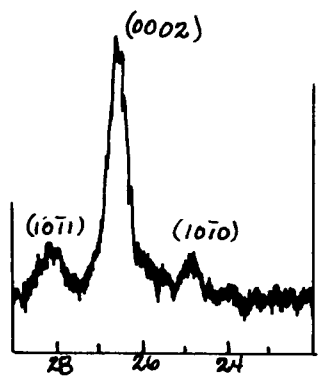

FIGURE 62

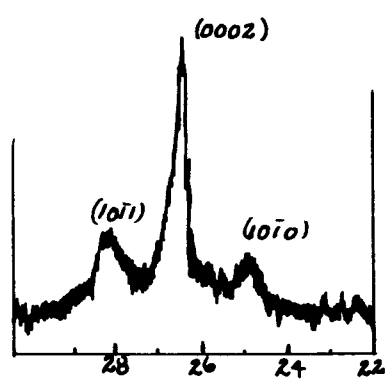

FIGURE 63

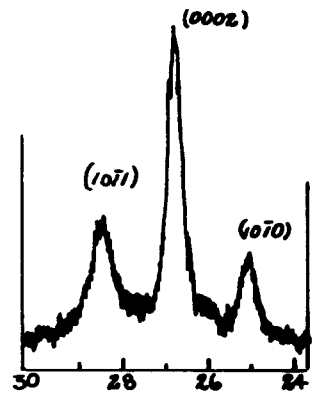

FIGURE 64

X-ray Diffractographs of CdS Films of Varying Crystallinity

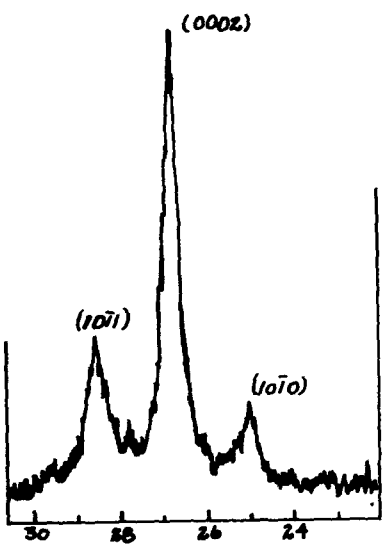

FIGURE 65

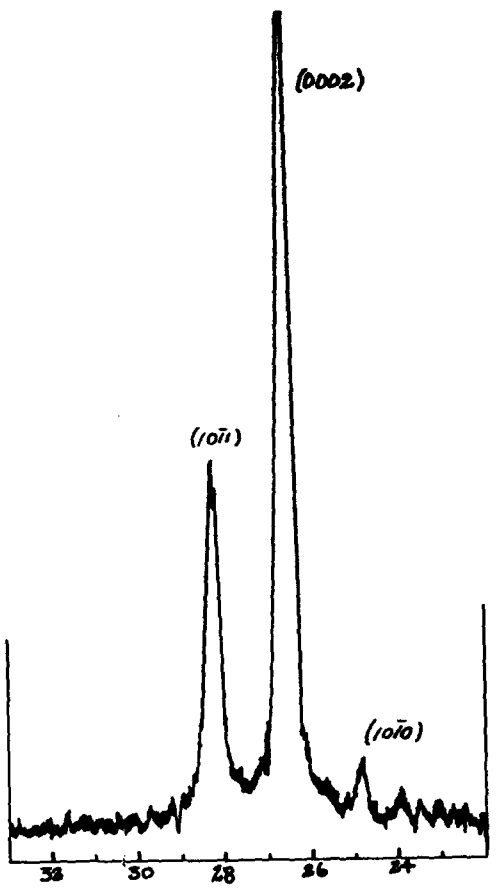

FIGURE 66

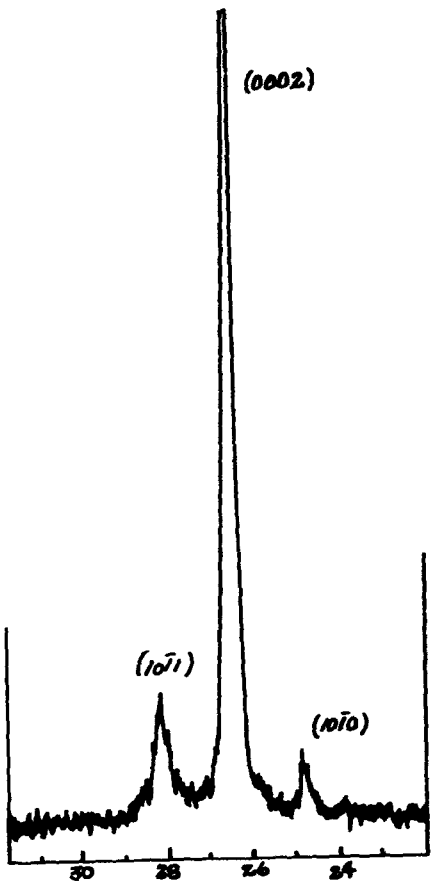

FIGURE 67

X-ray Diffractographs of CdS Films of Varying Crystallinity

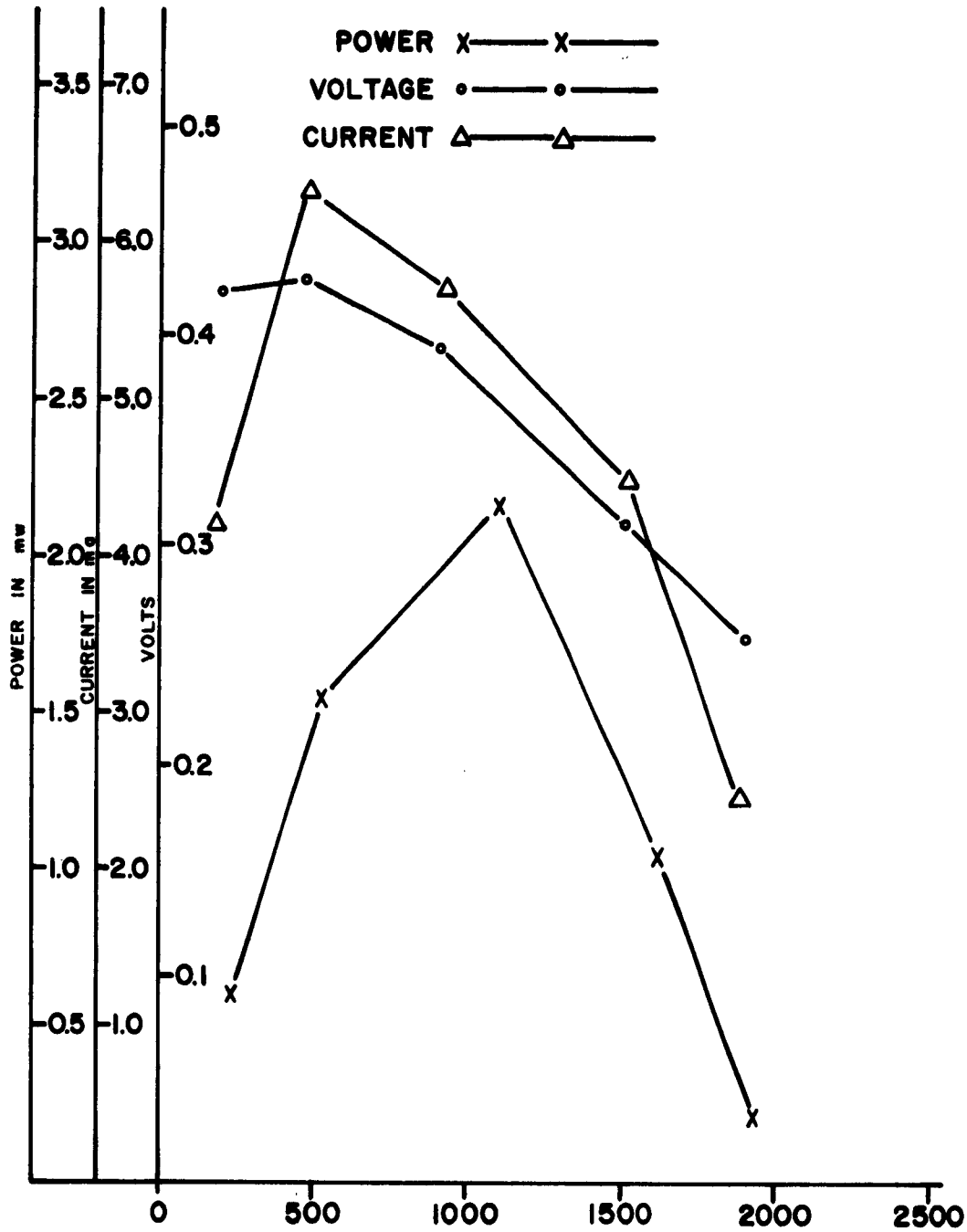

FIGURE 68
Solar Cell Characteristics vs Thickness of the Cu_xS_y Film

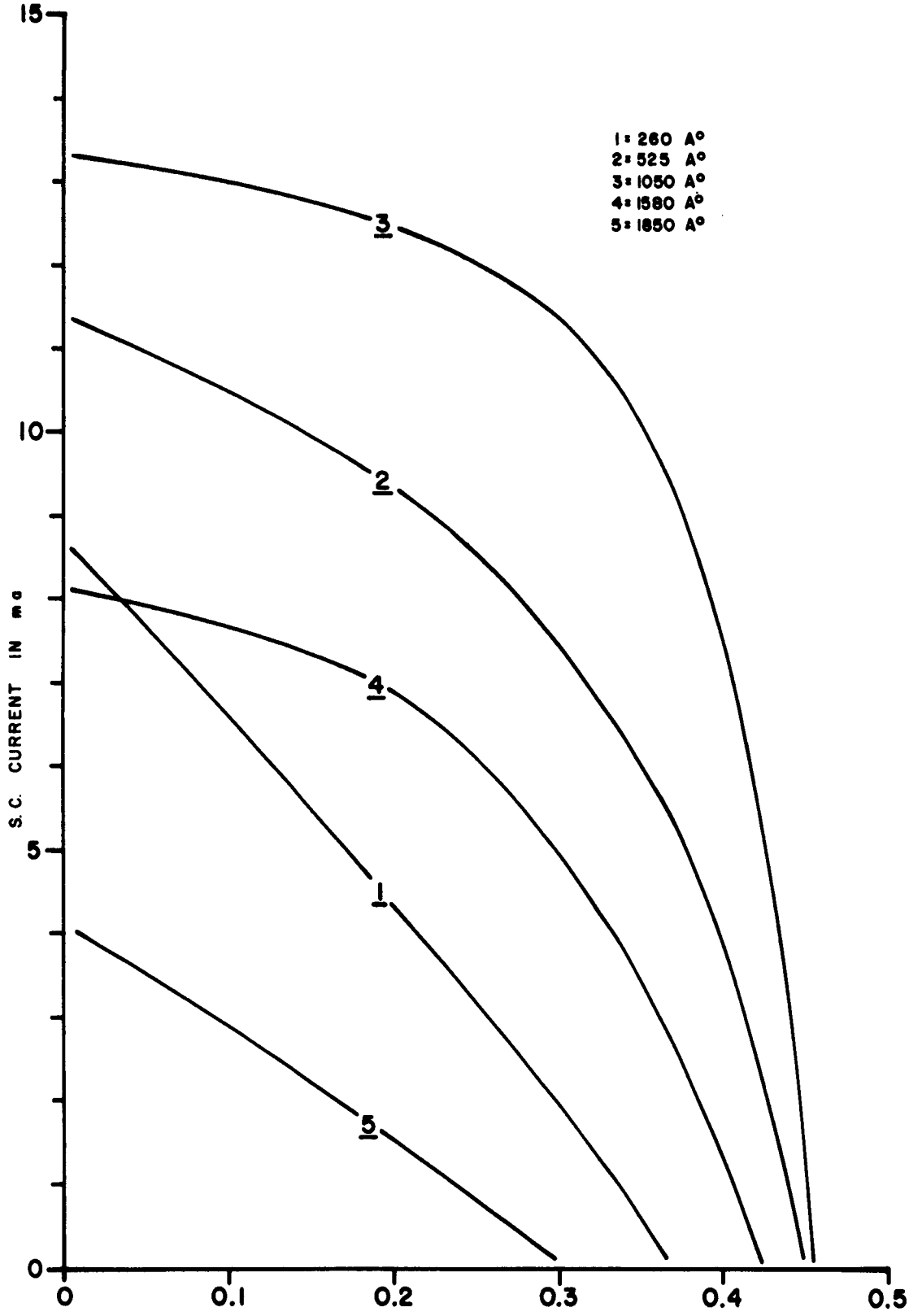

FIGURE 69
Cell I-V Characteristics vs Thickness of Cu_xS_y Film

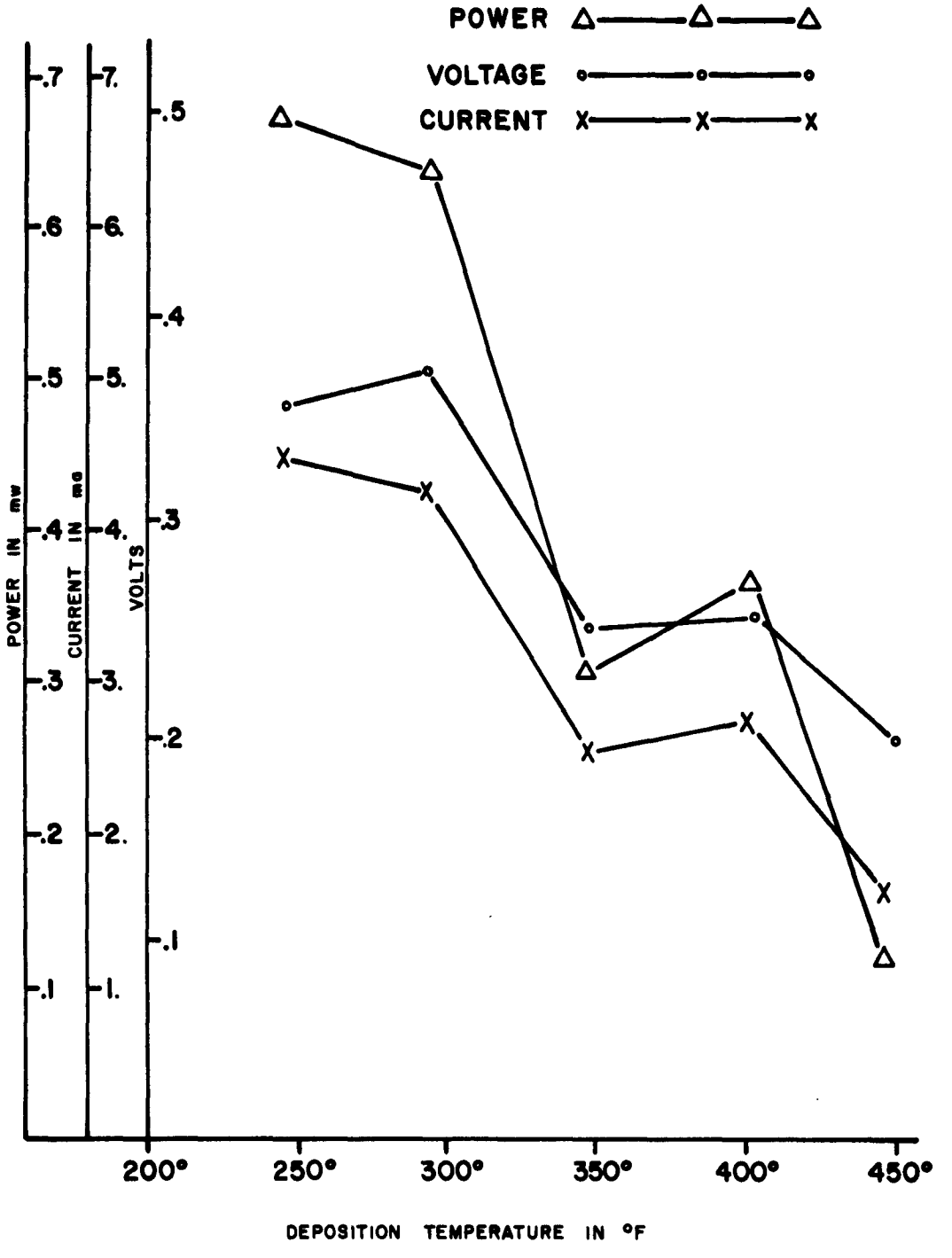

FIGURE 70
Barrier Formation by Cu_xS_y Film vs Deposition Temperature

TABLE 13

Photovoltaic Response of Various CdS Films having Different Crystallinity and Orientation

All values are for 1 cm^2 at an irradiation level of 100 mw/cm^2

Sample No.		I_{sc}	V_{oc}	P
1	A	.30 ma	.001 V	
	B	.25 ma	.001 V	
	C	.15 ma	.001 V	
2	A	1.4 ma	.18 V	.126 mw
	B	1.5 ma	.16 V	.120 mw
	C	1.6 ma	.18 V	.144 mw
3	A	1.24 ma	.33 V	.205 mw
	B	1.47 ma	.32 V	.235 mw
	C	1.45 ma	.33 V	.236 mw
4	A	5.5 ma	.13 V	.350 mw
	B	5.6 ma	.34 V	.950 mw
	C	5.7 ma	.33 V	.930 mw
5	A	2.0 ma	.27 V	.260 mw
	B	2.3 ma	.24 V	.271 mw
	C	2.2 ma	.26 V	.285 mw
6	A	3.9 ma	.33 V	.741 mw
	B	4.2 ma	.36 V	.758 mw
	C	4.3 ma	.35 V	.750 mw
7	A	7.6 ma	.37 V	1.406 mw
	B	6.1 ma	.39 V	1.156 mw
	C	6.5 ma	.38 V	1.235 mw

just prior to the application of the current collecting electrode enhances the photovoltaic characteristics. Figure 71 shows that heat treatment, at temperatures between 275 and 310° C, gives the greatest increase in the efficiency of the cell. The experiment was carried out in an air atmosphere as well as in an inert atmosphere. The change in atmosphere had no apparent effect on the photovoltaic properties of the cells. This immunity to the atmosphere indicates that the heat treat is necessary for the diffusion of the junction at the interface between the CdS and Cu_xS_y. The decrease in efficiency at higher temperatures is probably due to thermal decomposition of the Cu_xS_y.

d. Current Collector

The reasons for chosing copper as the current collector electrode on the back wall cells have been discussed earlier. Experiments, however, indicate that after the deposition of the copper it is necessary to give the cell another short heat treat to maximize the photovoltaic response. Results of the experiments, designed to indicate the optimum heat treat parameters, show that one to two minutes in air at 300° C generally gives the highest conversion efficiency; however, this varies slightly from cell to cell. If a cell has not been heat treated after the copper electrode is deposited, it usually has a low open circuit voltage. Since the copper electrode has as its only purpose the contacting of the Cu_xS_y it is assumed that the low open circuit voltage is due to shorting paths found by the evaporated copper contacting the CdS layer at discontinuities in the Cu_xS_y layer. Heat treatment appears to cause oxidation of the shorts and thus results in increased open circuit voltage as shown in Table 14.

TABLE 14

	No Heat		2 min. in air at 300° C		2 min. in N_2 at 300° C	
Sample No.	O. C. V.	S. C. C.	O. C. V.	S. C. C.	O. C. V.	S. C. C.
11-15 B_1	.05	1.8	.33	4.6		
11-15 B_2	.04	1.4			.08	2.6
11-15 B_3	.11	1.25	.39	3.9		
11-6KK C1	.18	2.9			.21	2.7
11-6KK C_2	.07	1.9	.42	5.2		
11-6KK C_3	.10	2.4			.24	3.1

Current collecting electrodes made from silver paint and evaporated copper are compared in Table 15. The cells used for this study were all prepared on the same glass substrate and were of the SnO_x-CdS-Cu_xS_y type. From the data in this table it can be seen that the height of the barrier is controlled by the CdS-Cu_xS_y junction and not the "metal-semiconductor" interface.

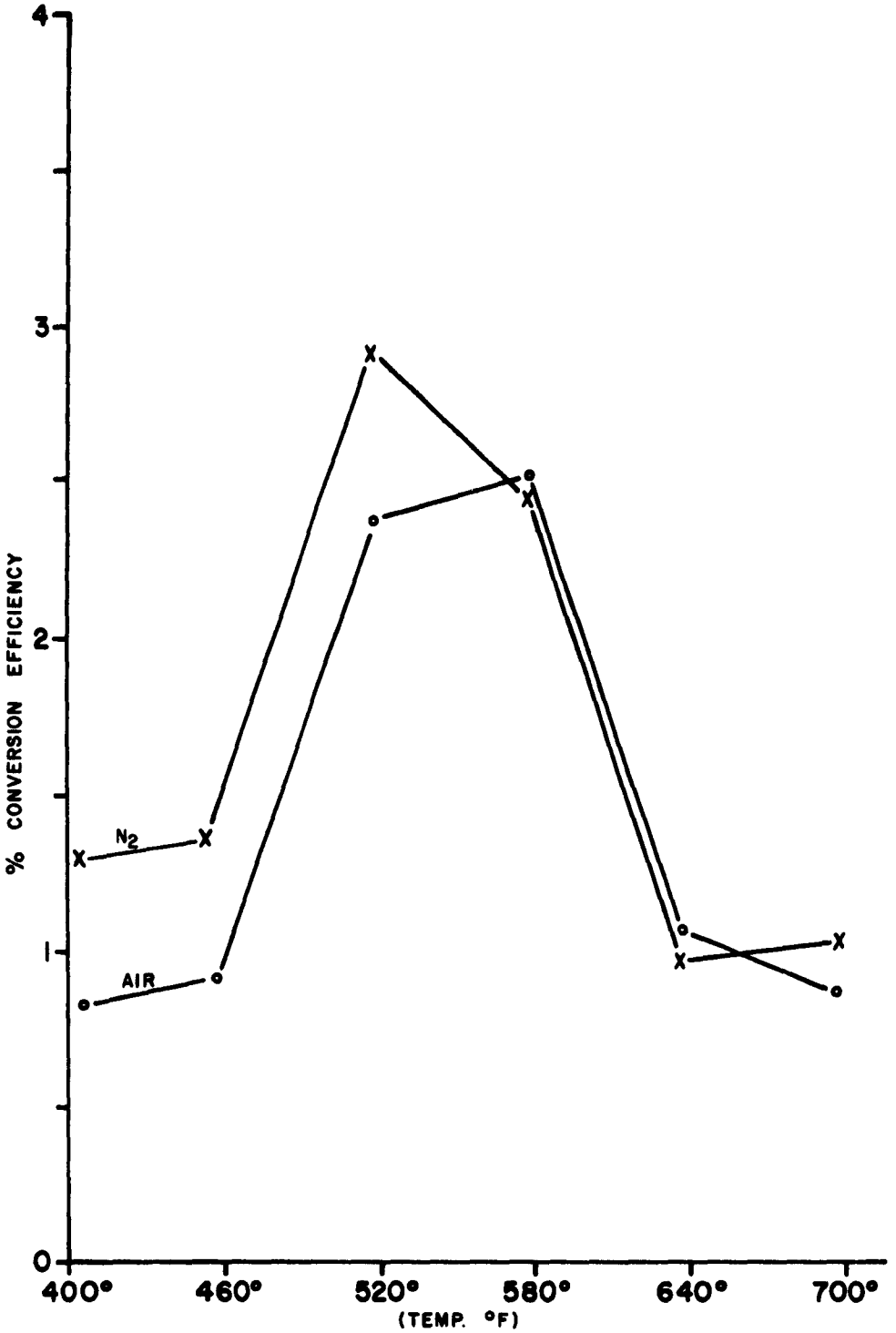

FIGURE 71
Barrier Formation by Cu_xS_y Film vs Heat Treatment

TABLE 15

Sample No.	O. C. V.	S. C. C.
1-21E1A Ag Paint	0.42 V	2.3 ma
1-21E1C Ag Paint	0.40 V	2.6 ma
1-21E1E Ag Paint	0.44 V	2.0 ma
1-21G3A Ag Paint	0.42 V	1.9 ma
1-21G3B Ag Paint	0.41 V	2.7 ma
1-21E1B Evaporated Cu	0.46 V	6.3 ma
1-21E1D Evaporated Cu	0.40 V	4.2 ma
1-21E1F Evaporated Cu	0.45 V	5.7 ma
1 21G3C Evaporated Cu	0.44 V	3.9 ma
1-21G3D Evaporated Cu	0.43 V	5.4 ma

6. Typical Cell Characteristics

Tabulated in this section are those characteristics which are considered typical of SnO_x-CdS Cu_xS_y-Cu photovoltaic cells. The cells used in these measurements were fabricated in accordance with techniques that have been shown by the various optimization experiments to be the most likely to produce a high conversion efficiency cell.

a. Effect of Area

Figure 72 is the voltage-current curve produced by varying the load resistance for cells of various size. An increase in cell area causes a decrease in conversion efficiency as this figure shows. This loss in efficiency seems to be due to a decrease in the ratio of forward to reverse diode characteristics. With increased area comes a decrease in internal reverse resistance that leads to an internal shunting effect. To experimentally verify this assumption a 1 cm^2 cell with "square" I V characteristic curve was shunted externally with a 50 ohm resistor and the I-V curve was again measured. The results are shown in Figure 73. The shape of the curve changed in the manner predicted. Typical diode characteristics are shown in the photographs in Figure 74. Measurements of the diode characteristics for many cells of different areas have also supported the assumption that reduction in efficiency of large area cells is due to "softening" of the diode.

b. Intensity

The open-circuit voltage reaches a maximum level at relatively low illumination levels whereas the short circuit current increases

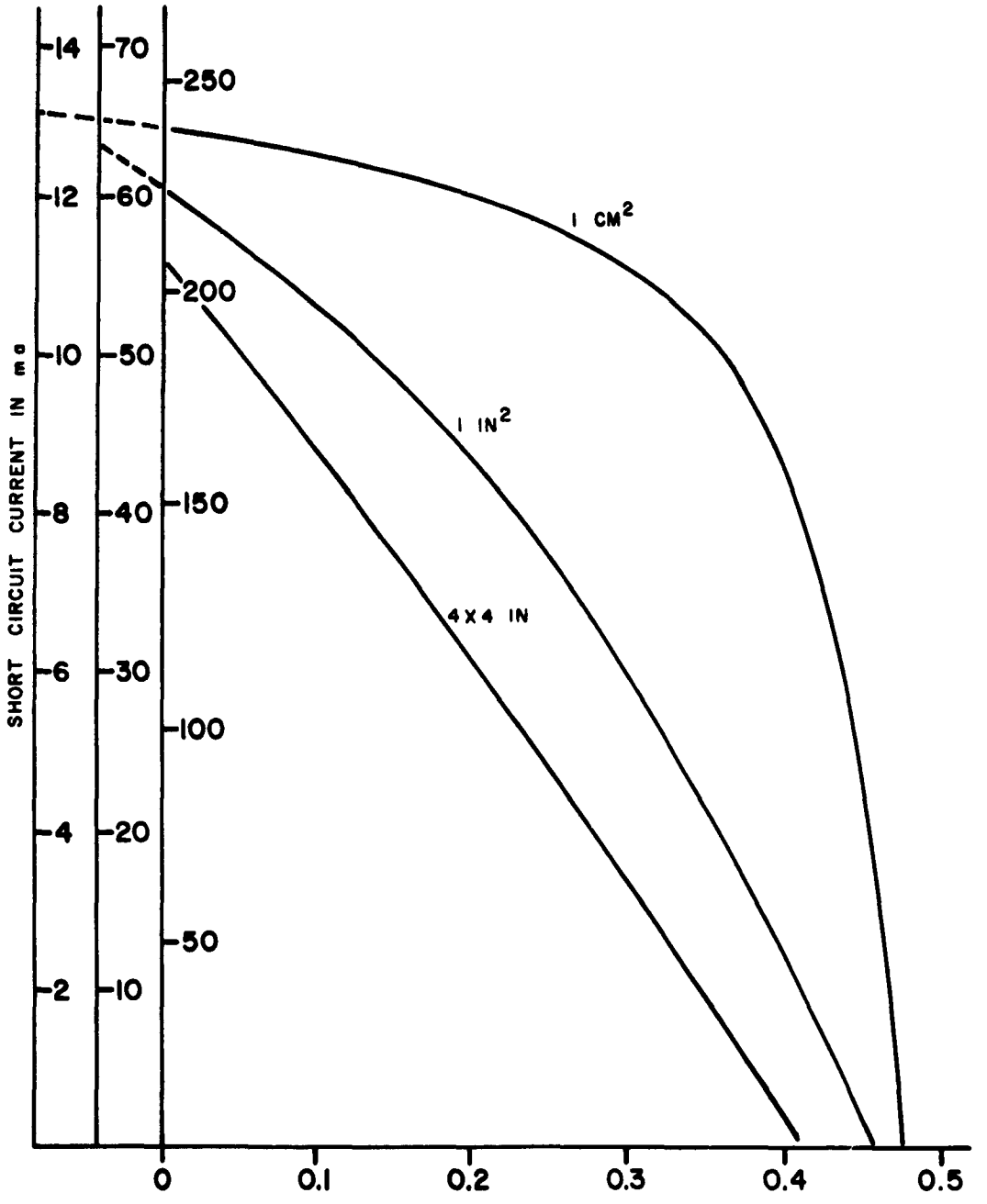

FIGURE 72
Effect of Area Size on I-V Characteristics of Cell

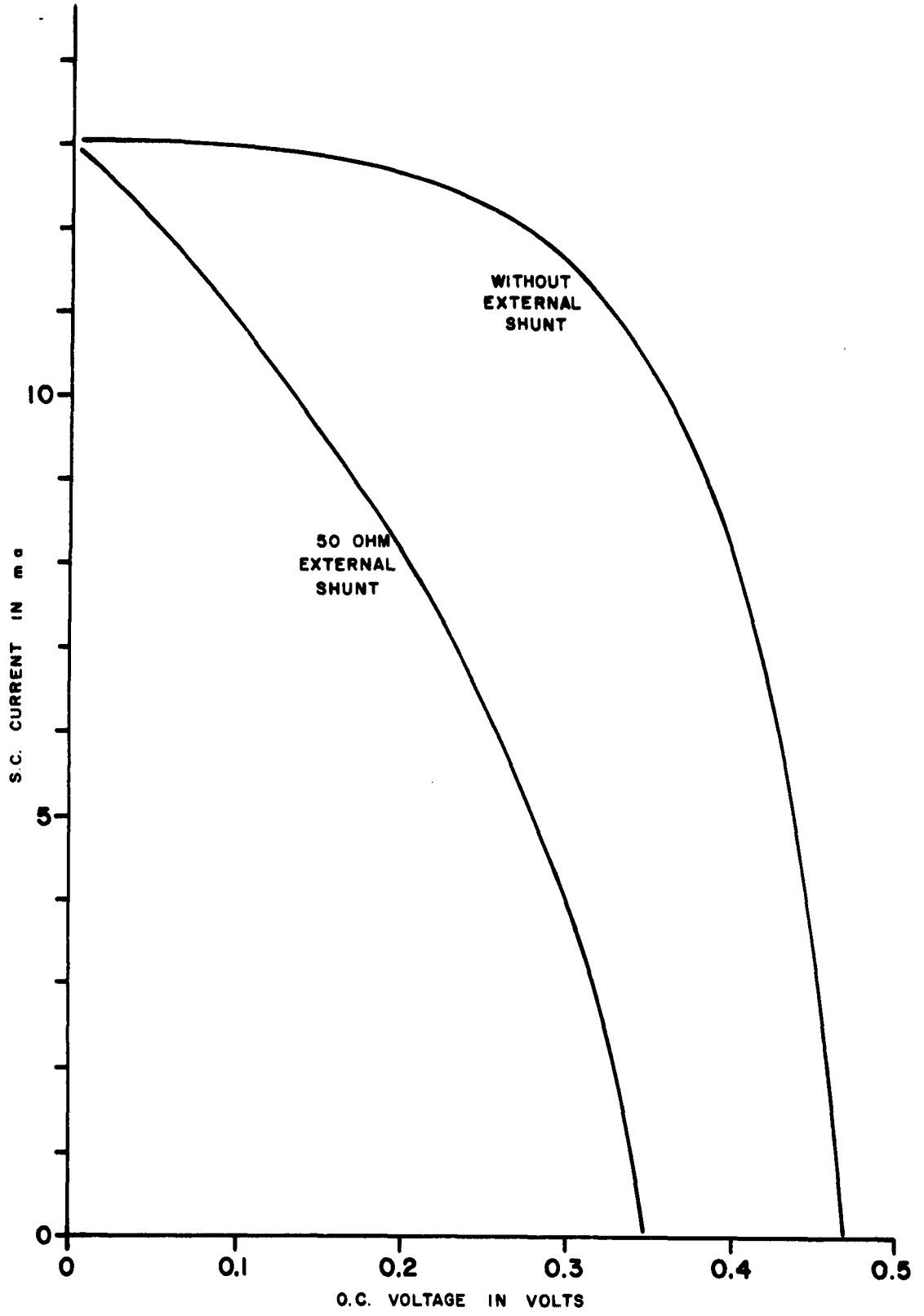

FIGURE 73
Effect of Shunting on a Cell's Diode Characteristic

FIGURE 74a

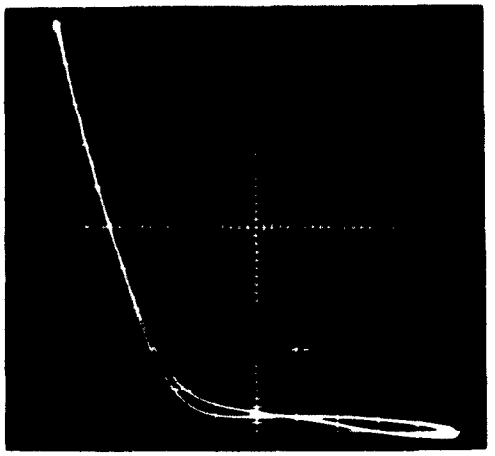

1 cm^2

FIGURE 74b

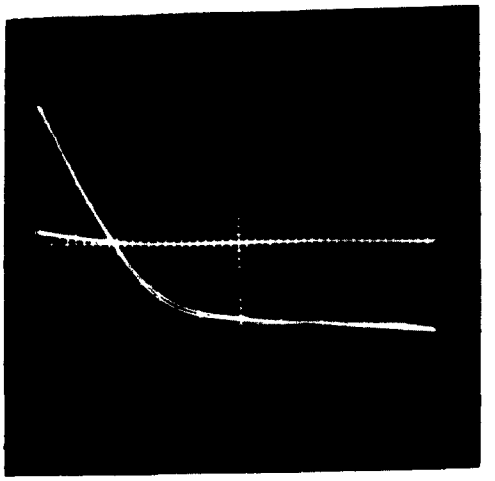

1 inch square

FIGURE 74c

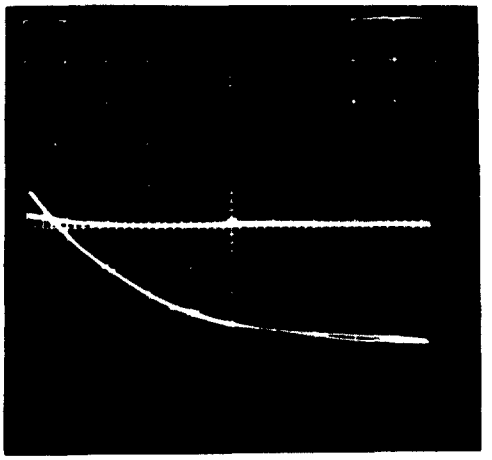

4" x 4"

Typical Diode Characteristics of Cells of Different Areas

in a linear fashion as the illumination level is increased, as shown in Figure 75. The non-linearity of the voltage-intensity curve is due to the open circuit voltage being dependent entirely on the height of the barrier. Consideration of the non-linearity of the voltage characteristics dictates that all spectral response and other phenomena involving the illumination level be measured by monitoring the short circuit current.

c. Response Time

Although not of any particular importance in power applications, it has been found that a typical thin film cell has a very short response time. The response time of the photovoltaic cells was measured by monitoring the voltage output of the cell on an oscilloscope. The light source was a pulsed 100 watt mercury arc lamp. Shown in Figure 76 is the response of the photovoltaic cell compared to the response of a 1P21 photomultiplier tube. As indicated in the figure the rise time of the light source (to 90% of the final brightness level) is about 12 μ seconds. The photovoltaic cell reaches saturation voltage in about 6 μ seconds, at an illumination level that is somewhat lower than the full-"on" illumination of the source, however, it is obvious that measurement of the cell's response time is limited by the rise time of the light source. To accurately measure the response time it will be necessary to use a light source that has a faster response than the photovoltaic cell.

d. Temperature Characteristics

An experiment was conducted to determine the effect of operating temperature on the conversion efficiency of the photovoltaic cell. The cell was placed in the environmental test chamber (Figures 77 and 80) and then the chamber was evacuated to a pressure of approximately 10^{-3} mm of Hg. There was no noticeable change in the cell characteristics due to the decrease in pressure. Figure 78 shows the relation between temperature of the cell and the open circuit voltage, short circuit current, and the power. Since these measurements were made under constant illumination the power curve is directly related to the conversion efficiency curve. The open circuit voltage appears to approach a maximum value of about 0.6 volts as the temperature is decreased. The power is at a maximum at a temperature between 0 and -100° C, however, the decrease in power is most rapid at temperatures above 75° C. At this temperature both the current and voltage begin to decrease.

e. Angle of Incidence

The effect of the angle of incidence of the illumination on the open circuit voltage and short circuit current for front wall and back wall cells is clearly shown in Figure 79. The illumination level used for these measurements was greater than that needed to bring the voltage level to saturation and thus the voltage remained constant until the angle of incidence was great enough to cause appreciable reflection losses. The current, as mentioned above, is linear with intensity and therefore is capable of exhibiting greater variations with fluxations in the energy reaching the photovoltaic junction.

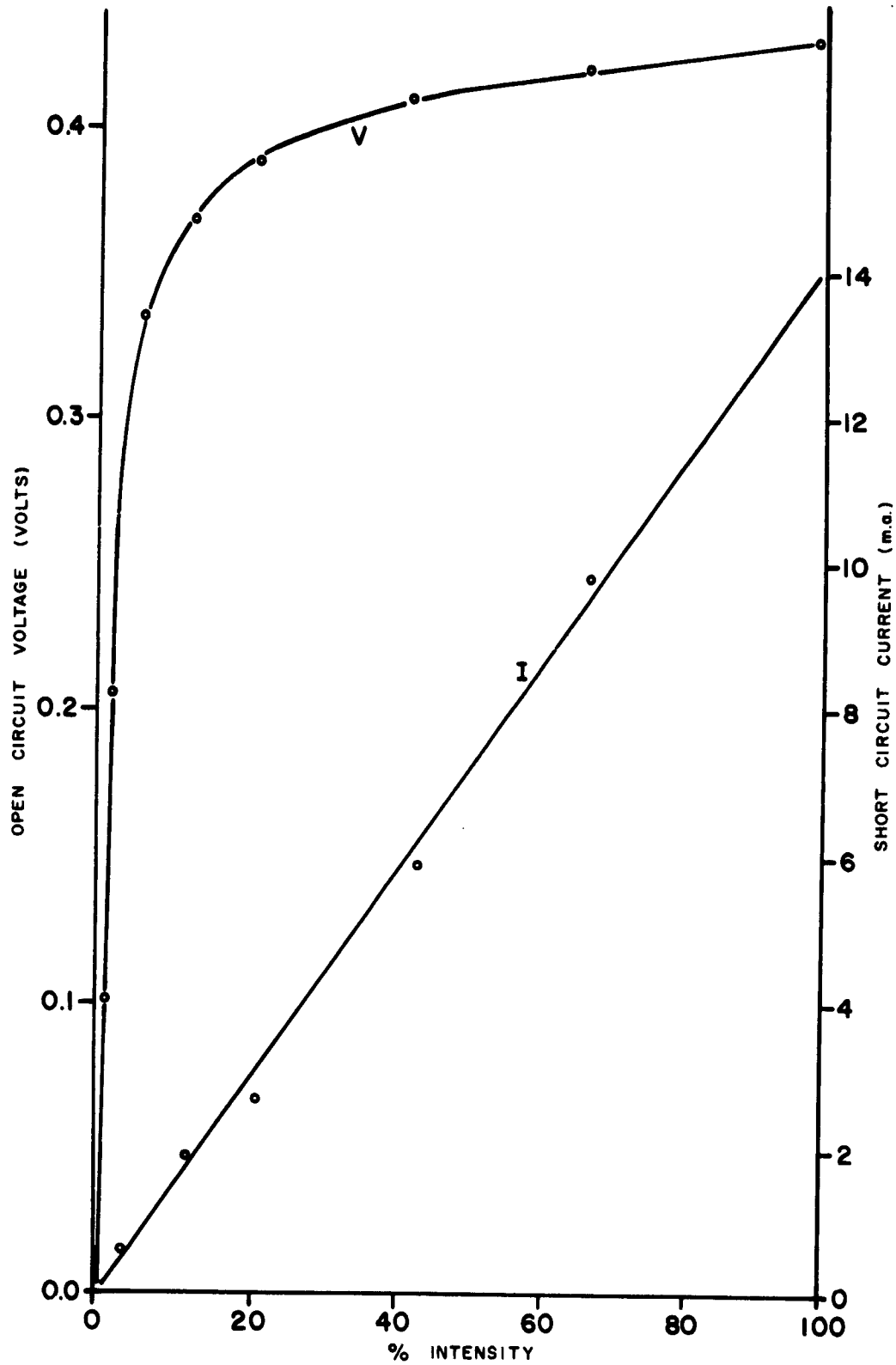

FIGURE 75
Current and Voltage vs Light Intensity

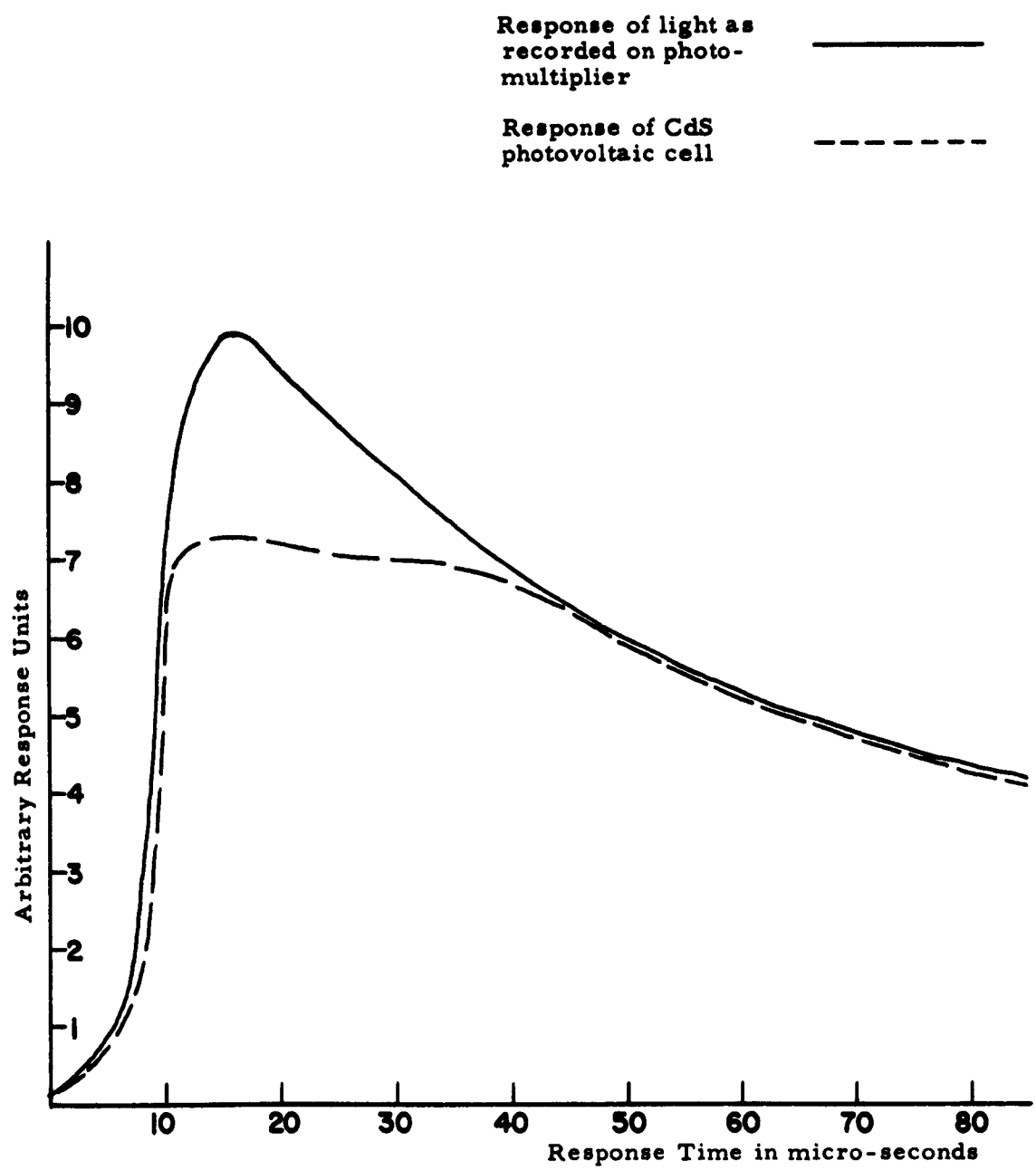

FIGURE 76
Graphical Display of Response Time

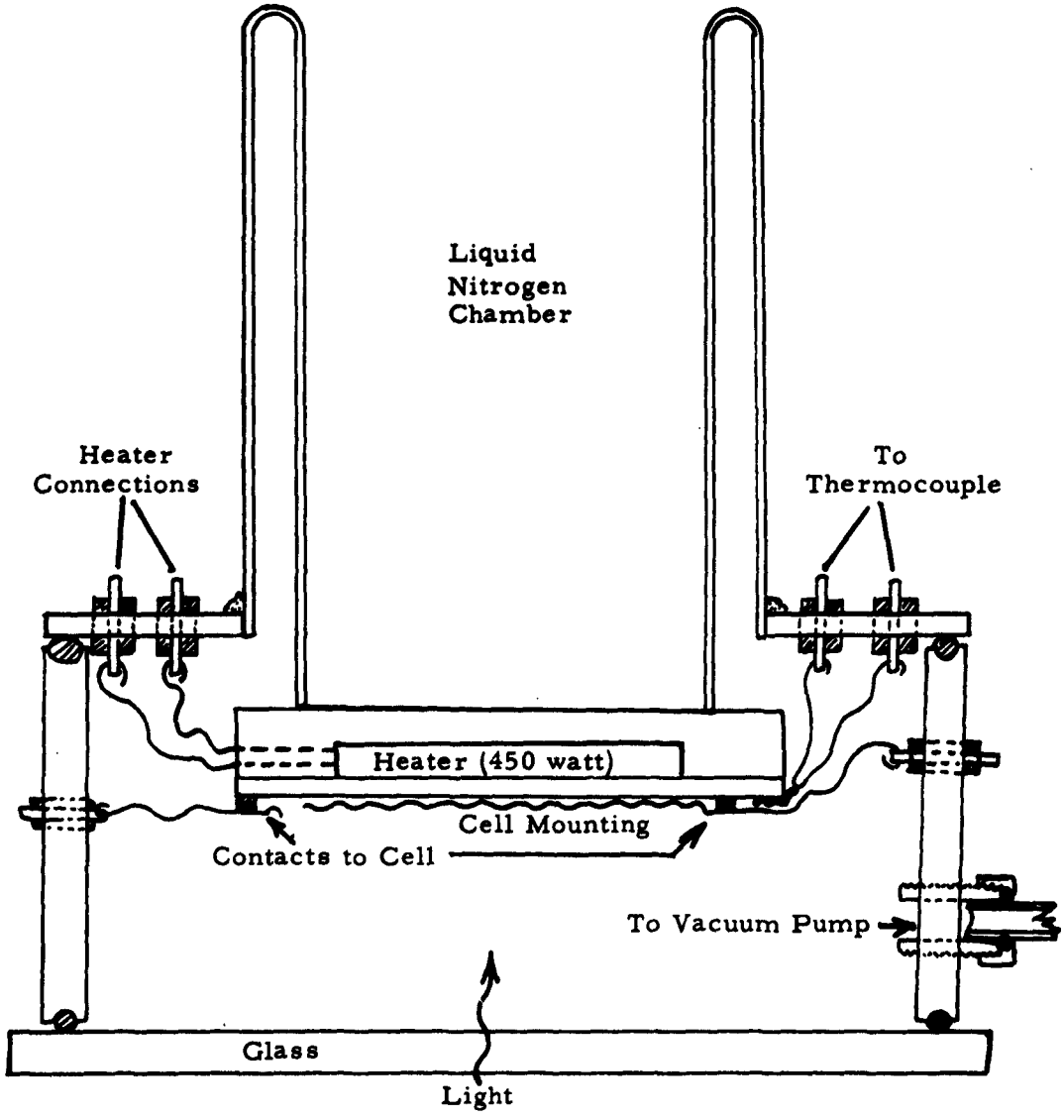

FIGURE 77
Environmental Test Chamber

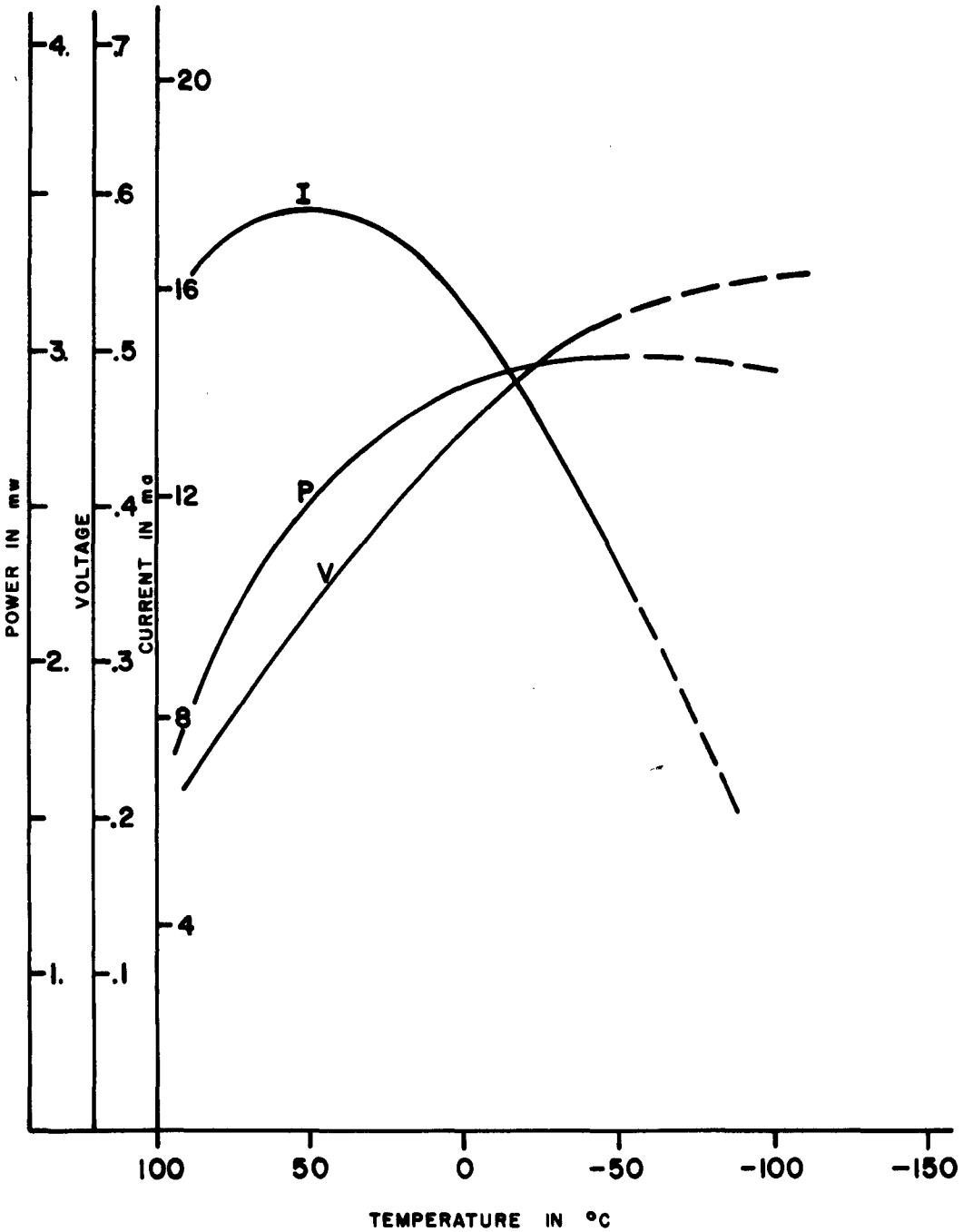

FIGURE 78
Current, Voltage and Power vs Temperature

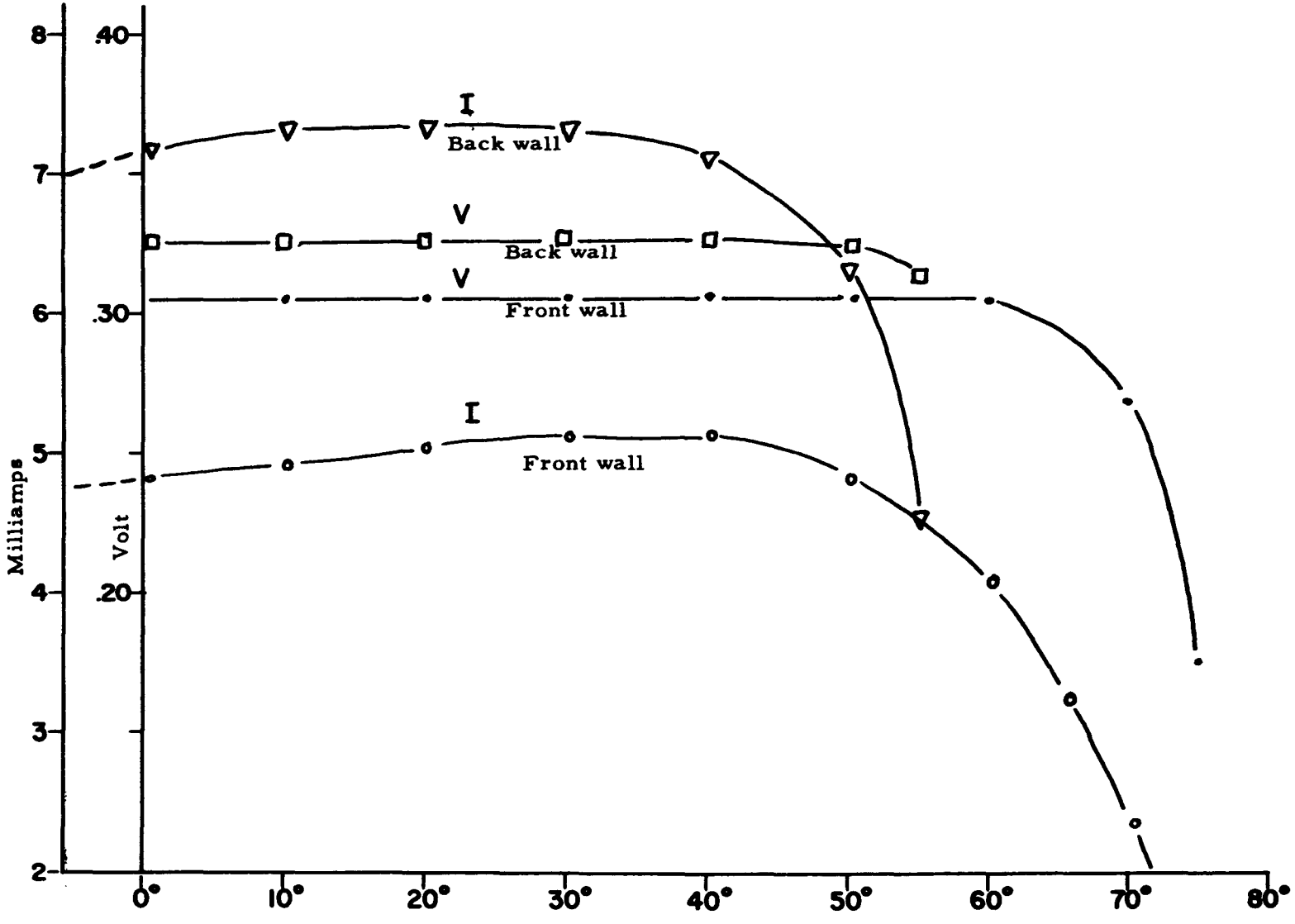

FIGURE 79
Current and Voltage vs Angle of Incidence

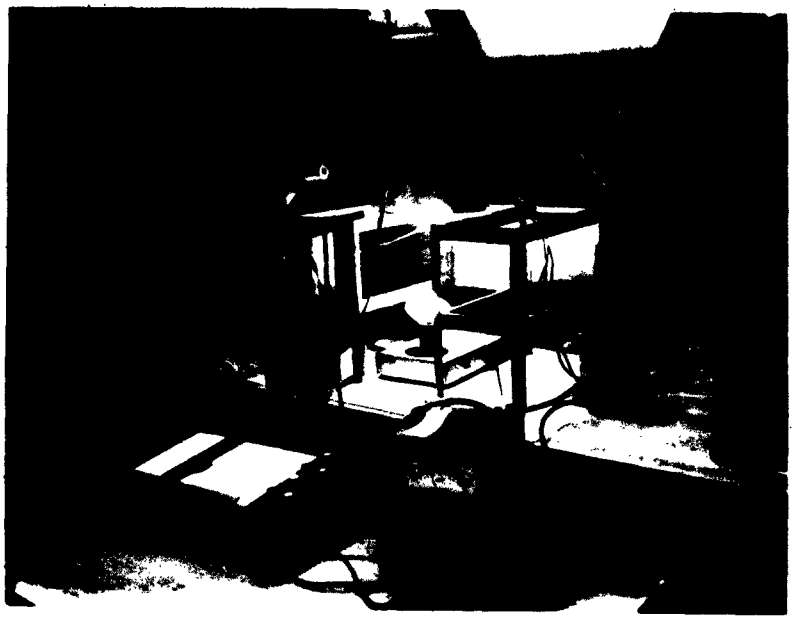

FIGURE 80
Environmental Test Chamber

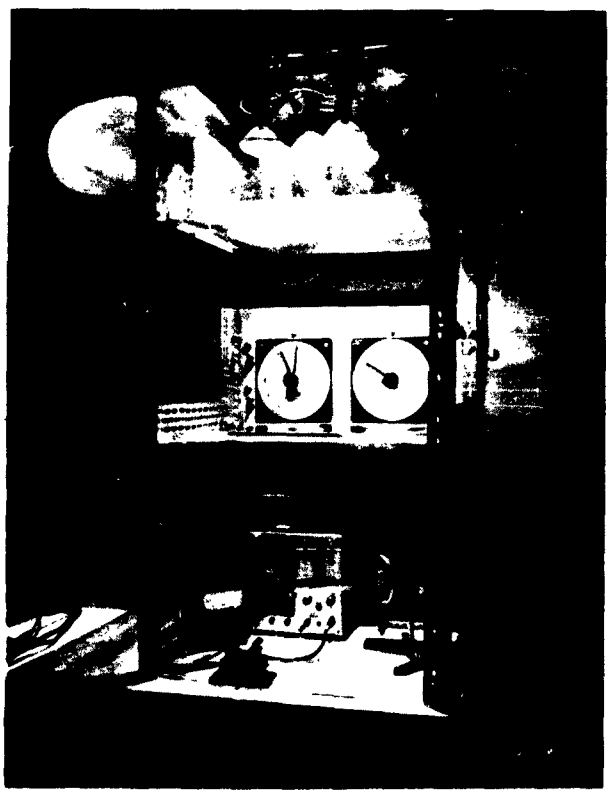

FIGURE 81
Artificial Sun Apparatus

Further evidence of the voltage saturation is evident from the fact that the current displays a negative slope at angles greater than 30° whereas the voltage in some cases remained flat even at 60°.

In the front wall cell the current at an incidence angle of 35° is increased by 6% over the current at normal incidence. This may be accounted for by considering that the light in a front wall cell is partially blocked by a current collecting grid of silver paint and as the light is allowed to impinge on the cell, at some angle other than 90°, the area under the electrodes is partially illuminated and thus contributes to the current.

f. Stability

The problem of shelf-life has not been one of major investigation on this program, however, those measurements that were made are worthy of note.

Cells made using the evaporated copper as the barrier layer were found to have unpredictable life. In many cases it was found that the photovoltage after 24 hours had decreased to less than 25% of its original value of 0.35-0.42 volts. Cells of the SnO_x-CdS-Cu_xS_y-Cu type have been found, however, to display very stable characteristics. A group of cells of this type were tested after 3 months exposure to the normal laboratory atmosphere (20° C at ≈30-40% humidity) and were found to have undergone no degradation in voltage or current. As a matter of fact, in some cases the voltage was found to have increased from 0.40 volts to 0.42-0.44 volts. The apparent immunity to atmosphere can be accounted for by considering the location of the photosensitive junction. In a cell of the SnO_x-CdS-Cu_xS_y-Cu types the junction is at the interface between the CdS and the Cu_xS_y, thus the continuous Cu_xS_y film plus the copper current collector electrode act as a protective coating sealing off the photosensitive region from contact with the atmosphere. In cells of the SnO_x-CdS-Cu type, the junction or barrier region, produced by diffusion of the copper into the CdS, is exposed to the ambient atmosphere and naturally is more susceptible to degradation.

SUMMARY AND CONCLUSIONS TO CELL FABRICATION

During this study solar cells were produced, using the chemical spray technique, that exhibited conversion efficiencies as great as 3.9% for a 1 cm^2 cell. The deposition of a barrier layer by the chemical spray technique was also shown to be feasible and indications are that a barrier formed in this manner is more stable, more uniform and more easily controlled than those produced by any other method. Experiments indicated the necessity of crystallinity and orientation in the CdS films. The techniques necessary to spray highly crystalline, strongly oriented films were developed and used to produce efficient photovoltaic cells. Cell deterioration was briefly investigated and the results showed that a cell of SnO_x-CdS-Cu_xS_y-Cu type is more stable than cells utilizing barriers produced by other techniques. Further investigation and experimentation is necessary to explore the possibilities of increasing the carrier concentration in the CdS and the Cu_xS_y in order to increase the conversion efficiency. Additional experiments are needed to optimize the basic physical properties that will lead to increased area and power to weight ratio.

TECHNICAL SUMMARY

The fabrication of thin film CdS photovoltaic cells by a chemical spray process has been shown feasible. Small (1 cm^2) CdS cells have been fabricated with efficiencies of greater than 3.5%.

The CdS cells fabricated during this research period covered by this report are, except for two very important features, similar to cells fabricated by standard vacuum deposition techniques. The features which are unique to cell mode by the chemical spray process are: (1) the barrier is formed by the deposition of a distinct and separate p-type film of copper sulfide, and (2) the total thickness of the semiconducting film combination is less than 1 micron.

Although this research effort covered only the demonstration of feasibility using the chemical spray process and not the chemical spray process itself, it can be shown that this process does make possible the continuous deposition of an entire photovoltaic structure.

Several new thin film combinations were tried, their photovoltaic response demonstrated, and their spectral responses reported.

The large area (16 $inch^2$) cells of CdS which were delivered under this contract had average efficiencies of 0.2% which is well below the 3.5% shown possible in 1 cm^2 cells. It has been shown, however, that this low efficiency of the large area cells is not due to the current collecting ability of either the top or the bottom electrode, but rather due to the condition of the junction formed between the n-type and p-type films.

The condition of this junction, and hence the efficiency of the large area cells, should lend itself to improvement much more readily than improving what appears to be already sufficient current carrying ability of the top and bottom electrodes.

APPENDIX A

CHARACTERISTICS OF LARGE AREA SOLAR CELLS

The thermal and electrical characteristics for several of the large area CdS cells that were prepared for delivery are given in this section. The cells prepared from CdS films are 16 square inches in area and range in efficiency from 0.1 to 0.2%. The two cells produced from CdSe are photovoltaic but the maximum efficiency obtained in a large area cell (9 square inches) is 0.01%. Because of the low efficiency the characteristic data were not determined for CdSe cells.

Solar Simulator

The dependence of open circuit voltage and short circuit current on the angle of incidence and intensity of the light was measured on the solar simulator shown in Figure 81. Figure A-1 shows the intensity uniformity of the area illuminated by the solar simulator. The solar simulator light is supplied by a bank of five 300 watt photo-spot bulbs. A 3 cm water filter is used to produce a spectral distribution that is more nearly similar to the sun's distribution than unfiltered tungsten light.

1. The apparatus described in Figures 77 and 80 is used to measure the temperature characteristics of cells that are as large as 4-1/2" x 4-1/2". The temperature of the cell is assumed to be the same as that measured by the thermocouple in contact with the surface of the brass cell mounting block on which the cell is mounted. The current voltage curves shown in Figure A-2 are for temperatures from -110° C to + 110° C.

2. The intensity characteristics were measured by varying the light intensity in the solar simulator with neutral density filters made from various size mesh screens. These measurements are shown in Figure A-4. A blower was used to insure a minimum amount of heating of the cell during measurements in the solar simulator.

3. Figure A-3 describes the effect of incident angle of the illumination on the open circuit voltage and short circuit current for two of the 16 square inch CdS cells. Contact to the copper current collector on large area cells was made by a soft indium mesh held under pressure by a pc. yfoam sponge. The cells were rotated around an axis perpendicular to the light beam on a Nippon Kogaku goniometer.

Effect of cell area on efficiency is discussed in Section IV.

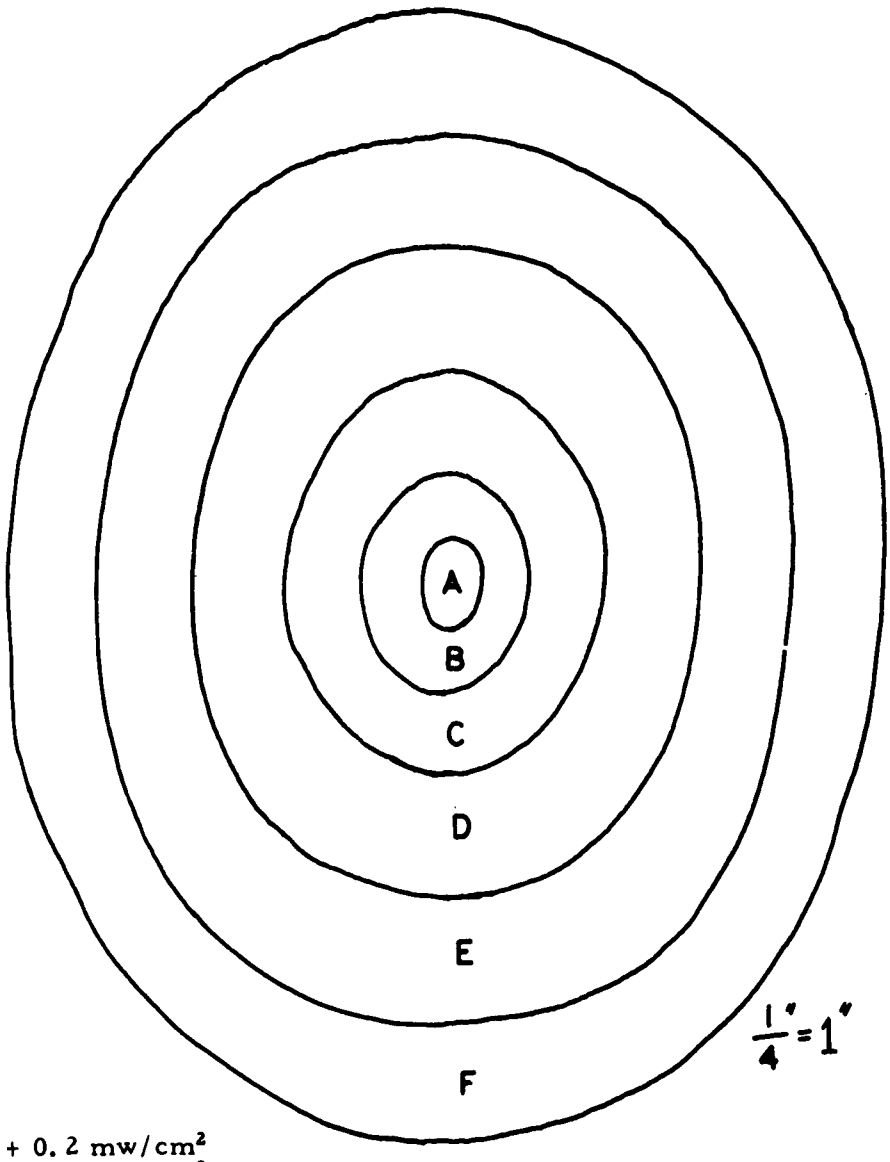

A	$140 + 0.2$ mw/cm^2
B	140 ∓ 2.0 mw/cm^2
C	135 ∓ 3.0 mw/cm^2
D	128 ∓ 4.0 mw/cm^2
E	110 ∓ 15.0 mw/cm^2
F	70 ∓ 30 mw/cm^2

FIGURE A-1

Area Uniformity of Light Source

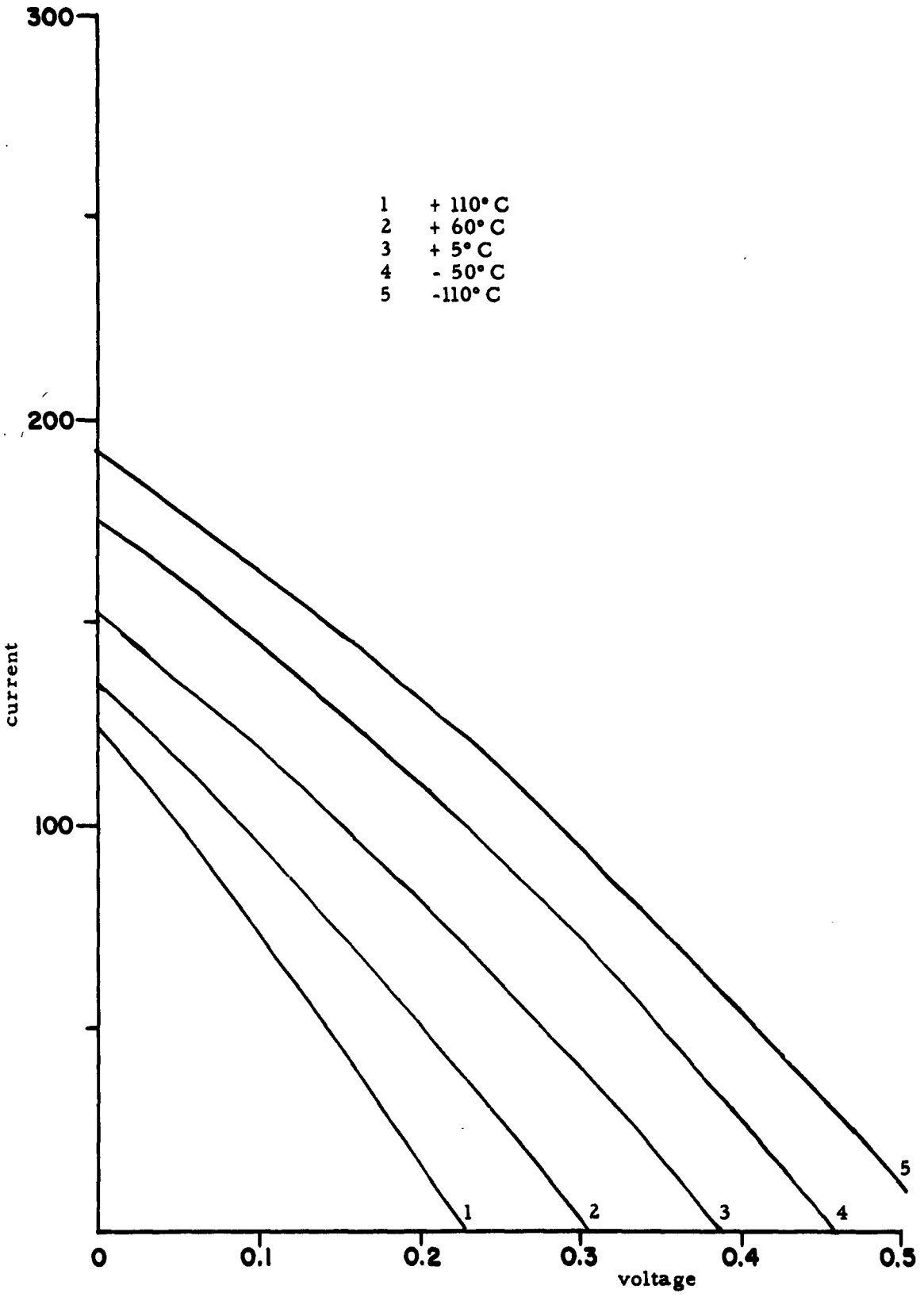

FIGURE A-2
Current and Voltage vs Temperature

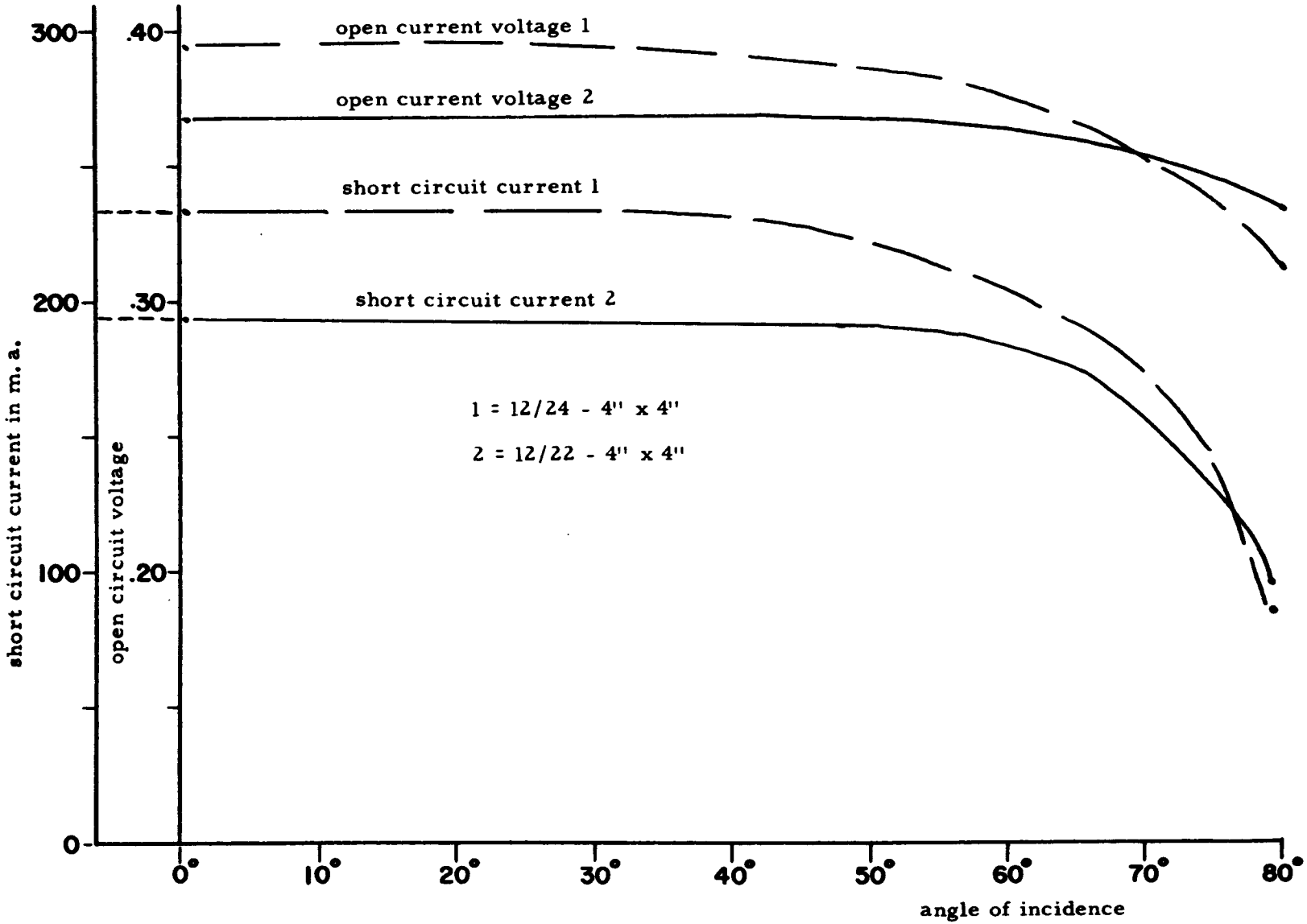

FIGURE A-3
Current and Voltage vs Angle of Incidence

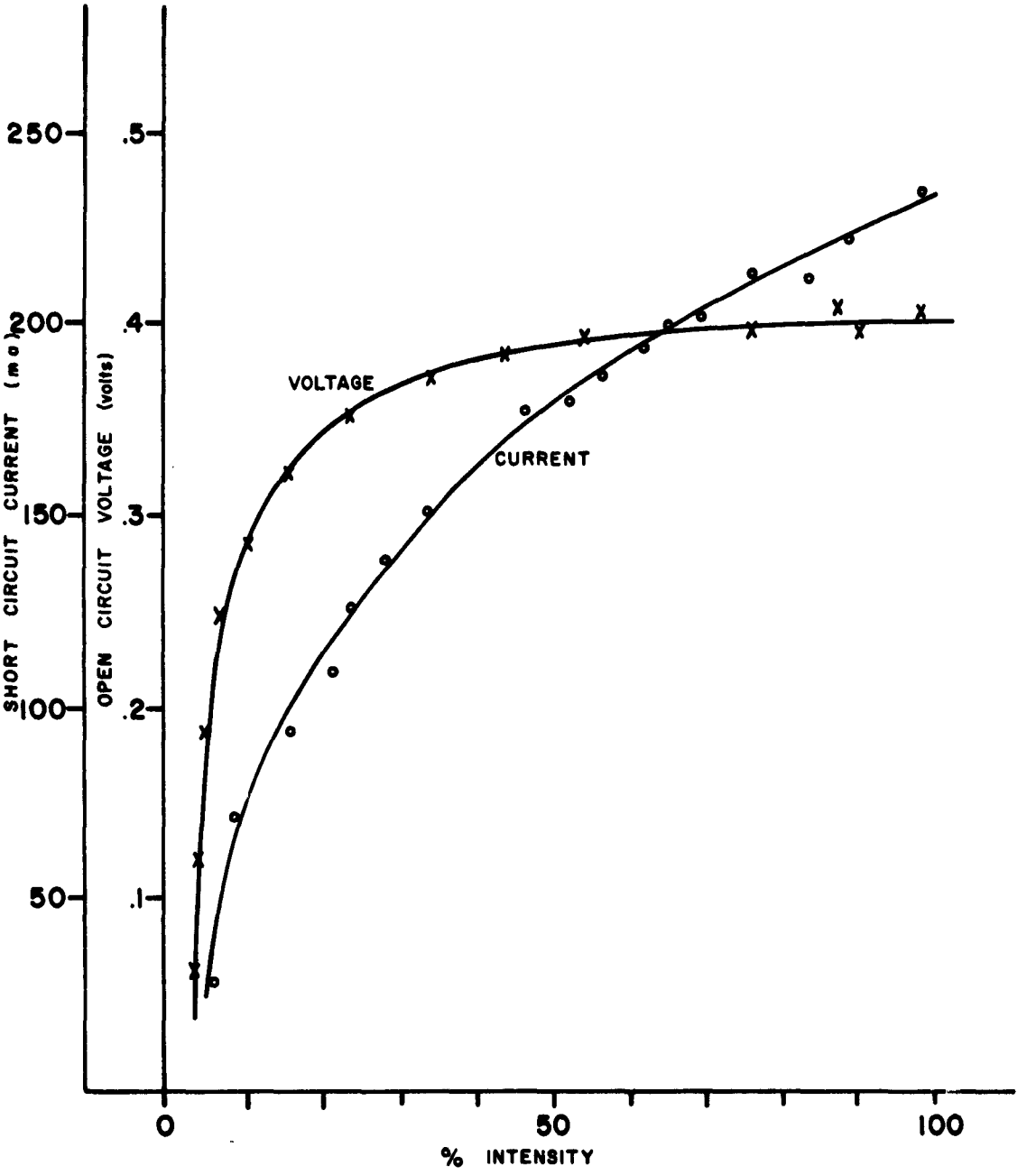

FIGURE A-4
Current and Voltage vs Intensity

LIST OF REFERENCES

1. Carlson, A., "Research on Semiconductor Films", WADC Technical Report 56-62, January 1956

2. Shirland, F. A., "Photovoltaic Cadmium Sulfide", ARL Technical Report 60-293, August 1960

3. Addiss, R. R. et al, "Solar Cell Array Optimization", ASD Technical Report 62-69, Vol. II, December 1962

4. Research on Solar Energy Conversion Employing Cadmium Sulfide, ASD Technical Report 62-69, Vol. II, December 1962

5. "Solar Cell Array Optimization", ASD Technical Documentary Report 61-11, Vol. III, December 1962

6. Shirland, F. A. et al, "Research on Solar-Electrical Energy Conversion Employing Photovoltaic Properties of Semiconducting Cadmium Sulfide", ASD Technical Report 62-69, January 1962

7. Putsieko, E. K., "Determination of the Sign of the Carriers of Photoelectric Current by the Condenser Method", Doklady, Akad Nauk SSSR 67, 1009 (1956)

8. Dunlap, W. C. Jr., "An Introduction to Semiconductors", p. 189, Wiley and Sons, New York, 1957

9. Jezek, Ak. Ceska, Rox., 29, No. 26 (1920)

10. NBS Circular 539, Vol. IV, pp 15-16 (1955)

11. Giles, J. M. and VanCakenberghe, J., Solid State Physics in Electronics and Telecommunications 2, 900 (1960); Part 2, Semiconductors, Academic Press, Inc. (London)

12. Vitrikhovskii, N. I. and Mizetskaya, I. B., "Preparation of Mixed CdS-CdSe Monocrystals from the Vapor Phase and Some of Their Properties", FTT 1, 397 (1959) (Soviet Physics-Solid State, Vol. 1, page 358

13. Wolf, E., "Progress in Optics", Vol. 1, pp 226-228, Interscience, 1961

14. Vasicek, A., "Optics of Thin Films", p. 207, Interscience, 1960

15. Bannon, J., Nature 157, 446 (1946)

16. Bateson, S. and Bachmeier, A. J., Nature 158, 133 (1946)

17. Tolansky, S., "Multiple-Beam Interferometry of Surfaces on Films", p. 144-147, Oxford Press, London, 1949

18. Wolf, E., "Progress in Optics", Vol. 1, pp 214-251, Interscience, 1961

19. Korosy, F., "A Volatile Compound of Copper", Nature, 160, 21 (1947)

Aeronautical Systems Division, Dir/Aeromechanics, Flight Accessories Lab., Wright-Patterson Air Force Base, Ohio Rpt. Nr. ASD-TDR-63-223, Part I. FEASIBILITY INVESTIGATION OF CHEMICALLY SPRAYED THIN FILM PHOTOVOLTAIC CONVERTERS. Final report, March 63. 111 p. incl. 85 illus., 15 tables, 19 refs.

UNCLASSIFIED REPORT

This technical report presents the results of the first phase of Contract AF 33(657)-7919. The objectives were: (1) demonstrate the feasibility of fabricating a thin film photovoltaic converter using a chemical spray process, and (2) fabricate for delivery six experimental cells. Research with these materials has shown the feasibility of fabricating photovoltaic converters using thin films of cadmium and copper sulfide (.6 μ and .05 μ respectively) and has shown that the deposition process used is applicable to large area, multiple layer (CdS-CdSe-Cu_2S) configurations, solid solution (Cd(S, Se)-Cu_2S) cells, and continuous line production. This research has also shown that a heterogeneous junction photovoltaic converter can be formed using CdS. The four CdS cells had an average efficiency of .2% and the two CdSe cells had an average efficiency of less than .01%. CdS cells of one square inch were made with 1.2% efficiency and CdS cells of one square centimeter were made with 3.5% efficiency. All of these cells were of the back wall (incident irradiation travels through the substrate) configuration using one eighth inch hard glass as the substrate.

(over)

1. Feasibility Study
2. Photovoltaic Converters
3. Semiconducting Films
4. AFSC Project 8173 Task 817301
5. Contract AF 33(657)-7919
6. National Cash Register Company Dayton, Ohio
7. R. R. Chamberlin et al.
8. Aval fr OTS
9. In ASTIA collection

Aeronautical Systems Division, Dir/Aeromechanics, Flight Accessories Lab., Wright-Patterson Air Force Base, Ohio Rpt. Nr. ASD-TDR-63-223, Part I. FEASIBILITY INVESTIGATION OF CHEMICALLY SPRAYED THIN FILM PHOTOVOLTAIC CONVERTERS. Final report, March 63. 111 p. incl. 85 illus., 15 tables, 19 refs.

UNCLASSIFIED REPORT

This technical report presents the results of the first phase of Contract AF 33(657)-7919. The objectives were: (1) demonstrate the feasibility of fabricating a thin film photovoltaic converter using a chemical spray process, and (2) fabricate for delivery six experimental cells. Research with these materials has shown the feasibility of fabricating photovoltaic converters using thin films of cadmium and copper sulfide (.6 μ and .05 μ respectively) and has shown that the deposition process used is applicable to large area, multiple layer (CdS-CdSe-Cu_2S) configurations, solid solution (Cd(S, Se)-Cu_2S) cells, and continuous line production. This research has also shown that a heterogeneous junction photovoltaic converter can be formed using CdS. The four CdS cells had an average efficiency of .2% and the two CdSe cells had an average efficiency of less than .01%. CdS cells of one square inch were made with 1.2% efficiency and CdS cells of one square centimeter were made with 3.5% efficiency. All of these cells were of the back wall (incident irradiation travels through the substrate) configuration using one eighth inch hard glass as the substrate.

(over)

1. Feasibility Study
2. Photovoltaic Converters
3. Semiconducting Films
4. AFSC Project 8173 Task 817301
5. Contract AF 33(657)-7919
6. National Cash Register Company Dayton, Ohio
7. R. R. Chamberlin et al.
8. Aval fr OTS
9. In ASTIA collection